DEPARTAMENTO DE INVESTIGACIÓN Y DOCTORADO

MODELOS ORIENTADOS PARA CONTROL INCLUYENDO VARIACIONES INTRAPACIENTE PARA SISTEMAS DE PÁNCREAS ARTIFICIAL

AUTOR: M.Eng. Marcela Moscoso-Vásquez

DIRECTOR: Ricardo S. Sánchez-Peña, Ph.D

CO-DIRECTOR: Dr.Ing. Patricio H. Colmegna

TESIS PRESENTADA PARA OPTAR AL TÍTULO DE

DOCTOR EN INGENIERÍA

Jurado

Dr.Ing. Santiago Rivadeneira   Dr.Ing. José F. García-Tirado   Dra. Marta Basualdo

CIUDAD AUTÓNOMA DE BUENOS AIRES
Agosto 2019

M.Eng. Marcela Moscoso-Vásquez: MODELOS ORIENTADOS PARA CONTROL IN-CLUYENDO VARIACIONES INTRAPACIENTE PARA SISTEMAS DE PÁNCREAS ARTIFICIAL. *Tesis presentada como requisito parcial para acceder al grado de* **DOCTOR EN INGENIERÍA** *del Instituto Tecnológico de Buenos Aires.*

DEPARTAMENTO DE INVESTIGACIÓN Y DOCTORADO

CONTROL-ORIENTED MODELS WITH INTRA-PATIENT VARIATIONS FOR ARTIFICIAL PANCREAS SYSTEMS

AUTHOR: M.Eng. Marcela Moscoso-Vásquez

ADVISOR: Ricardo S. Sánchez-Peña, Ph.D

CO-ADVISOR: Dr.Ing. Patricio H. Colmegna

A THESIS SUBMITTED AS A REQUIREMENT FOR THE DEGREE OF

DOCTOR EN INGENIERÍA

Commitee

Dr.Ing. Santiago Rivadeneira   Dr.Ing. José F. García-Tirado   Dr. Marta Basualdo

CIUDAD AUTÓNOMA DE BUENOS AIRES
August 2019

M.Eng. Marcela Moscoso-Vásquez: CONTROL-ORIENTED MODELS WITH INTRA-PATIENT VARIATIONS FOR ARTIFICIAL PANCREAS SYSTEMS. *A thesis submitted in partial fulfillment of the requirements for the degree of* **DOCTOR EN INGENIERÍA** *of Instituto Tecnológico de Buenos Aires.*

"Sometimes science is more art than science, Morty. Lot of people don't get that."

Rick Sanchez

Acknowledgments

First and foremost, I would like to express my profound gratitude to my advisor, Ricardo Sánchez-Peña, for giving me this wonderful research opportunity and for his continued support, encouragement and his patience despite my mistakes and shortcomings with such understanding and encouraging attitude. I feel privileged for all the support he offered from the start, for offering me his friendship, his wise words, and for allowing me to grow integrally during these years of working together. I would also like to express my gratitude to my co-advisor, Patricio Colmegna for his willingness to help me with every aspect of this research, his encouraging attitude and enriching advise and comments. His constance, discipline, and attention to detail have become an inspiration for continuing on this path. To both Ricardo and Patricio, I owe special thanks for the personal and professional lessons they instilled in me.

I would also like to acknowledge Dr. Ignacio Más, Dr. Demián García-Violini, Dr. Marcelo Frías, Lic. José Rojas, and Gustavo Pierotti, who offered me their friendship and experience, and who have been incredibly supportive and helpful both professionally and personally. Also, I would like to acknowledge the DiabeTeam from Universidad Nacional de La Plata, Dr. Fabricio Garelli, Dr. Hernán De Battista, Eng. Emilia Fushimi, Eng. Nicolás Rosales, Eng. Cecilia Serafini, and their partners from LEICI, for their camaraderie and welcoming spirits, and the enjoyable times we shared both inside and outside the office. To all of them, including my teaching partners Dr. Dardo Marqués and Eng. Juan Martín Maffi, thanks for your support, encouragement and warmth that make me reaffirm the choice of the academic field for my life.

To my family, who from the distance have always given me their unconditional love and support, proudly sharing my achievements, and pushing me to continue pursuing what I love to do despite the difficulties that came along. To my friends, who have made of Buenos Aires a home away from home, for their company, advise, inspiration, motivation, and basically, sharing wonderful times over these years. I'm honored to rely on such wonderful friends. Finally, I would like to acknowledge my friends back home, Viviana Palacio, Gloria Monsalve, Luis Betancur and Alex Alzate, with whom I share this "crazy" goal of pursuing a doctoral degree in different parts of the world. Each one of them has been an inspiration and motivation to continue in this path, and helped shape my way of facing new challenges. Special thanks are due to Alex, who became an essential partner during this experience both academically and personally.

"I almost wish I hadn't gone down the rabbit-hole -and yet-and yet- it's rather curious, you know, this sort of life!"

- Alice.

Resumen

En los últimos años se ha incrementado el número de investigaciones orientadas al desarrollo de un Páncreas Artificial (AP) para la regulación automática de glucosa en pacientes con Diabetes Mellitus Tipo 1 (T1DM). Sin embargo, el riesgo de hiper- e hipoglucemia sigue siendo un impedimento para una regulación adecuada de la glucemia en algunos casos. Una fuente importante de limitaciones se origina a partir de la incertidumbre del modelo, y la alta variabilidad inter- e intra-paciente que afecta la dinámica de la regulación de la glucosa. Por lo tanto, considerando que se requieren herramientas para el diseño de estrategias de control robustas y variables en el tiempo que permitan considerar estos aspectos, esta tesis se centra en desarrollar modelos que permitan integrarlos en la etapa de diseño del controlador.

Con el fin de caracterizar las variaciones intra-paciente en sujetos con T1DM, se realiza una revisión de su origen y la fisiología subyacente relacionada con esta variabilidad, obteniendo un resumen de las variables que afectan los requerimientos diarios de insulina de cada paciente. Además, se analizan los enfoques para modelado/simulación de las variaciones de sensibilidad a la insulina (S_I) y las diferentes maneras en las que se han tenido en cuenta estas variaciones en los modelos orientados a control.

En el marco del control robusto, se obtienen diferentes modelos orientados al control de T1DM incluyendo las variaciones en S_I. Primero, a partir de un modelo lineal de parámetros variantes (LPV) desarrollado previamente, usando técnicas de invalidación, un conjunto de modelos de bajo orden capaz de "cubrir" las variaciones intra-pacientes con límites de incertidumbre dinámica. Este conjunto de modelos es fundamental para el diseño de controladores robustos que garanticen estabilidad y desempeño. En segundo lugar, se incluyen variaciones intra-pacientes durante la etapa de identificación del modelo, lo que permite integrarlas dentro de una estructura LPV de bajo orden adecuada para el diseño de controladores LPV. La eficacia de este nuevo modelo se evalúa de la siguiente forma. Por un lado, se computa el error cuadrático medio (RMSE) entre las desviaciones de glucosa predichas por los modelos LPV con y sin variaciones intra-paciente y el simulador. Por otro lado, se miden las distancias entre ambos modelos y el simulador a través del ν-gap, a fin de determinar las diferencias de desempeño a lazo cerrado. Finalmente, se desarrolla un modelo LPV que permite dar cuenta de los efectos de la hiperglucemia/hiperinsulinemia en la sensibilidad a la insulina y su efectividad se evalúa nuevamente en lazo abierto y lazo cerrado.

Abstract

Research on the development of a closed-loop artificial pancreas for automatically regulating the blood glucose level in Type 1 Diabetes Mellitus (T1DM) patients has intensified in the past years. However, the risk of hyper- and hypoglycemia remains an impediment to adequate glycemic control in some cases. A significant source of limitations originates from model uncertainty, and the extremely high inter- and intra-patient variability that affects the dynamics of glucose regulation. Therefore, considering that tools are required for the design of robust and time-varying control strategies that consider these issues, this thesis focuses on developing control-oriented models that allow considering them in the controller design stage.

In order to characterize intra-patient variations in T1DM, a review of the sources and underlying physiology related to intra- and inter-day variability is made, obtaining a summary of the variables affecting daily insulin requirements. Moreover, modeling/simulation approaches of Insulin Sensitivity S_I variations that have been adapted for T1DM are analyzed. Additionally, the different ways they have been accounted for in control-oriented models are reviewed.

Following a robust control framework, different control-oriented models including variations in S_I are obtained. First, invalidation techniques are applied to a previous linear parameter varying (LPV) model to develop a set of low-order LPV models that "covers" intra-patient variations with dynamic uncertainty bounds. This model set is instrumental for obtaining robust controllers that guarantee stability and performance. Secondly, intra-patient variations are included during the model identification stage to embed them within a low-order LPV model structure that is amenable for LPV controller design. The performance of this new model was evaluated in comparison with the previous LPV model without intra-patient variations in terms of their open- and closed-loop differences with the UVA/Padova model. In open-loop, the analysis is made through the Root Mean Squared Error (RMSE) between the glucose deviation predicted by the models and the UVA/Padova simulator. In closed-loop, the ν-gap metric was used, which measures the distance, in terms of performance, between two models. Finally, an LPV model that allows to account for the effects of hyperglycemia/hyperinsulinemia on insulin sensitivity is developed and evaluated both in open- and closed loop.

Contents

List of Figures

List of Tables

Symbols and Abbreviations

Letters

Symbol	Description
A	System Matrix
B	Input Matrix
C	Output Matrix
D	Input related output matrix
S_I	Insulin Sensitivity
$S_{I,nom}$	nominal insulin sensitivity
$S_{I,VF}$	Insulin Sensitivity Variation Factor
$S_{I,VFs}$	Insulin Sensitivity Variation Factors

Greek Letters

Symbol	Description	Units
α	Coefficients for average gain polynomial fitting	
γ	Uncertainty weight	
λ	Coefficients for pole polynomial fitting	

Abbreviations

AP   Artificial Pancreas

AUC   Area Under the Curve

BG   Blood Glucose

BW   Bandwidth

CBR   Case-Based Reasoning

CGM   Continuous Glucose Monitoring

CGM   Continuous Glucose Monitoring

CHO   Carbohydrate

CR   Carbohydrate Ratio

CSII   Continuous Subcutaneous Insulin Infusion

CVGA   Control Variability Grid Analysis

DCG   DC Gain

DP   Dawn Phenomenon

EGP   Endogenous Glucose Production

FDA   Food and Drug Administration

GEZI   Glucose Effectiveness at zero insulin

GH   Growth Hormone

GT   Glucose Tolerance

HG   Hyperglycemia

HGHI   Hyperglycemic-Hyperinsulinemic

HGO   Hepatic Glucose Output

HI   Hyperinsulinemia

ICR   Insulin-to-Carbohydrate ratio

IIR   Insulin Infusion Rate

IOB   Insulin On Board

IR   Insulin Resistance

LPV   Linear Parameter-Varying

LQG   Linear Quadratic Gaussian

LTI   Linear Time Invariant

MPC   Model Predictive Control

PF   Pareto Front

RMSE   Root Mean Square Error

T1DM   Type 1 Diabetes Mellitus

T1DM   Type 1 Diabetes Mellitus

TDI   Total Daily Insulin

UC   Unfalsified Control

Chapter 1

Introduction

Type 1 Diabetes Mellitus (T1DM) is a chronic disease characterized by the inability to produce insulin due to the destruction of the pancreatic β-cells. Typical treatments require constant patient interaction with glucometers and insulin injections, or in the best scenario, glucose sensors and insulin pumps. This way of treatment is burdensome and subject to human errors that lead to complications and therefore, to an increased health expenditure on their treatment. In consequence, the goal is to develop systems that improve patients quality of life and reduce the extremely demanding self-management plan and lifestyles they follow. In this regard, the Artificial Pancreas (AP) a long-awaited alternative for T1DM management and its development was triggered by recent developments of Continuous Glucose Monitoring (CGM) and complex simulation models. The AP is a control engineering problem that is challenged by the significant delays in insulin absorption, variability in system dynamics between patients and within the same patient, meals, exercise, and sensor/pump errors. Controller design for AP needs to focus on the balance between system complexity, clinical benefits, and patient convenience. In this regard, mathematical modeling and computer simulations allow optimization of controller designs before their clinical testing.

Considering that large intra-subject variability represents a big challenge for both modeling and control tasks, this thesis focuses on developing a mathematical model that reflects this time-varying and nonlinear dynamic behavior, while maintaining a simple structure that allows reliable and robust control synthesis techniques to be used, and produce a controller that can be implemented in real-time. In this Chapter, a brief overview of the motivation and results of this thesis are presented. In Section 1.1 the current advances and challenges for the development of the AP control system are discussed. Objectives and main accomplishments of this work, along with dissemination of partial results are gathered in Sections 1.2 and 1.3, respectively. Finally, Section 1.4 maps out the thesis outline.
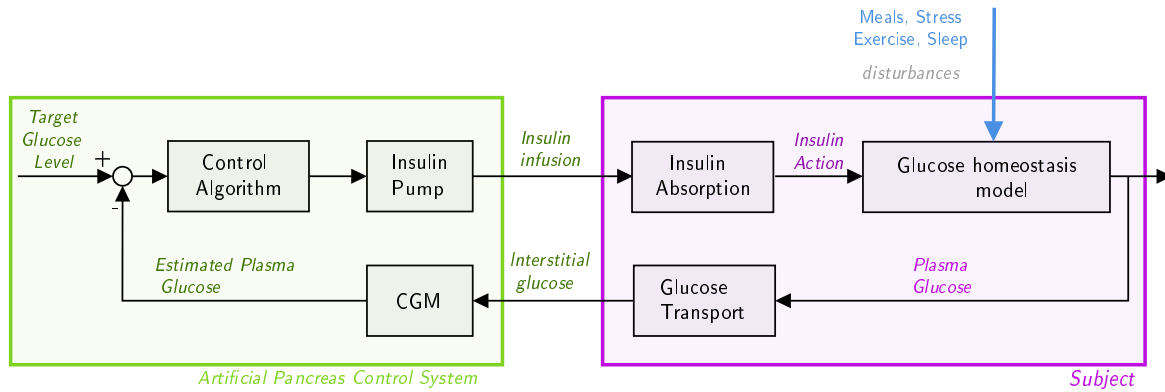
Figure 1.1: Block diagram for the closed-loop glucose regulation (Artificial pancreas).

1.1   Motivation

T1DM patients require intensive insulin therapy to control their glycemia and avoid the hazardous complications that may arise [1, 2]. According to the conventional therapy, they should monitor their glucose concentration levels and administer insulin injections every day for the rest of their lives, which makes T1DM a burdensome disease for both the patients and their families. Usually, patients not only have to adjust a basal insulin delivery to stabilize his/her glucose levels during fasting periods, but also need to count the Carbohydrate (CHO) content of every meal before eating in order to determine how much insulin to infuse to counteract its effect. Unfortunately, in real life this calculation is far from accurate and therefore, patients are continuously exposed to hyper- and hypoglycemic events originated from under- and overestimating the ingested carbohydrates. Moreover, hyper- and hypoglycemic risks increase due to many other situations related to every-day life, like mood, sleep cycle or physical activity, which have an impact over the glycemic levels of the patient, and therefore, in his/her quality of life [3].

The AP was conceived to automate the information collection, decision making, and insulin management of a person with T1DM to maintain euglycemia, despite various daily disturbances. In this way, an AP has three essential elements: sensors, insulin pumps, and a decision-making algorithm (controller) to close the loop. A representation of the AP and its role in glucose regulation is presented in Figure 1.1.

Initially, the intravenous route was considered for both insulin infusion and glucose monitoring. Afterwards, alternative routes were analyzed, but the most significant breakthrough was in the 1990s with the appearance of the CGM [4, 5], which allowed the transition from having just a few measurements to obtaining them every five minutes through a minimally invasive procedure. The main disadvantage of these sensors is the delay between the interstitial glucose measurements and the plasma glucose levels.

Contrary to the pancreas, an AP cannot have direct portal circulation for insulin infusion. The first Continuous Subcutaneous Insulin Infusion (CSII) pump appeared around 1978 [6]. Implantable insulin pumps that infuse insulin into the peritoneum represent a more suitable alter-

native from the physiological point of view, but their invasiveness limits their application [7]. In turn, subcutaneous pumps, being less expensive and invasive, are the ones considered feasible [7]. However, this subcutaneous infusion represents another source of delay since the insulin molecule has to be absorbed through the capillary wall in order to have effective action. Finally, the control algorithm is in charge of calculating the adequate amount of insulin to be infused by the CSII according to the CGM readings, and this decision is usually based on a mathematical model that describes the glucose-insulin dynamics.

In order to automate the decision of how much insulin to infuse, several control algorithms have been tested in clinical trials, e.g., Model Predictive Control (MPC), Proportional-Integral-Derivative (PID) control, switched Linear Quadratic Gaussian (LQG) or fuzzy logic controllers [8–20]; and *in-silico*, e.g., $\mathcal{H}_\infty$ control, Linear Parameter-Varying (LPV) and switched LPV [21–29], or adaptive control [30–32]. A recent state-of-the-art of the current activities and developments in this area can be found in [33]. Despite vast improvements in glycemic control achieved with the AP, there is still no efficient and safe system able to normalize glucose levels in T1DM patients regardless of the numerous disturbances that affect the system [7, 34]. Besides sensor/actuator failure, the major challenges for closed-loop control include:

1. The delay associated with the CGM measurements and the actual plasma glucose levels introduced by the subcutaneous route. This delay is attributed to physiology (glucose transport) and technology factors (numerical filtering), and is around 10-15 minutes [7]. Additionally, CGM devices usually need to be periodically calibrated, and even body movement and sensor location can affect the resulting measurement [34], compromising their reliability. Such lags and differences between sensor and blood glucose measurements have a detrimental effect on controller performance [35, 36]. This challenge can be overcomed with the development of more accurate and reliable sensors [35, 37], like the Dexcom G6 (Dexcom, San Diego, CA) and Freestyle libre II (Abbot, Chicago, IL) sensors which do not require calibration and the measurement delay is significantly reduced.

2. Like subcutaneous measurements, there is a significant delay associated with the insulin infused at a subcutaneous level. Such delay is originated from the slow absorption dynamics that even "rapid-acting" insulin analogues (insulin aspart, lispro or glulisine) exhibit, and from the delayed insulin action, i.e., the time for the peak glucose-lowering effect [7, 38]. Overall, the total lag time from insulin infusion to insulin action is around 80-120 minutes, and it remains active in the organism for several hours [7, 39–41]. Although the absorption times have been reduced with insulin analogues like FIASP (Novo Nordisk, Denmark), the insulin duration time remains similar to other insulin analogues.

   Slow insulin absorption combined with its prolonged action, leads to what is known as insulin "stacking". When the controller continues to infuse insulin in response to increasing glucose concentrations, an over-accumulation of insulin occurs and might lead to controller-induced hypoglycemia [7, 38]. Therefore, considering that for single-hormone controllers, insulin's effect cannot be counteracted by the controller, closed-loop controllers have to ac-

count for the slow insulin absorption to avoid insulin overdosing. Moreover, insulin "stacking", accompanied by prolonged glucose appearance, may lead to Hyperinsulinemia (HI), a condition that leads to impaired Insulin Sensitivity (S_I) [42–46].

In order to address this challenge, several control algorithms include modifications over the insulin delivery according to a real-time estimate of plasma insulin concentration, or Insulin On Board (IOB) [17, 47, 48].

3. The response to the same insulin dose varies from patient to patient, which is referred to as inter-patient variability. Different dynamics reflect different biological characteristics of each subject, and in this case, are mostly related to differences in insulin sensitivity, requirements and absorption/action times [18, 35]. These variations are larger than in healthy individuals [49] and preclude the possibility of obtaining a unique control algorithm that works for everyone. In consequence most recent research efforts are focused on model personalization [18, 19, 21, 50–57]. Some approaches use patient-specific clinical variables like Total Daily Insulin (TDI), Carbohydrate Ratio (CR) or body weight to individualize the Linear Time Invariant (LTI) or LPV model's gain [21, 50]. Other strategies involve MPC algorithms that are individualized by using patient-specific model parameters or personalizing the MPC cost function weights [7, 58]. Adaptive algorithms (like run-to-run control) that adjust and individualize controller parameters have also been proposed.

4. Insulin needs also exhibit day-to-day variations within the same patient (intra-patient variability), which often presents in ultradian (less than 24-hour periods), circadian (24-hour periods) or circannual (365-day periods) rhythms [59]. In T1DM, insulin requirements to control glycemia vary across the daytime [60], attributed to circadian changes in Glucose Tolerance (GT), i.e., the relative amount of glucose taken up by peripheral tissue [61], and S_I [62], which corresponds to the ability of insulin to stimulate glucose utilization and inhibit glucose production [63]. Many factors like meals, exercise, sleep architecture, stress, and rhythms of counterregulatory hormones also influence this variability [52, 59, 64, 65], but the underlying mechanisms are not fully understood [66]. A better understanding of how these factors are involved in S_I variations is crucial to developing models to improve glucose control, minimizing glucose variability and thus, reduce possible complications [49]. In this regard, several approaches to tackle intra-patients variations in closed-loop control have been explored, like adaptive predictive controllers or adaptive PID controllers. These strategies include real-time estimation of S_I to adjust controller coefficients according to the estimated S_I, both in single-hormone [30, 31, 67] and dual-hormone controllers [68, 69]. However, developing models and algorithms to overcome this variability remains an active research area.

5. Large disturbances affect the dynamics of the system that have a significant effect on glucose concentration, like meals, physical exercise or stress. Usually, meals are tackled by a feedforward action, where the patient announces meal time and CHO content of the meal, and matching insulin boluses are infused according to his/her CR. Although the injection of an open-loop bolus based on the CHO intake facilitates the reduction of postprandial

glucose values [70], CHO counting is prone to errors and burdensome for the patients [71]. Moreover, meal composition, rather than CHO contents alone, also influences insulin requirements. For example, high-fat meals require more insulin than a meal with low-fat content, even when having the same CHO ammount [7]. Meal-related insulin requirements are also different in days when the subject has been physically active compared to resting ones, and these factors are not considered by solely counting CHOs. Therefore, several alternatives for eliminating the CHO counting have been tested, relying on CGM measurements to control post-prandial glucose levels. However, this approach generally leads to prolonged hyperglycemia due to the significant insulin absorption delays compared to meal absorption [7, 41]. Recently, unannounced meals have been tackled by informing the controller that a meal is happening but providing partial information (meal size classification) that may deliver a partial bolus [72–75] or trigger the switching between two different controllers together with an adjustment of limits on insulin infusion [17].

Exercise represents another important source of variations in glucose concentrations, having significant impacts over insulin sensitivity [41]. These variations are, in turn, influenced by many factors related to the exercise itself (type, intensity, duration) and the subject's glycemic control (starting blood glucose, last insulin bolus, and insulin injection site). Moreover, the sudden exercise-induced glucose variations are challenging for CGM devices to detect, due to lag in measurement readings. Several approaches for managing exercise during closed-loop control, like basal insulin suspension, CHO ingestion prior to exercise and feedforward action by making an announcement 20 minutes before exercise starts, have been proposed. However, hypoglycemia remains a challenge, and other approaches like adding heart-rate or activity sensors, or feedforward control in bi-hormonal systems appear as promising alternatives. Ultimately, the goal is to achieve automated meal and exercise recognition and control that achieves glucose regulation despite meal and exercise challenges [38, 41].

6. Another source of limitations is model uncertainty. In addition of intra-patient variability, uncertainty also appears in key physiological processes as meal absorption, subcutaneous insulin absorption, and subcutaneous measurement delays [35, 66]. For realistic variations in the model parameters of the actuator, plant (subject) and sensor, the achievable closed-loop bandwidth is severely restricted [34, 35]. These limitations impose a limit on the feasible response time and hence, on the achievable controller performance. Unfortunately, such limitations are unavoidable and independent of the control algorithm, being inherent of the system (patient) itself [34]. Therefore, the control algorithm must be designed with robustness properties that guarantee that the system will be stable and meet performance requirements under worst-case scenarios of model uncertainty and ultimately make closed-loop control reliable and safe [18, 19, 35, 65]. In this regard, several robust control strategies have been explored [26, 27, 76, 77], with encouraging results for robust control tools in the glucose regulation problem.

Besides advances in hardware improvement, progress in computational models of the insulin-

glucose dynamics has played a fundamental role in the acceleration in AP systems development. Numerous mathematical models of glucose regulation have been proposed and are used for three main purposes: *(i)* to support physiology studies [78, 79], *(ii)* to be used in controller design (control-oriented models) [31, 50, 57, 69, 80] and *(iii)* simulation and *in-silico* testing of controllers [81–85].

The primary goal of T1DM simulation models is to provide a blood glucose prediction as close as possible to a real situation. However, given their mathematical complexity, they are usually simplified for controller synthesis. Moreover, using complex models for synthesis does not necessarily guarantee better closed-loop performance [86] nor reduce the inter- and intramodel variability which arises due to other factors [34]. Therefore, control-oriented models have to represent the underlying dynamics, but with a simple mathematical formulation that facilitates the controller design.

Considering the uncertain, time-varying characteristics of the glucose-insulin dynamics, adaptive MPC or robust control emerge as suitable and promising control strategies for AP applications. In the first approach, the prediction model's parameters are constantly updated using controller performance criteria (run-to-run control) or real-time identification by least squares minimization of the prediction error. Based on simulation models, in the second approach, *(i)* LTI or LPV models with dynamic uncertainty bounds (model-set) [27, 86] and *(ii)* LPV models have been obtained [57, 87] and used for designing $\mathcal{H}_\infty$ LTI control [25–29], switched LQG [17], LPV and switched LPV [21–24] and Unfalsified Control (UC) [88] strategies.

These LPV strategies are able to capture the non-linear dynamics while maintaining a simple model structure for its real-time implementation with guaranteed stability and performance properties of the controller, contrary to adaptive identification strategies that may lead to unstable models [31]. It is worth remarking that, among these strategies, the reliability and representation capabilities of the prediction model are directly correlated with the efficiency and achievable performance, since the model dynamics are inherited by the controller.

1.2   Objectives

Considering the advantages of LPV controllers, the main objective of this thesis is to develop control-oriented models for the glucose-insulin dynamics that include intra-patient variations related to insulin sensitivity, while maintaining a low order structure for allowing its use in robust controller design. In particular, the following objectives are pursued:

- **State of the art:** Review of physiological phenomena underlying intra-patient variations, in order to understand underlying mechanisms and determine modeling and simulation strategies that have been adopted for these variations.

- **Control-oriented models:** Review of control-oriented models, analyzing the different ways

in which inter- and intra-patient variations are included, and the advantages or disadvantages of each approach.

- **Models with intra-patient variations:** Development of models with intra-patient variations suitable for designing $\mathcal{H}_\infty$ or LPV controllers, analyzing their representation capabilities and benefits for controller design.

1.3 Major findings and dissemination of results

As a result of the realization of this thesis, the following aspects are highlighted:

1. Participation in the first AP clinical trial without pre-meal insulin boluses in Latin America. In this trial, the ARG algorithm [17] was validated in a pilot study on five T1DM, where it was able to safely regulate the glucose level, minimizing risks of hypo- and hyperglycemia. The following publications derived from this experience:

   > R. Sánchez-Peña, P. Colmegna, F. Garelli, H. De Battista, D. García-Violini, **M. Moscoso-Vásquez**, N. Rosales, E. Fushimi, E. Campos-Náñez, M. Breton, *et al.*, "Artificial pancreas: Clinical study in latin america without premeal insulin boluses," *Journal of diabetes science and technology*, vol. 12, no. 5, pp. 914–925, 2018

   > P. Colmegna, F. Garelli, E. Fushimi, **M. Moscoso-Vásquez**, N. Rosales, D. García-Violini, H. D. Battista, and R. Sánchez-Peña, "Artificial pancreas: The argentine experience," *Science Reviews*, vol. 1, no. 1, 2019

2. A review of the underlying physiological mechanisms of intra-patient variations was made, that allowed to narrow down their primary source to insulin sensitivity variations. Moreover, modeling/simulation approaches of S_I variations that have been adapted for T1DM were analyzed, finding that most approaches are for controller testing rather than synthesis. From this work, the following congress publication was made:

   > **M. Moscoso-Vásquez**, P. Colmegna, and R. Sánchez-Peña, "Intra-patient dynamic variations in type 1 diabetes: A review," in *2016 IEEE Conference on Control Applications (CCA)*, pp. 416–421, Sept 2016

3. An LPV model set, instrumental in robust controller design was obtained through (in)-validation techniques, considering parametric uncertainties in insulin sensitivity. The advantages of this model set were exploited by designing a switched-LPV controller, that proved useful in presence of dynamic and parametric uncertainties, compared to a nominal LPV model. This result conducted to the following publication:

F. Bianchi, **M. Moscoso-Vásquez**, P. Colmegna, and R. Sánchez-Peña, "Invalidation and low-order model set for artificial pancreas robust control design," *Journal of Process Control*, 2019. https://doi.org/10.1016/j.jprocont.2019.02.004

4. The development of an average LPV structure that allows to include both inter- and intra-patient variations with a control-oriented focus using patient's clinical data in a non-invasive way. Additionally, the structure has the flexibility to be used together with a real-time insulin sensitivity estimator. Related to this result, the following paper has been submitted for publication:

   M. Moscoso-Vásquez, P. Colmegna, and R. Sánchez-Peña, "Control-oriented model with intra-patient variations for glucose regulation in type 1 diabetes." Submitted to Biomedical Signal Processing and Control, February 4th 2019

5. A preliminary model for including the effects of insulin on board in the reduced insulin sensitivity characteristic of hyperglycemic/hiper-insulinemic conditions. The model maintains the low-order structure amenable for control structure design. The following congress publication is under elaboration:

   M. Moscoso-Vásquez, P. Colmegna, and R. Sánchez-Peña, "Model of Hyperglycemia-Hyperinsulinemia effects for the Artificial Pancreas control," Oct 2019. *submitted to 2019 IEEE Colombian Conference Automatic Control (CCAC)*

1.4   Thesis outline

This thesis is organized as follows:

Chapter 2 presents the review of physiological phenomena underlying intra-patient variations, and the modeling and simulation strategies that have been adopted in the literature.

In Chapter 3 a review of control-oriented models is made, analyzing the personalization strategies and ways to include intra-patient variations. The personalized LPV model in [57] is selected as a base model for the development of models with S_I variations, and therefore, it is formally presented in this chapter. Moreover, model invalidation techniques are described, as a way to consider the inherent uncertainties of glucose-regulation in a control-oriented model.

Invalidation of the LPV model is carried out in Chapter 4, obtaining a model-set suitable for robust controller synthesis purposes. Based on this model-set, a switched LPV controller is designed and tested *in-silico* in the distribution version of the UVA/Padova simulator, demonstrating the advantages of this approach under different sources of uncertainty.

In order to consider intra-patient variations within the model's structure, in Chapter 5 an LPV model including a parameter related to insulin sensitivity variations is developed. The model tested both for simulation and control design purposes against the UVA/Padova simulator and the LPV model of [57].

Insulin stacking effects on S_I are considered in Chapter 6, where a preliminary model for describing the effects of hyperglycemia-hyperinsulinemia on insulin sensitivity is presented. The LPV model [57] is expanded by including a parameter dependent on the IOB. This model is tested in open-loop to test its representation capabilities.

Finally, conclusions and future work are discussed in Chapter 7.

Chapter 2

Intra-Patient Variations in Type 1 Diabetes

Circadian variations in glucose regulation have been demonstrated in both healthy and subjects with diabetes. This variability leads to large intra- and inter-patient uncertainty that can be a limiting factor to the performance of open- and closed-loop insulin therapies [62, 94]. Therefore, a better understanding of how these factors are involved in glucose homeostasis is crucial to develop physiological models that help improve glucose control, minimize glucose variability, and reduce morbidity and complications subjects with diabetes.

In this Chapter, a review of the physiological explanation underlying intra-patient variability is analyzed. To this end, the main factors that influence these phenomena in T1DM subjects are determined in Section 2.1. Then, in Section 2.2, a review of the current strategies that account for intra-patient variations in T1DM glycemic control is made, analyzing their advantages and limitations. Additionally, some suggestions for addressing the modeling of intra-patient variations are presented.

2.1 Diurnal Variations in Insulin Requirements

Insulin dose requirements are influenced by many factors, including weight, food uptake, sleep and wakefulness, sleep deprivation, stress, exercise and temperature changes [30, 52, 62]. Because some of these factors oscillate with pulsatile ultradian, circadian and circannual frequencies, it is desirable to include them when designing glucose controllers [95].

A study of fasting Blood Glucose (BG) response to insulin doses at different times of day performed in healthy adults [96], found that the hypoglycemic response to insulin is markedly more pronounced in the morning, compared to the afternoon (see Figure 2.1). This suggests that both GT and S_I are higher in the morning and decline as the day progresses, implying they experience a circadian variation [62]. For example, in [60], it is detected that in insulin- and non-insulin-dependent subjects with diabetes, there is a morning to evening improvement in GT.

Variations in GT lead to fluctuations in insulin requirements as illustrated in Figure 2.2, where low insulin requirements are observed during sleep, and peaks appear after meals. In this regard,
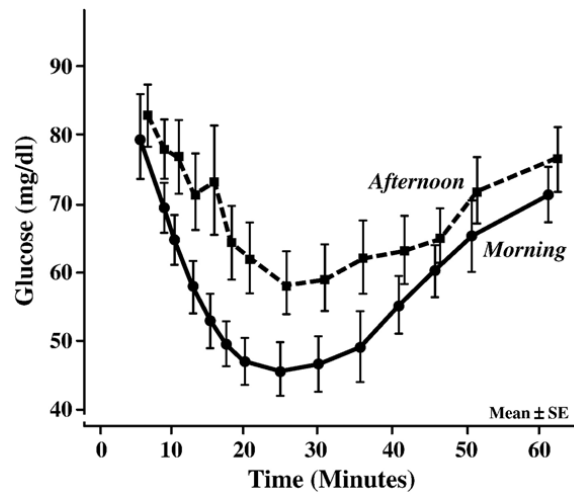
Figure 2.1: BG response to an intravenous injection of insulin ($0.05U/kg$) at different times of
day. From [62].

insulin needs are higher after breakfast, compared to other meals. This is known as the Dawn
Phenomenon (DP) [60, 62, 94, 97] and describes a state of hyperglycemia in the early morning
hours, when the increased insulin requirements are not met [60]. The magnitude of the DP varies
considerably among subjects [94], but it is highly reproducible within the same subject if factors
that influence insulin action remain constant [98]. Furthermore, this phenomenon is not specific
to subjects with diabetes, but rather a physiological event related to a circadian variation of S_I.
In T1DM, DP is also attributed to other variables, like duration of diabetes, quality of precedent
glycemic control, and state of the counter-regulation system to hypoglycemia [60, 94, 98].
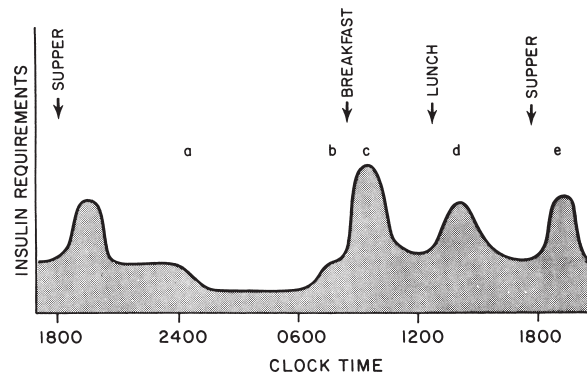
Figure 2.2: Schema of daily insulin requirements. From [94].

In order to explain the causes of the DP, multiple mechanisms that differ from the idea of a cir-
cadian variation of S_I, have been explored. One considers that insulin availability may decrease dur-
ing the second part of the night because of waning of insulin injected subcutaneously the evening
before or, when an insulin pump is used, due to degradation of the infused insulin [60]. However,
previous studies linked these variations to differences in Growth Hormone (GH) secretion [60, 98].
On a different view, Blackard et al. [94] have detected that the higher insulin requirement for
breakfast is connected with decreased insulin needs for subsequent meals, because of a prolonged
insulin action remnant from previous insulin boluses. Moreover, the higher insulin requirement is

attributed to an expected increase in glucose production during awakening compared to sleep [94].

However, most authors agree with the aforementioned hypothesis that relates DP to the circadian variation of S_I. Thus, they consider that reduced S_I during the morning may result in increased glucose production and/or impaired glucose utilization during the latter part of the night [60, 98, 99]. Also, because S_I reflects the insulin ability to stimulate glucose utilization [100], changes in S_I produce variations in metabolic activity that affect the Hepatic Glucose Output (HGO) level, and therefore, the insulin requirements [61].

In this regard, the diurnal variation of S_I was evidenced based on clinical information of 20 subjects with diabetes [49]. Based on triple-tracer tests, differences in postprandial insulin action for breakfast, lunch, and dinner were found, and for each meal, S_I was estimated with the oral minimal model [101]. Results for each subject, are presented in Figure 2.3, showing that every patient exhibits his/her own specific pattern over the day. These variations are around $\pm 40 - 60\%$ the average value observed for each patient. However, there was no significant difference in the average S_I for each meal, which shows that there is no uniformly diurnal pattern of postprandial S_I that could be generalized to the T1DM population as a whole.
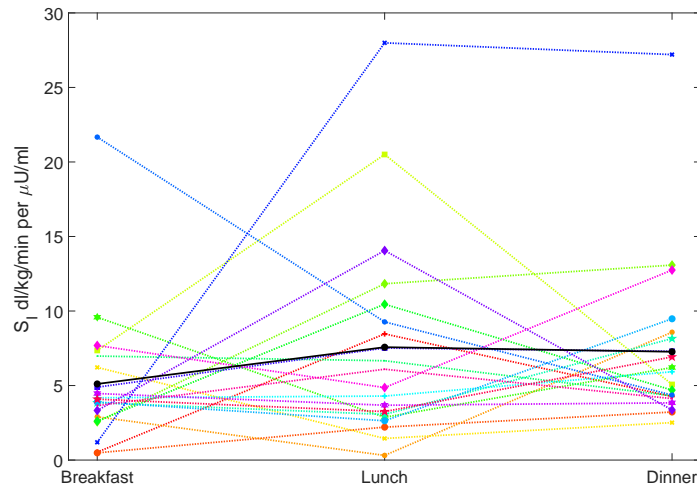
Figure 2.3: Model-based S_I for different subjects (colored dotted lines) and average estimate (black solid line) for meals at different times of day. Adapted from [49].

As mentioned before, hormonal cycles also impose an effect on glucose metabolism. Particularly, rhythmicity of counter-regulatory hormones (GH, cortisol, glucagon, catecholamines), which increase during the early morning hours, modifies tissue S_I [62]. Thus, impaired secretion of counter-regulatory hormones relates to the magnitude of the DP [98]. Evidence indicates that early nocturnal GH pulses play a more significant role in the development of the DP than other hormones [60, 62, 99, 102]. However, the precise mechanism by which GH contributes to the DP remains unclear. Its contribution to this phenomenon is related to the effects of GH on glucose metabolism, insulin clearance, and lipolysis regulation elevating free fatty acids level, which compete for glucose utilization and stimulate gluconeogenesis [60].

The quality of current BG control is another important factor that affects the magnitude of

the DP. It has been found that poor glycemic control is associated with the enlarged manifestation of the DP and *vice versa* [98]. In this regard, conversion from conventional to intensive insulin therapies can produce a significant reduction in both frequency and magnitude of the early-morning rise in BG [60].

Determination of appropriate basal insulin levels is an essential component of insulin therapy. Basal insulin requirements typically vary throughout the day and night based on endogenous glucose output and peripheral S_I [99]. Analysis of basal patterns obtained in fasting tests on 322 T1DM subjects undergoing pump therapy, revealed differences between juvenile (under 20 years old) and adult (over 20 years old) basal insulin patterns as shown in Figure 2.4. Because no significant differences were found between men and women, the magnitude and pattern of insulin requirements might reflect timing and magnitude of cortisol and GH secretion within each age category [99].
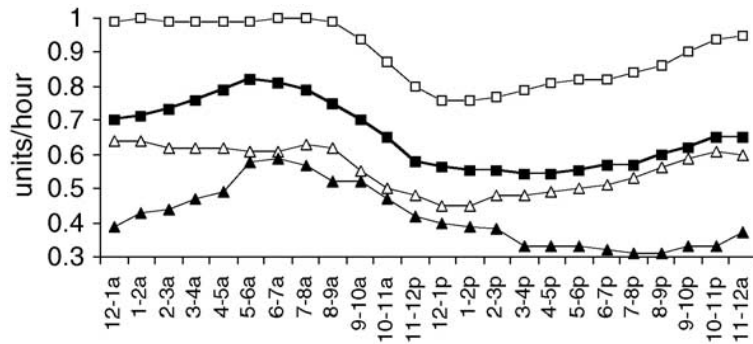
Figure 2.4: Average basal rates by age group. Open triangles: Age 3-10. Open square: Age 11-20. Solid square: Age 20-60. Solid triangles: Age >60. From [99].

Either GT or S_I circadian rhythms can thus explain the DP. However, GT variations are regulated by S_I, which stimulates glucose disposal [61, 103]. Therefore, intra-patient variability can be modeled by a suitable description of S_I circadian variation. Such description should include time of day, physical activity, stress, and sleep structure. The following section focuses on reviewing current approaches for including S_I into available T1DM models.

2.2   Modeling/Simulation Of Intra-Patient Variability

Intra-patient variation of S_I has been accounted for in different ways [47, 52, 85, 95, 103–106]. Although exact values of model parameters are unknown, they can be bounded by intervals that characterize the observed variability [59]. In that regard, parametric uncertainties in IS and insulin absorption models can be included in well-known simulation models, like the Cambridge [105], and UVA/Padova [107] models, in earlier versions that lacked intra-patient variations in their formulations [108].

Another approach is to consider that some model parameters are time-varying. For example, in [47], sinusoidal variations of 20% amplitude and 19- and 29-hour periods for S_I and insulin absorption, respectively, are included in the UVA/Padova model. In [104], the parameters V_{mx} (parameter related to insulin-dependent glucose utilization) and k_{p_3} (parameter governing amplitude of insulin action in the liver) of the same model were modified as follows:

$$\rho(t) = \rho_0 + \rho_0 * k_\rho(t) \sin\left(\frac{2\pi}{24 \cdot 60}t + 2\pi R_{nd}\right) \tag{2.1}$$

where $\rho(t)$ represents the time-varying parameter (V_{mx} or k_{p_3}), ρ_0 is the default value in the simulator, R_{nd} is a randomly uniformly generated number from the interval $[0, 1]$, and $k_\rho(t)$ is a time-varying parameter defined as:

$$k_\rho(t) = \begin{cases} 0.7 & \rho(t) \leq \rho_0 \\ 0.3 & \text{otherwise.} \end{cases} \tag{2.2}$$

As mentioned before, the Cambridge model can also be used to describe the intra-patient variability. In that regard, in [105], multivariate log normal distributions obtained from clinical data, are considered to define S_I-related parameters of the Cambridge model. In [85], time-varying parameters are included in that model, where the S_I variation is represented by superimposing sinusoidal oscillations of 5% amplitude and 3-hour period on the nominal values of selected model parameters. Moreover, each one of those parameters has a different phase generated randomly from a uniform distribution $U[0, 3h]$.

Diurnal variations of S_I have been recently implemented into the UVA/Padova T1DM simulator [83, 109] by linking each *in-silico* subject to a time-varying S_I profile [106]. These profiles were obtained based on the results in [49] (see Figure 2.3). The S_I of each subject, estimated with the oral minimal model [101] for breakfast, lunch, and dinner, was classified as *high (h)* or *low (l)*, according to a fixed threshold, and the resulting trend (pattern) between meals was observed. In Table 2.1, the S_I profile and the estimated probability of each of the seven identified S_I patterns are presented. These patterns are transformed into the corresponding time-varying profile by an almost stepwise-line signal that varies three times a day (at 4 a.m., 11 a.m., and 5 p.m.), where the 40% of the nominal value in the simulator is assigned to the *low* values, and a 100% to the high ones. Deviations from these profiles are allowed, modulating the nominal pattern by multiplicative random noise. As an example, the procedure for the class-5 profile is illustrated in Figure 2.5. Finally, each *in-silico* subject is randomly assigned to one of the seven classes, according to the estimated probability of each class.

In [110], intra-patient variations are considered not for modeling, but for closed-loop glycemic control purposes, using a Case-Based Reasoning (CBR) approach. CBR is an artificial intelligence technique, widely applied in medicine, that tries to solve new problems by applying solutions previously learned [110, 111]. The patient's current situation is recognized based on the time of

Table 2.1: S_I pattern classes included in the UVA/Padova T1DM simulator. B, breakfast; D, dinner; L, lunch.

Class	S_I pattern	S_I profile	Probability
1	*l-l-l* or *h-h-h*		0.1
2	*h-h-l*		0.05
3	*h-l-h*		0.05
4	*h-l-l*		0.1
5	*l-h-h*		0.2
6	*l-h-l*		0.2
7	*l-l-h*		0.3

day, BG, meal intake, external disturbances, and IOB. Then, the following steps take place: *(i)* Retrieve the most similar situation (case) from a base case, *(ii)* reuse the information on that case to solve the problem, i.e., determining the S_I and Insulin-to-Carbohydrate ratio (ICR), *(iii)* revise the proposed solution based on the outcome, and *(iv)* retain parts of the experience that are likely to be useful in the future. In this way, intra-patient variability and external perturbations are considered, granting robustness against uncertain inputs [110]. The basal insulin I_b and insulin
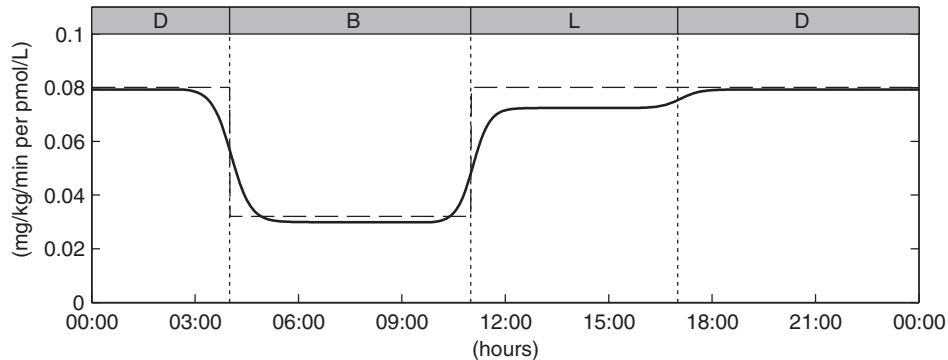
Figure 2.5: Nominal (dashed line) and time-varying (continuous line) S_I profiles for a virtual class-5 subject. B: breakfast; L: Lunch; D: Dinner. From [106].

bolus I_B are corrected to the actual delivery, I_b^d and I_B^d, respectively, according to:

$$I_B^d = I_B K_D \tag{2.3}$$

$$I_b^d = I_b K_D K_A \tag{2.4}$$

with K_A a gain to simulate circadian variability, which randomly takes a value from the interval $[0.8, 1.2]$ every day, and

$$K_D = \begin{cases} 0.7 & t \in [0 - 4] \text{ h} \\ 1 & t \in [4 - 10] \text{ h} \\ 1.5 & t \in [10 - 18] \text{ h} \\ 2.5 & t \in [18 - 24] \text{ h.} \end{cases} \tag{2.5}$$

In [30], a similar approach is applied to modify the plasma insulin concentration $IOB(t)$ from the model proposed in [105]. There, circadian changes in S_I are modeled by introducing a modulating gain that affects the sensitivities of each insulin action mechanism, k_{b1}, k_{b2}, and k_{b3}, equally. This is performed by replacing $IOB(t)$ with the following variable $IOB'(t)$:

$$IOB'(t) = k_m(t) IOB(t) \tag{2.6}$$

where the modulating gain $k_m(t)$ is given, in the Laplace domain, by:

$$k_m = \frac{e^{-\tau\delta s}}{(15s + 1)(s + 1)} k_p(s) \tag{2.7}$$

with the input $k_p(t)$ a step profile corresponding to the desired gain for each segment of the day, as defined in (2.5). The dynamics are set according to expected behavior [30], and the delay introduced in the input $\tau\delta$, is relative to when the segment of the day changes, considering that the change in sensitivity is known to start earlier. This parameter is optimized such that the desired infusion profile maintains the BG concentration as close to normal conditions as possible [30].

In [52], an S_I variation function is defined based on clinical studies on the DP. There, the evening S_I is defined as the nominal value, and Insulin Sensitivity Variation Factors ($S_{I,VFs}$) are defined for several other times of the day. Then, those values are interpolated to obtain a polynomial description of the time-varying nature associated with the S_I (see Figure 2.6). The profile obtained through this procedure considers mean population values that agree with the mean values found in [106], and its daily evolution coincides with the class-5 S_I pattern previously defined (see Figure 2.5).

Several indexes for estimating S_I have been developed, based on hyperinsulinemic-euglycemic clamps [112], intravenous glucose tolerance test [101] and meal and oral glucose tolerance test
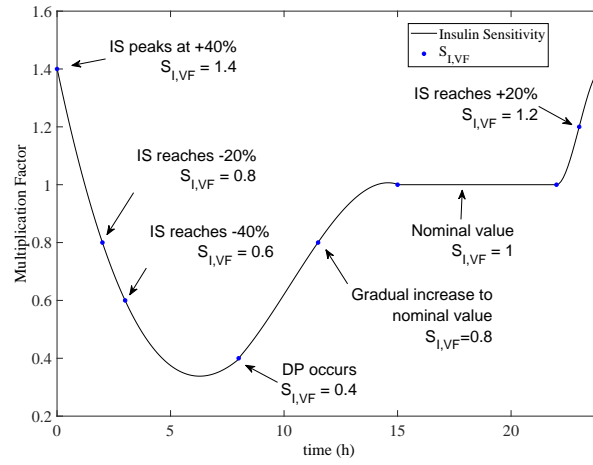
Figure 2.6: S_I variation curve. Adapted from [52].
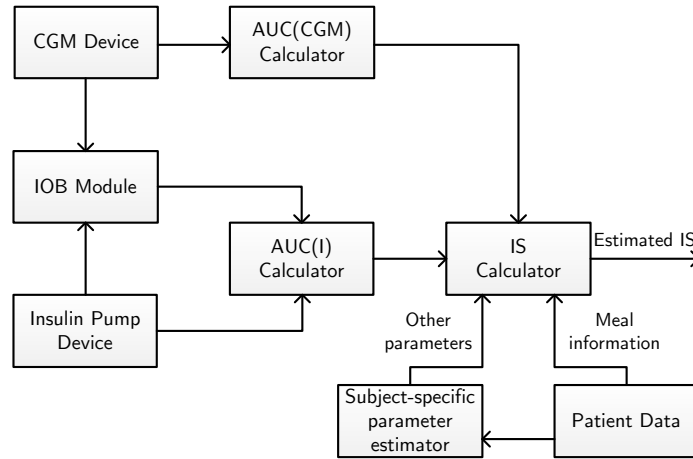
Figure 2.7: Schematic diagram for the calculation of the Pump–CGM S_I Index. Adapted from [63].

based on the minimal model [113, 114]. However, they require plasma glucose and insulin concentrations, and therefore their application in everyday life is not feasible. In this regard, a method to determine a patient's S_I index based only on CGM and insulin pump data is presented in [63, 103]. The procedure, which is depicted in Figure 2.7, implies a minimally invasive technique for estimating S_I. The Area Under the Curve (AUC) of the CGM data and the estimated IOB is calculated. These magnitudes, together with patient physical parameters and meal information are used to compute the patient's S_I index via a simple algebraic operation [63, 103]. This index has also been used to assess inter-day variability in 20 subject's with AP under free living conditions, obtaining a Markov chain model of each subjects' day-to-day S_I variations [115].

Considering that from a mathematical perspective intra-patient variations represent uncertainty in model parameters, in [59, 95] these variations are described through the representation of parameter values as intervals when simulating a model. These simulations produce an envelope (see Figure 2.8) that represents all the possible glucose excursions that might be experienced by

the patient, or "interval models". Such envelopes are found through modal interval analysis, considering the lower and upper bounds for uncertainties in food intake and patient's S_I [95]. Worst-case bound envelopes allow a safer prediction of possible hyper- and hypoglycemia episodes [95]. Limits on the adjustable parameters can be established for a model in two ways: *(i)* taking into account that the limits are not widely divergent for the initial parameter value [95], or *(ii)* through an identification procedure with BG measurements or CGM data in order to obtain an interval model [116]. Bounding all glucose measurements using an interval model with time-varying parameters considered as intervals, can help to increase the robustness of the derived therapies or control algorithms [116].
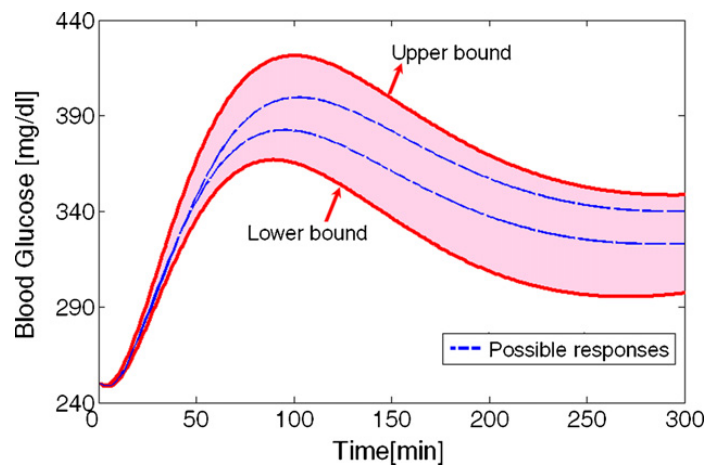
Figure 2.8: Output of an interval dynamic model: All possible system responses (shaded area) are limited by upper and lower bounds. From [95].
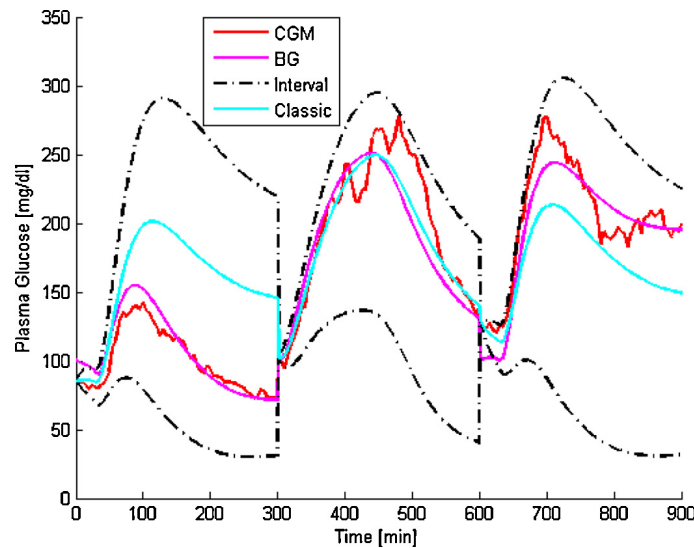
Figure 2.9: Comparison of classic and interval identification using CGM data. Three 5 hour postprandial periods in consecutive days are shown. From [116].

Interval models can be obtained through multi-objective optimization of both fitting error and interval width. This optimization leads to a family of solutions, Pareto Front (PF), in which an element cannot be replaced for improving an objective without worsening another.

The PF represents all the possible solutions from a zero-width/non-zero error problem (classic identification) to a minimum-width/zero error problem (interval approach). A comparison of both identification approaches is presented in Figure 2.9. Here, it is worth noting that models identified using CGM data have wider intervals that the ones from reference BG measurements. Such difference implies an overestimation of actual intra-patient variability since it is confounded by CGM measurement error [116]. However, given that practically neither the optimal width nor the possibility of overlapping several BG postprandial periods are available, correlations can be found between the CGM-based and the BG-based width, and thus, the optimal CGM-based width can be found through such regressions. Variation throughout a 15-day simulation of the S_I-related parameters S_{IT}, S_{ID}, S_{IE}, k_e and pump error (random time-varying error for the insulin infusion rate) is shown in Figure 2.6.
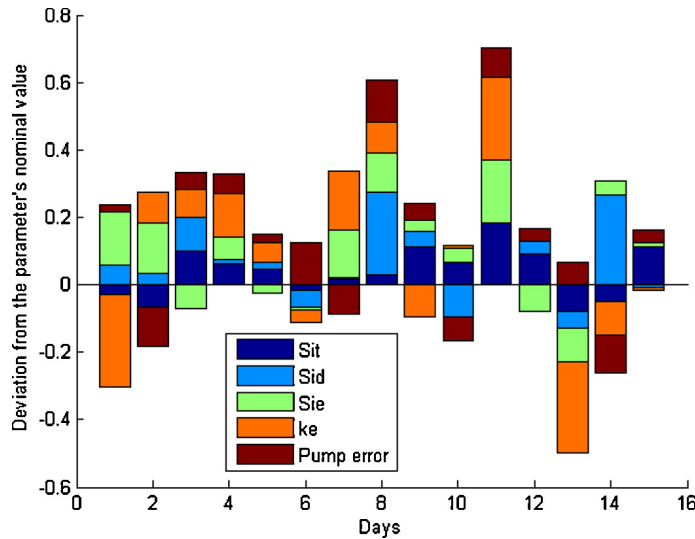
Figure 2.10: Parameter variation within the 15 day experiment. From [116].

Variation is computed as relative to the nominal parameter, being positive if it induces decrements in glucose concentration and negative otherwise. It is worth mentioning that the magnitude of the deviation does not directly correlate to the magnitude of the effect since not all the model parameters have the same sensitivity [116]. However, this provides helpful information on the final influence of variability on the model's output for a particular day, and could be useful in deriving more robust glycemic control strategies.

Parametric variations were also considered in [117], where the Medtronic Virtual Patient (MVP) model is identified for ten different subjects based on closed-loop glucose-insulin data and the oral minimal model [101]. Intraday parameter variations for each patient was allowed in cases when, if considered constant, lead to unsatisfactory identification results. In such cases, parameters S_I, Glucose Effectiveness at zero insulin (GEZI) and Endogenous Glucose Production (EGP) were structured to assume one of two values during three windows inside a 24-hour time period. Parameters assumed the same value during windows one and three, and a different one for the second window. Start and end times of each window were identified to minimize the fitting error in all three windows. S_I variations were identified in six of the ten subjects of the study,

obtaining $\pm 30 - 70\%$ variations between time-windows. Moreover, window times and duration were also different for each subject, which reinforces the need for subject-specific S_I profiles.

As mentioned in Section 2.1, intra-patient variability can be described by changes in S_I, which in addition, are influenced by meals, stress, sleep architecture and physical activity. In order to summarize the relationship between some of these variables, a block diagram is depicted in Figure 2.11. Note that correlations between all variables are not illustrated, since their causal relations are not fully understood, as is the case, for example on the effect of excercise on S_I. Moreover, rhythms of counterregulatory hormones and quality of BG control also influence daily variations in insulin requirements, by modifying the patient's S_I. Therefore, a description of the S_I circadian variation should be representative of the daily variations in glucose metabolism in each patient.
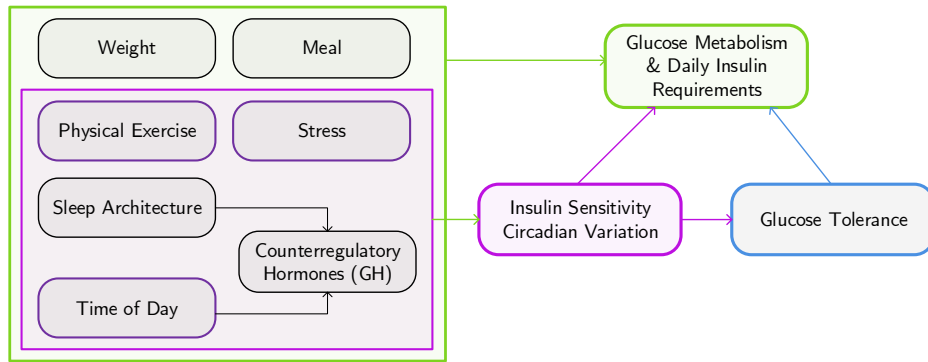
Figure 2.11: Variables involved in intra-patient variability.

2.3   Concluding Remarks

In this Chapter, the physiological sources of intra-patient variability and the different approaches for its modeling/simulation that have been adapted for T1DM were summarized. The following aspects are worth highlighting:

- Circadian intra-patient variations are influenced by many factors (meals, stress, sleep architecture, physical activity, rhythms of counterregulatory hormones and quality of BG control) that, ultimately, reflect on the patient's S_I, making it vary during the day. Thus, intra-patient variability could be described by suitable modeling of circadian S_I variation.

- Several T1DM simulation models have been adapted in order to reflect the time-varying nature of the problem. Considering the high interpatient variations it is fundamental to obtain subject-specific patterns of S_I that can be implemented in a control algorithm, and, to date, there is no general consent on how to determine or represent such variations. In this regard, the sensor–pump S_I index presented in [63, 103] seems to be a promising tool. Once the S_I is estimated, its daily pattern can be identified and included at the controller design stage. Moreover, other factors like stress, should continue being explored in order

to include their effects on the insulin-glucose dynamics, and therefore, obtain more robust and reliable glucose controllers.

- Intra-patient variability can be accounted for as uncertainty in model parameters and/or initial conditions. Developing dynamic models that consider this uncertainty could be helpful to improve model accuracy as well as implementing robust control algorithms for the AP.

Chapter 3

Control-Oriented Models

Understanding and modeling the dynamics of glucose regulation has lead to improvements in diabetes treatment. A large number of models of glucose regulation have been proposed, with different purposes and levels of detail according to their intent: physiology studies, simulation or control purposes (design, tunning or validation), patient management, health care intervention or systems biology.

In this Chapter, the different models used for describing glucose regulation, with a focus on control-oriented models, are reviewed. In Section 3.1 a broad classification of available models is carried out, outlining their characteristics and applications. Then, a review of models used in controller design is carried out in Section 3.2, analyzing how the inclusion of intra- and inter-patient variability is performed. Focusing on robust control strategies, which can account for parametric and dynamic uncertainty, Section 3.3 describes a personalized LPV model that represents the time-varying nature of the T1D problem. Section 3.4 introduces (in)-validation techniques that allow obtaining uncertainty bounds by comparing a nominal model with experimental data and can be used for robust controller design. Finally, some concluding remarks are presented in Section 3.5.

3.1   Models in T1DM

Mathematical models of glucose regulation have been proposed and studied since the 1960s, and have become instrumental in developing therapeutic tools and assessing their effectiveness. These models can be classified in two broad categories: *minimal models* which describe the key components of system functionality and are capable of measuring fundamental processes of glucose regulation, and *maximal models* which include a detailed and comprehensive description of the underlying physiology and are able to simulate the glucose-insulin system.

Minimal Models

Minimal models are the simplest possible models of the glucose regulatory system. Starting from dynamic data and a given structure, using system-identification techniques, model parameters

that represent metabolic variables are then estimated using the data. Mathematical models in this category are usually of low order with the following features: *(i)* physiologically based, *(ii)* simple and reliable estimation of parameters from a single dynamic response of the system, *(iii)* parameters that vary inside physiologically plausible ranges and *(iv)* ability to describe system dynamics with the smallest number of identifiable parameters [7, 108]. These models can be used in physiology studies to estimate metabolic variables such as insulin sensitivity [101], beta-cell responsiveness [79], and glucose effectiveness [118], using dynamic experiments like the intravenous glucose tolerance test. Minimal models are often used for controller design and estimation strategies.

Maximal Models

In contrast to minimal, maximal models are complete comprehensive descriptions that attempt to fully incorporate all the available knowledge of metabolic regulation into a non-linear model of a high order with a large number of parameters, that is generally non-identifiable without massive experimental and invasive investigations on an individual [108]. Many maximal models have been used as test beds for examining the empirical validity of models intended for clinical applications, or to perform experiments over the glucose system, that otherwise would be very dangerous, expensive or unethical to carry out. These simulation models provide the opportunity to investigate diabetes from additional viewpoints and alternative objectives.

Simulation environments (such as AiDA [119]) were developed for educational purposes to allow patients and clinicians to gain quantitative understanding of glucose dynamics, or to assess closed-loop delivery systems [82–85]. In the last decade, the Food and Drug Administration (FDA) has accepted simulation models for the approval of different medical devices. The UVA/Padova metabolic simulator [82] was accepted in 2008 as the first *in-silico* model that can substitute animal studies in preclinical testing of AP systems. Detailed analysis and comparison of different model structures are reported in the literature [120].

3.2   Control-oriented models

Glucose models have also constituted an integral part of closed-loop predictive glucose controllers. Most control design methods make use of compact, low order models, whose main task is capturing systems dynamics at a detail enough to achieve satisfactory regulation performances [7, 108]. These models can be parametric low-order models (minimal), parametric high-order models but with few free parameters to allow real-time estimation or non-parametric models such as ARMAX models or impulse response models. These can be derived from existing minimal models, by simplifications of maximal models or be derived specifically for their used in closed-loop controllers.

Obtaining a model for any particular dynamical system, in general, is usually obtained through an identification process. The drawback here is that this procedure, in the case of T1DM patients,

is very invasive, and most metabolic parameters related to the insulin-glucose system are not easily identifiable in practice. Hence, usually average models are proposed as a first approach for describing insulin-glucose dynamics. However, the large inter-patient variability precludes the possibility of obtaining a single controller for all possible patients with a satisfactory performance, and obtaining personalized models has been widely studied in order to tackle this issue [18, 19, 21, 50–57, 121–125].

One approach to obtaining a personalized T1DM control-oriented model is to adapt a low-order model structure based on the patient's clinical data, such as weight, TDI, the CR, among others [108]. Hence, the control-oriented models are tuned taking into account easily available information, that the patients use daily for their glucose control. For example, given the patient's TDI, an insulin sensitivity factor can be obtained using the 1800 rule (1800/TDI) [126]. From the medical point of view, the 1800 rule indicates the maximum drop in glucose concentration, measured in mg/dl, after a 1 U injection of rapid-acting insulin. Since the work in [50], that rule has been used in several studies, both *in-silico* and clinical, to tune the gain of an LTI model to a particular patient [21, 32, 50, 57, 65, 127].

In [18, 53], three different approaches to obtain a personalized LTI model are presented: *(i)* based on the patient's CR, *(ii)* a non-parametric approach using historical input-output data to perform black-box identification, and *(iii)* a gray-box identification with a known fixed structure. For the first approach, each *in-silico* subject of the UVA/Padova simulator is associated with a 13-th order LTI average model that is personalized according to his/her CR. CR is a parameter that is part of the conventional therapy of the patient and represents how many carbs are covered by one unit of insulin. Groups are defined by selecting patients having low ($\overline{CR} \leq 12$), medium-low ($12 < \overline{CR} \leq 15$), medium-high ($15 < \overline{CR} \leq 19$) and high ($\overline{CR} > 19$) S_I, where $\overline{CR}$ corresponds to the average value of the daily CR profile of each subject in the UVA/Padova simulator. Then, the model corresponding to the patient's group is used as a one-step-ahead prediction model to synthesize a customized MPC. For the second approach, a non-parametric approach is used to identify an LTI prediction model, that is subsequently converted to a state-space representation of a given dimension, but there is no control on the order of the resulting model. Finally, a gray-box identification is carried out through constrained optimization, maintaining a 13-th order LTI structure.

Other model personalization approaches consist of gray-box identification from a subject historical clinical data. In [128] a fifth-order LTI model is proposed, which through a least-square cost function is able to fit clinical data over a two-day period. Its parameters are identified from CGM data, insulin dosages, and carbohydrate estimate. This model was further expanded to a fifth-order LTI model, to achieve parametric interpretability [129]. From these models, an estimate of S_I can be obtained through model parameters, but the obtained value would correspond to an average value over the estimation window. A similar approach is considered in [130] where a fifth-order order linear model that fits data up to 84 days is identified, allowing S_I, time-to-peak insulin absorption and time-to-peak gut absorption to assume different day-to-day values,

thus capturing the inter-day variability of each subject, with the intra-day variations yet to be described. In a related manner, data-driven models that are identified with historical clinical data have been developed in [131–133]. In these works, Wiener-type or ARX models include an input (mostly time) to account for the effects of the circadian rhythms on glucose metabolism.

Intra-subject variability is an additional important challenge for the AP and has not been addressed in the aforementioned control-oriented personalized models. Moreover, as mentioned in Chapter 2, although S_I variations have been generally considered to test glucose controllers through extensive simulations, better closed-loop performance may be obtained if these variations were included in the synthesis stage. In this regard, adaptive control systems consider intra-patient variations by embedding the model in the controller and adjusting controller parameters as the behavior of the system changes. Other adaptive control systems update the parameters of the model recursively as new data are collected from the system, and use the latest model in the controller [31]. Moreover, the S_I index based on pump and CGM data [103] could potentially be useful for run-to-run control strategies to adapt basal insulin patterns [30, 134], insulin boluses [104, 110], or MPC cost functions [19]. It is worth noting that real-time parametric identification can help improve closed-loop performance. However, the ability of real-time identification algorithms to track time-varying parameters need to be carefully assessed, especially considering that for some subjects parameters can present substantial differences over time. Model identifiability analysis could be carried out, for example, using the methodological approach described in [135].

Another approach to cope with intra-patient variability is to compute tight-solution bounds on prediction models [59, 66, 116]. In this case, parametric variations over a glucose-insulin model are used to compute all the possible responses (solution envelope) and define upper and lower bounds that can be computed in real time and employed as prediction models in control structures like MPC. Similarly, in [86] an LTI model-set was obtained based on the Sorensen's model [84], by covering the modeling error as additive uncertainty, between the complete model and a sixth-order LTI model.

A good control-oriented model should have a structure that allows a well-known, reliable and numerically robust control synthesis technique to produce a controller that can be implemented in real-time. Considering the time-varying characteristics of the glucose regulation problem, LPV models are good candidates and can result in LPV or switched LPV (LTI) control strategies. Examples of LPV models that have been proposed to describe the insulin-glucose dynamics can be found in [23, 25, 26, 76, 87, 136]. In [76] and [23], the Bergman minimal model [78] was considered and transformed into a quasi-LPV model by an appropriate choice of parameters. In [25, 26, 87], the Sorensen compartmental model [137] was linearized at different points, which were defined as the vertexes of an affine-LPV model that covers the original nonlinear one. This model was used as an uncertainty LTI model set, and an $\mathcal{H}_\infty$ controller was designed to control it; hence, the time-varying characteristics were not exploited. Finally, in [136], the Cambridge model [138] was represented with an LPV system by a particular selection of scheduling variables. The LPV system was used to obtain a robust LPV controller that was tested on different *in-silico*

scenarios, showing the benefits of including uncertainty on the controller synthesis.

In this regard, the personalized LPV model developed in [57] reflects the time-varying and nonlinear nature of the problem, while maintaining a third-order structure, which is not the case with previous control-oriented models [21, 50, 65]. This more accurate description of the problem allowed the possibility of designing a switched LQG controller [17] that has been successfully tested on the complete *in-silico* adult cohort of the UVA/Padova metabolic simulator, and in the first clinical trials in Latin America [89]. Considering its advantages, this model will be extended to include intra-patient variations, which will be explored in two different ways: *(i)* treating them as uncertainty, and therefore, covering possible S_I variations with a dynamic uncertainty bound, and *(ii)* modifying the average structure of the model to include parametric variations in S_I. The next section presents a detailed description of this model and its identification procedure.

3.3 Control-oriented LPV model

The control-oriented LPV model was developed in [22, 57] based on the UVA/Padova metabolic simulator [81]. It has a low-order structure akin to the one presented in [50], where the input corresponds to the subcutaneous insulin infusion (in pmol/min) and the output is the glucose concentration deviation (in mg/dl):

$$G(s) = k \frac{s + z}{(s + p_1)(s + p_2)(s + p_3)} e^{-15s}. \tag{3.1}$$

An average model was first identified at a glucose concentration $g = 235$ mg/dl, where the 1800-rule was found to be rendered correct for the nonlinear model. Then, its domain of validity was extended by allowing parameter p_1 to vary with g in order to fit the average Bandwidth (BW) of the linearized models at different glucose values, keeping all other parameters fixed ($z = 0.1501$, $p_2 = 0.0138$ and $p_3 = 0.0143$). The following piecewise-polynomial function was used to approximate pole $p_1(g)$:

$$p_1(g) = \phi_{1,i}\, g^3 + \phi_{2,i}\, g^2 + \phi_{3,i}\, g + \phi_{4,i} \quad \text{with} \quad i = \begin{cases} 1 & \text{if } g \geq 300 \\ 2 & \text{if } 110 \geq g < 300 \\ 3 & \text{if } 65 \geq g < 110 \\ 4 & \text{if } 59 \geq g < 65 \\ 5 & \text{if } g \leq 59 \end{cases} \tag{3.2}$$

and with coefficient values given in Table 3.1.

In this way, a simple manner of replicating changes in the model's gain according to the glucose value was obtained, since the time-varying parameter p_1 relates both the BW and DC

Table 3.1: Parameter values of $p_1(g)$ from (3.2).

i	$\phi_{1,i}$	$\phi_{2,i}$	$\phi_{3,i}$	$\phi_{4,i}$
1	0	0	-3.4321×10^{-6}	4.4706×10^{-3}
2	0	9.0580×10^{-8}	-5.3562×10^{-5}	1.1357×10^{-2}
3	-4.2382×10^{-8}	1.1402×10^{-5}	-9.1676×10^{-4}	2.5849×10^{-2}
4	0	1.7321×10^{-4}	-2.3080×10^{-2}	7.7121×10^{-1}
5	0	0	-2.8336×10^{-5}	1.4083×10^{-2}

Gain (DCG) of the model.

The average glucose-dependent model (3.1) can then be tuned to a specific subject by adjusting parameter k with his/her TDI as follows. For each subject #j, the LPV model at 235 mg/dl is excited with a 1 U insulin bolus and the value of k_j is determined so that the glucose drop matches the one predicted by the 1800-rule ($1800/TDI_j$). Here, it is worth remarking that parameter k_j is time-invariant but specific to each subject.

A state-space representation of the personalized LPV model (defined as LPV$_g$ model) is given by:

$$\dot{x}(t) = \boldsymbol{A}(p_1)x(t) + \boldsymbol{B}u(t)$$
$$y(t) = \boldsymbol{C}x(t)$$

(3.3)

with u and y the insulin delivery and glucose signals, and

$$\boldsymbol{A}(p_1) = \begin{bmatrix} 0 & 1 & 0 \\ 0 & 0 & 1 \\ 0 & -p_2 p_3 & -(p_2 + p_3) \end{bmatrix} + p_1 \begin{bmatrix} 0 & 0 & 0 \\ 0 & 0 & 0 \\ -p_2 p_3 & -(p_2 + p_3) & -1 \end{bmatrix},$$

$$\boldsymbol{B} = \begin{bmatrix} 0 & 0 & 1 \end{bmatrix}^T, \quad \boldsymbol{C} = k_j \begin{bmatrix} z & 1 & 0 \end{bmatrix}.$$

(3.4)

Note that a delay of 15 min should be added to the output and that the LPV$_g$ model is affine in parameter p_1, which is an advantageous characteristic for the design of LPV controllers. The LPV$_g$ was compared to the UVA/Padova simulator in in open- and closed-loop by means of the Root Mean Square Error (RMSE) and the ν-gap metric respectively, achieving better fit than control-oriented models presented previously in this field [21, 50, 65].

Bearing in mind that this model in intended for controller design, the ν-gap metric is used for quantifying the difference between the closed-loop performance of two different loops before the controller is designed [57]. The performance is quantified by means of a generalized stability margin, $b_{P_1,K}$. For LTI models, given a controller K and a model P_1, both transfer functions,

this margin is defined by [139, 140] as:

$$b_{P_1,K} = \left\| \begin{bmatrix} P_1 \\ I \end{bmatrix} (1 - KP_1)^{-1} \begin{bmatrix} -K & I \end{bmatrix} \right\|_\infty^{-1} \tag{3.5}$$

where larger values of $b_{P_1,K}$ correspond to better performance of the feedback system comprising P_1 and K. This performance measure/stability margin is related to the ν-gap, $\delta_\nu(P_1, P_2)$, by the inequality:

$$b_{P_2,K} \geq b_{P_1,K} - \delta_\nu(P_1, P_2) \tag{3.6}$$

with both $b_{P_i,K}$ and $\delta_\nu(P_1, P_2)$ taking values only in the range $[0, 1]$. Thus, $\delta_\nu(P_1, P_2)$ is a measure of the difference between P_1 and P_2, with smaller numbers corresponding to P_1 and P_2 being more similar and $\delta_\nu(P_1, P_2) = 0$ only if $P_1 = P_2$. The ν-gap is defined as:

$$\delta_\nu(P_1, P_2) = \left\| (I + P_2 P_2^*)^{-1/2} (P_2 - P_1) \cdot (I + P_1^* P_1)^{-1/2} \right\|_\infty \leq 1 \tag{3.7}$$

This metric indicates that any controller K that stabilizes P_1 with a margin $b_{P_1,K} > \beta$, is also guaranteed to stabilize P_2 with a stability margin of at least β, if P_2 is a second model satisfying $\delta_\nu(P_1, P_2) < \beta$. In other words, any plant at a distance less than β from P_1 will be stabilized by any controller K that stabilizes P_1 with a certain level of performance.

The ν-gap can also be interpreted as an uncertainty measure. In this way, the largest model set that can be stabilized by a controller K stabilizing P_0 with $b_{P_0,K} > \beta$ is $\{P : \delta_\nu(P_0, P_1) \leq \beta\}$ [139, 140]. Note that for its computation, only the plant models are required, and therefore their closed-loop performances can be compared without having to design the controller.

The ν-gap is of particular interest in this work, considering that if P_1 and P_2 represent alternate models of the same system (the UVA/Padova model and the LPV_g for example), a small $\delta_\nu(P_1, P_2)$ indicates that the differences between both models are negligible from a feedback perspective.

3.4 Model (in)validation

As mentioned in Section 3.2, interval models have been used to describe model uncertainty for analysis and simulation purposes and time-varying parameters have been included in intervals to reflect how intra-patient variability propagates through the nonlinear dynamics in order to analyze the robustness of a specific control design [59, 66, 95, 116]. Nevertheless, no uncertainty quantification has been introduced for controller synthesis. In a robust control framework it is possible to tackle nonlinear/time-varying dynamics and uncertainty, through well-established and numerically robust techniques. In this regard, robust-control oriented identification deals with the interplay between identification, uncertainty and worst-case performance.
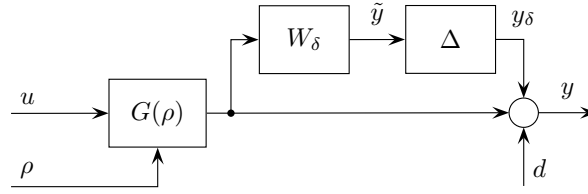
Figure 3.1: Model (in)validation setup.

Robust control models describe system uncertainty with both unknown additive signals and unknown dynamic disturbances. These unknown, but bounded components, lead to a model-set description [141]. Robust identification techniques allowed to obtain an uncertain model-set in coherence with the robust control methodology to be used. However, the uncertainty bounds were too conservative. In order to reduce this conservativeness, model (in)-validation appeared as a promising approach, where a robust control framework was used to determine the minimum levels of external noise and model uncertainty which do not (in)validate the experimental data [86]. The theory for model invalidation was proposed initially in [141, 142] and extented to LPV systems in [143].

The idea behind model (in)validation[1] is to verify if a given model is consistent with an experimental data set $(u(t_k), y(t_k), \rho(t_k))$ with $k = 0, \ldots, N-1$, where $u(t_k)$, $y(t_k)$ and $\rho(t_k)$ are the measures of the input, output, and varying parameter, respectively. In order to accommodate small differences between the model output and the experimental information, the system is usually described by a set of models parameterized by a nominal LPV model $G(\rho)$, a (dynamic) uncertainty bound Δ, and an output disturbance d. For instance, the model set may be defined as illustrated in Figure 3.1, that is,

$$\mathcal{G} = \{G(\rho)(1 + W_\delta(s)\Delta), \ \Delta \in \mathbf{\Delta}\} \tag{3.8}$$

where

$$\mathbf{\Delta} = \{\Delta \in \mathcal{H}_\infty \ : \ \|\Delta\|_\infty \leq \gamma\}, \tag{3.9}$$

$W_\delta(s)$ is a stable transfer function specifying the uncertainty dependence on frequency, $\mathcal{H}_\infty$ is the set of stable transfer functions with suitable dimensions, and $\|\Delta\|_\infty = \sup_\omega |\Delta(j\omega)|$. On the other hand, the disturbance is assumed in the set

$$\mathcal{D} = \{d \in \mathbb{R}^r \ : \ \|d\|_2/N \leq d_{\max}\}, \tag{3.10}$$

with $\|d\|_2 = \sqrt{\sum_0^N d(t_k)^T d(t_k)}$. Thus, the objective is to determine whether or not the measured values can be obtained with the assumed model $G(\rho)$, and the given set descriptions for the noise and uncertainty.

The relation among signals corresponding to the system description in Figure 3.1 can be ex-

---

[1]According to K. Popper [144], a theory can only be *falsified* or *invalidated* with certainty, never validated. This is because future data (that might (in)validate the theory) are not accessible. This also applies to dynamical models which mimic physical data.

pressed as:

$$T_z = T_{W_\delta} T_G T_u,$$
$$T_y = T_G T_u + T_d, \tag{3.11}$$
$$T_w = T_\Delta T_z,$$

where T_{W_δ}, T_G and T_Δ are the Toeplitz matrices associated with convolution kernels of $G(\rho)$, W_δ and Δ, respectively. The symbols T_z, T_u, T_y, T_d, and T_w, are the Toeplitz matrices associated with the sequences $\mathbf{u}$, $\mathbf{y}$, $\mathbf{d}$, and $\mathbf{w}$, respectively. The bold letters denote the respective truncated version of the signals, $\boldsymbol{\psi} = [\psi_0^T \ldots \psi_{N-1}^T]$, which are defined as follows:

$$T_\psi = \begin{bmatrix} \psi_0 & 0 & \cdots & 0 \\ \psi_1 & \psi_0 & \cdots & 0 \\ \vdots & \vdots & \ddots & \vdots \\ \psi_{n-1} & \psi_{n-2} & \cdots & \psi_0 \end{bmatrix} \tag{3.12}$$

The model set given by $\mathcal{G}$ is (in)validated against experimental data provided by vectors $\mathbf{u}$, $\mathbf{y}$, and $\boldsymbol{\rho}$, if there exist vectors $\mathbf{w}$ and $\mathbf{d}$ satisfying constraints (3.8) and (3.10). This is defined as consistency, and for the model, uncertainty and noise sets are *not* invalidated by the existing data. The (in)validation of the model in Figure 3.1 can be expressed as a convex optimization problem. More concretely, the measures of $u(t_k)$, $y(t_k)$, and $\rho(t_k)$ with $k = 0, \ldots, N - 1$ are consistent with the model in Figure 3.1 if the following optimization problem is feasible:

$$\underset{\mathbf{d}, \mathbf{w}}{\text{minimize}} \quad \gamma \tag{3.13a}$$

$$\text{subject to} \quad \begin{bmatrix} T_u^T (T_{W_\delta} T_G)^T T_{W_\delta} T_G T_u & T_w^T(\mathbf{w}) \\ T_w(\mathbf{w}) & \gamma^2 I \end{bmatrix} > 0, \tag{3.13b}$$

$$\begin{bmatrix} d_{max}^2 & \mathbf{d}^T \\ \mathbf{d} & I \end{bmatrix} > 0 \tag{3.13c}$$

where $\mathbf{d} = \mathbf{y} - \mathbf{w} - T_G \mathbf{u}$.

In this way, it is possible to find the minimum upper bound on the norm of the uncertainty $\Delta \in \mathbb{C}$ so that the initial LPV model, $G(\rho)$, is not invalidated by the available experimental information $[u(t), y(t), \rho(t)]$. The optimization process either fixes one bound and minimizes the other, or minimizes a weighted combination of both bounds (γ and d_{max}) simultaneously.

The model (in)-validation tools presented in this section are an useful component in the typically iterative procedure of modeling, identification, design and experimental assessment for control system development [141]. From an identification perspective, model parameters can be included as additional optimization variables and consider the problem of finding the model that describes the datum with the smallest ammount of noise and dynamic uncertainty; or the problem of

fine tuning of a model initially estimated by other means, like the robust identification/invalidation procedure presented in [145]. This framework is adequate for robust controller design methods, such as $\mathcal{H}_\infty$ optimal control, LPV or switched (LTI) LPV control.

3.5   Concluding Remarks

In this Chapter, several aspects related to robust control, and how intra- and inter-patient variations are tackled in control-oriented models are reviewed and discussed. In this regard, it is worth highlighting:

- Personalized control-oriented models include mostly LTI descriptions that have yet to include intra-patient variations for control design purposes.

- The most promising approaches that consider intra-patient variations include: *(i)* personalized model identification allowing S_I to be a time-varying parameter in specific cases, and *(ii)* intervalar models that include parametric uncertainty that can be used in predictive control strategies.

- Model (in)validation allows to obtain a robust control model (nominal model with uncertainty bounds) suitable for the design of $\mathcal{H}_\infty$ optimal control, LPV or switched (LTI) LPV control techniques that can tackle both dynamic and parametric uncertainties quantitatively.

Chapter 4

Invalidation and Low-Order Model Set

As mentioned in Section 3.2, two different approaches to account for intra-patient variations in the controller design stage are explored in this work. First, by covering them with a dynamic uncertainty bound, and second by formalizing them in an LPV model that includes these variations in a way that allows for the different representations or even real-time estimation of patients S_I daily variability to be coupled with the model.

In this Chapter, the first approach is explored by extending the LPV_g control-oriented model (nominal model) to a set of models to represent uncertain dynamics by means of the invalidation procedure described in Section 3.4. "Experiments" are obtained from the UVA/Padova metabolic simulator. Both noise and uncertainty bounds are minimized so that the nominal model with uncertainty could have produced the data. This procedure provides a quantification of the model error with respect to this simulator and produces an LPV *model set* that is amenable to design robust controllers that take into account several sources of uncertainty, e.g., non-linearities and variations in S_I.

Section 4.1 describes the LPV results of the invalidation procedure carried out over the LPV_g model. Section 4.2 illustrates the use of the model set with the design of a switched LPV controller that is tested on the *in-silico* adult cohort of the distribution version of the UVA/Padova simulator, in comparison to a nominal design. Finally, some concluding remarks are presented in Section 4.3.

4.1 LPV_g model invalidation of synthetic patients

In this section, the model (in)validation tools presented in Section 3.4 are used to test the consistency of the LPV_g model presented in Section 3.3 against the noiseless *experimental* evidence obtained from the UVA/Padova simulator. The output noise bound is thus set at a very small value, and the optimization problem (3.13) is solved to determine the minimum uncertainty bound γ.

The experimental data sets $[u(t_k), y(t_k), \rho(t_k)]$ were generated by extensive simulations using

two types of realistic insulin profiles. The first one represents a correction insulin bolus of the form:

$$u(t) = \begin{cases} \theta/T_s, & \text{if } t_0 \leq t \leq t_0 + T_s, \\ 0 & \text{otherwise,} \end{cases} \quad (4.1)$$

where $T_s = 5$ minutes is the sampling time and θ a random number in the range $[0.5, 1.5]$ U. The second profile is a basal insulin modulation signal:

$$u(t) = \sum_{k=1}^{n} (1 + \zeta) u_{\mathrm{b}} \phi(kT_p) \quad (4.2)$$

where u_{b} is the basal infusion rate, ζ is a random number in the range $[-0.5, 0.5]$, $\phi(t)$ is a pulse signal of width $T_p = 60$ minutes and nT_p is the total simulation time. This signal mimics the modulation of the basal insulin infusion rate during a closed-loop test, as the one that will illustrate these results in Section 4.2. The time-varying parameter, $\rho(t_k)$, represents parameter $p_1(g)$ from (3.2), and is computed using the experimental glucose signal, $y(t_k)$.

The difference between the *experiment* and the model during the invalidation process covers structural and/or parametric uncertainties. The first one involves the different dynamical behaviors of the system when moving from one glucose value to another. Specifically, this represents different LTI models moving over a nonlinear dynamical surface. In addition, intra-patient variations are included as parametric uncertainties in S_I. In order to consider this variability, for each *in-silico* adult of the distribution version of the UVA/Padova simulator, the nominal insulin sensitivity ($S_{I,nom}$) was affected with each one of the factors in the set $\{0.5, 0.7, 0.9, 1, 1.1, 1.3, 1.5\}$. These values were selected according to the clinical findings presented in [49]. Variations in S_I were implemented as changes in the model parameters V_{mx} and k_{p3} that represent the peripheral and hepatic insulin sensitivity, respectively.

To collect sufficient representative information of each *in-silico* adult, they were excited with three signals of the form (4.1) and five of the form (4.2). As an example, Figure 4.1 shows the excitation signals and glucose evolution corresponding to the experiments performed on Adult #001 with $S_{I,nom}$. The upper plots correspond to the input signals and the bottom plots correspond to the glucose responses obtained with the UVA/Padova simulator and the LPV_g model. Bearing in mind that different insulin sensitivities are used, effects of insulin modulations in a wider range are considered, at least in nominal conditions. For example, a 1.5 U bolus for $S_I = 1.5\, S_{I,nom}$ would be similar to a lower bolus with the nominal S_I, or a larger bolus with a lower S_I. Moreover, the range of insulin profiles used in this work was limited in order to guarantee that the glucose traces, in all cases, remain in the simulator's domain of validity, i.e., [40, 400] mg/dl.

The model (in)validation discussed above requires a discrete model. Therefore, the discrete first order approximation of the LPV_g model, with a 5-minute sampling time, results:
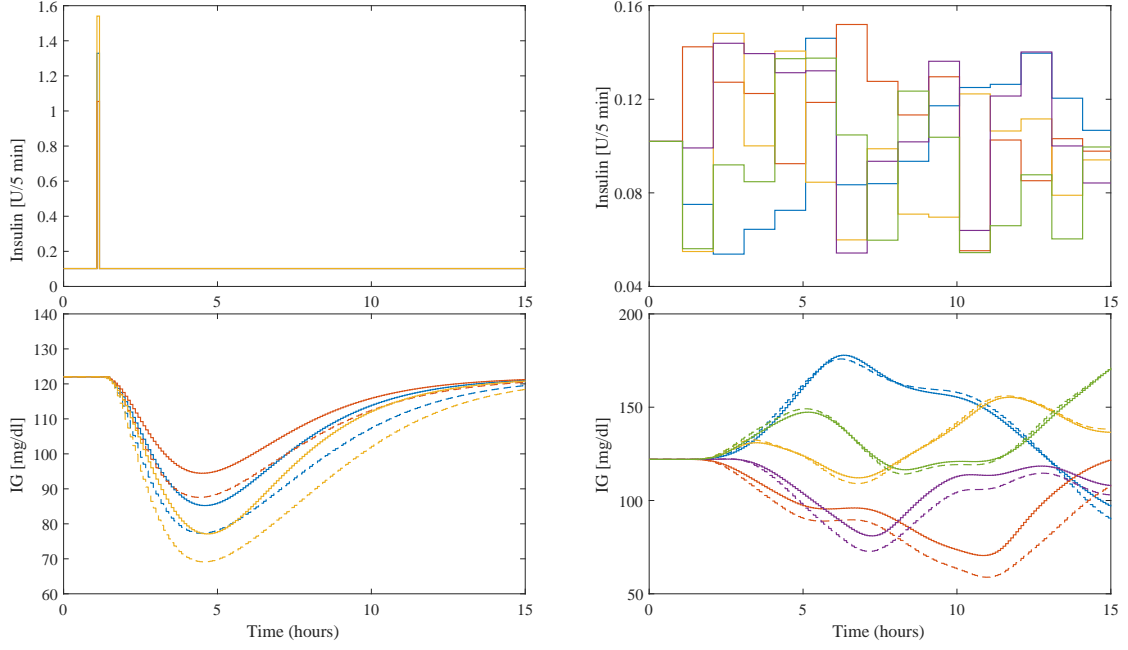
Figure 4.1: *In-silico* experimental results with the insulin bolus test signal (left) and the basal insulin modulation test signal (right) applied to Adult #001 with sensitivity $S_{I,nom}$. Insulin infusion rate (upper) and glucose response (lower) obtained with UVA/Padova simulator (solid line) with LPV model (dashed line).

$$x(t_{k+1}) = A_d[p_1(t_k)] \, x(t_k) + B_d \, u(t_k),$$
$$y(t_k) = C_d \, x(t_k),$$

where

$$A_d[p_1(t_k)] = \begin{bmatrix} I + T_s A[p_1(t_k)] & 0 \\ B_e C & A_e \end{bmatrix}, \qquad B_d = \begin{bmatrix} T_s B_e \\ 0 \end{bmatrix}, \qquad C_d = \begin{bmatrix} 0 & C_e \end{bmatrix},$$

$$A_e = \begin{bmatrix} 0 & 0 & 0 \\ 1 & 0 & 0 \\ 0 & 1 & 0 \end{bmatrix}, \qquad B_e = \begin{bmatrix} 1 \\ 0 \\ 0 \end{bmatrix}, \qquad C_e = \begin{bmatrix} 0 & 0 & 1 \end{bmatrix}.$$

The noise signal set was defined in (3.10) with $d_{max} = 0.05$, and the uncertainty weight in (3.8) as:

$$W_\delta(s) = 0.2 \, \frac{500s + 1}{50s + 1} \tag{4.3}$$

In model (in)validation, the differences between the experimental data and the model are "explained" by the model uncertainty Δ and a noise set bounded by d_{max} mg/dl. Here, noise-free results from the UVA/Padova simulator have been used as "experimental data", reason why such

a small noise bound $d_{\max}$ was selected. In addition the noise set serves to consider noisy data, but this bound has no implications in the control design. In next section more realistic noisy scenarios are considered to test the proposed robust controller, which does not affect the validity of the uncertain model.

Hence, all differences between the model and the experiment are attributed to non-linearities and unmodeled phenomena, which can affect stability and performance. Here, $W_\delta(s)$ is a high-pass filter because above a certain frequency, uncertainty impedes the stabilization of the closed-loop. The only designer's choice is the maximum achievable closed-loop bandwidth (2×10^{-3} rad/min in eqn. (4.3)) which was chosen according to the *a priori* knowledge on the system, in order to cover the nominal model's dynamics. Its magnitude depends on the *experimental* knowledge of the system, and is computed as an uncertainty bound γ in the set (3.9) which scales $W_\delta(s)$ during the controller design. The magnitude depends on the proposed uncertain model, and in general can be reduced if a more complex model set is used, e.g., higher order. Therefore, the 20% uncertainty that $W_\delta(s)$ has at low frequencies is only a starting point, since its actual magnitude is computed by means of the (in)validation procedure.

The uncertainty bounds γ obtained after solving the optimization problem (3.13) for each data set and for each *in-silico* adult are summarized in Figure 4.2. Adult #007 has been excluded because its TDI is not compatible with its S_I. In addition, the invalidation tests performed on this subject have shown a clear inconsistency between model and data, turning it into an outlier of the set in terms of model uncertainty. The red dots indicate the γ for each test and the red line the worst case bound for each combination of subject-S_I. The blue line indicates the worst-case uncertainty bound $\gamma_{ws,j}$ for each adult. This last bound can be used in LPV synthesis tools for the controller design by scaling the uncertainty weight as $\gamma_{ws,j}W_\delta(s)$. In this way, the model-set for each subject is described by:

$$\mathcal{G}_j = \{G(\rho)(1 + W_\delta(s)\Delta), \ \Delta \in \mathbf{\Delta}_j\} \tag{4.4}$$

where

$$\mathbf{\Delta}_j = \{\Delta \in \mathcal{H}_\infty \ : \ ||\Delta||_\infty \leq \gamma_{ws,j}\}, \tag{4.5}$$

The corresponding values obtained in the model (in)validation are listed in Table 4.1.

This modeling strategy can be carried out from real clinical data in a minimally invasive way. One alternative would be to use the patient's daily data recorded by the CGM and pump to invalidate the LPV$_g$ model and obtain the patient's particular model set, considering that the time-varying parameter (p_1) is computed with the CGM readings. In this way a robust controller can be designed, and tested clinically on the same subject. Using clinical data, which could have inputs with lower variability and therefore, lower capability to challenge the model (excitability), will not affect the procedure, since the difference between the clinical data and the model output is originated by the subject's individual response, and includes all possible sources of uncertainty
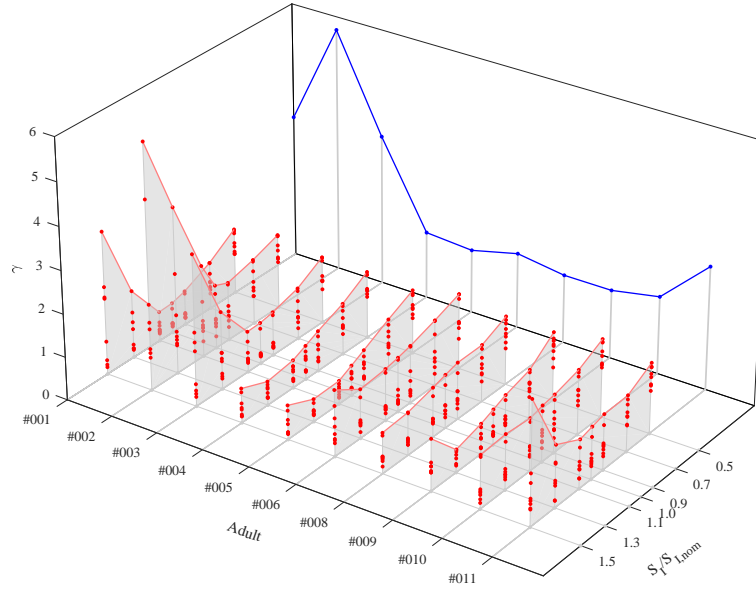
Figure 4.2: Summary of the uncertainty bounds γ obtained for the eight test signals applied to each *in-silico* adult with seven different S_I. The blue line indicates the worst-case uncertainty bound $\gamma_{ws,j}$

Table 4.1: Uncertainty bounds for each *in-silico* adult and each variation in S_I. The worst-case bounds are $\gamma_{ws,j}$.

$S_I/S_{I,nom}$	Adult									
	#001	#002	#003	#004	#005	#006	#008	#009	#010	#011
0.5	1.524	1.735	1.555	1.560	1.484	1.754	1.596	1.598	1.808	1.637
0.7	1.093	1.515	1.194	1.190	1.185	1.530	1.326	1.124	1.502	1.298
0.9	0.791	1.350	1.015	0.934	0.858	1.332	1.318	0.949	1.344	1.282
1.0	0.698	1.479	0.958	0.787	0.696	1.256	1.238	0.822	1.301	1.208
1.1	0.681	2.131	0.948	0.646	0.540	1.196	1.147	0.700	1.218	1.128
1.3	1.566	3.859	1.801	0.552	0.523	1.135	0.989	0.526	1.276	1.431
1.5	3.327	5.694	3.510	0.798	0.791	1.528	0.940	1.197	1.231	2.864
$\gamma_{ws,j}$	3.327	5.694	3.510	1.560	1.484	1.754	1.596	1.598	1.808	2.864

(not only in S_I). In this way, the model set obtained (which now represents this patient) is the one to be controlled.

4.2   Switched-LPV robust controller design

The use of the set of models obtained in Section 4.1 is illustrated in this Section designing a switched-LPV controller. To this end, each subject is represented by the set of models computed in

Section 4.1, and extending the ideas in [21, 57], a (robust) switched LPV controller is synthesized based on this set. This design switches between two LPV controllers: $K_1(\rho)$ that is conservative and performs slight changes on the basal insulin infusion rate, and $K_2(\rho)$ that is more aggressive and is triggered at meal times.

The design of LPV controllers follows similar procedures as $\mathcal{H}_\infty$ optimal control, but for time-varying systems. The controller is computed solving a convex optimization problem aimed at minimizing the $\mathcal{L}_2$ gain of the mapping from a generic disturbance w to an output z, i.e., minimizing a scalar $\eta > 0$ such that

$$\|z\|_2 < \eta \|w\|_2,$$

where $\|x\|_2 = \sqrt{\int_0^\infty x^T(t)x(t)\, dt}$. Therefore, the design involves selecting w and z according to the control specifications. In the case of the AP, the structure of weights and signals are illustrated in Figure 4.3. In this framework, a controller designed to cope with an uncertain system represented by a set of models, works properly when nominal performance and robust stability are satisfied.

Here, nominal performance pertains the minimization of two selected variables under a *set* of possible perturbations r. Thus, it is achieved by solving the minimization of a gain $\alpha > 0$ for all r bounded in $\mathcal{L}_2$ such that:

$$\left\| \begin{bmatrix} \tilde{e} \\ \tilde{u} \end{bmatrix} \right\|_2 < \alpha \|r\|_2, \tag{4.6}$$

where $\tilde{e}$ and $\tilde{u}$ are obtained after weighting the glucose error e and the control action u (insulin infusion) with the following weights:

$$W_p(s) = \frac{k_e}{10} \frac{10s + 1}{5000s + 1}, \tag{4.7}$$

$$W_u = k_{u,j}, \tag{4.8}$$

respectively. The variable $j \in \{1, 2\}$ corresponds to the controller index in the switching strategy.
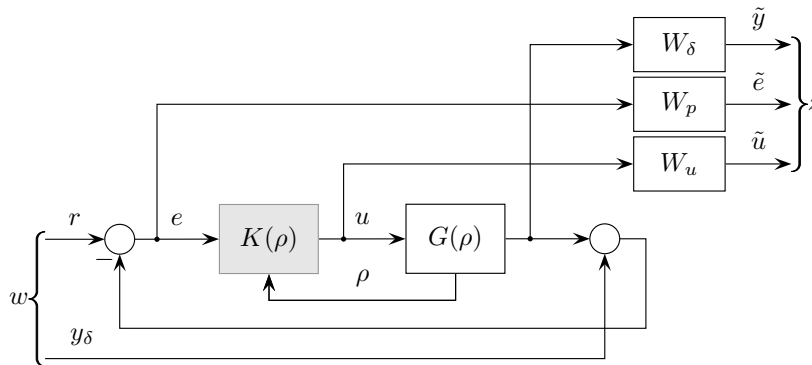
Figure 4.3: Robust LPV control design setup.

Table 4.2: Results corresponding to the LPV robust controller design for each *in silico* adult.

Adult	#001	#002	#003	#004	#005	#006	#008	#009	#010	#011
γ_{ws}	3.327	5.694	3.510	1.560	1.484	1.754	1.596	1.598	1.808	2.864
k_e	0.023	0.016	0.023	0.045	0.050	0.043	0.047	0.046	0.041	0.027
η_1	1.081	1.042	1.122	1.281	1.388	1.474	1.423	1.301	1.311	1.129
β_1	0.949	0.982	0.965	0.861	0.849	0.812	0.835	0.887	0.878	0.961
η_2	1.014	1.012	1.039	1.078	1.130	1.142	1.138	1.101	1.100	1.045
β_2	0.982	0.988	1.005	0.975	0.993	0.999	0.999	0.997	1.001	1.005

Weight $W_p(s)$ penalizes glucose deviations from the basal value (around 120 mg/dl [146]) and weight W_u penalizes large changes in the insulin injection. Both weights are the only controller tunning parameters, and are selected according to the designer's priorities by adjusting parameters k_e, $k_{u,j}$. The pole of W_p corresponds to the bandwidth of the nominal model. In this work, these performance weights have been selected in order to prioritize avoidance of hypoglycemia rather than the lack of hyperglycemia, considering the short and long term consequences of each state.

Robust stability consists in guaranteeing that the controller stabilizes the closed-loop system for any possible model in the set (3.8), and therefore stabilizes the underlying uncertain dynamics. To this end, the controller must be computed in order to ensure $\beta < 1$ where

$$\|\tilde{y}\|_2 < \beta \, \|y_\delta\|_2.$$

Variable $\tilde{y}$ is obtained after weighting y with the uncertainty dynamics (4.3) affected by the worst-case bound γ_{ws} corresponding to the particular subject, i.e., $\gamma_{ws}W_\delta(s)$.

Table 4.2 summarizes the controller design results, obtained through the Matlab Robust Control Toolbox$^{\text{TM}}$. For all subjects, the parameter in W_u was set as $k_{u,1} = 0.5$ and $k_{u,2} = 0.07$. Note that $k_{u,2}$ is significantly smaller than $k_{u,1}$, and therefore provides a lower weight on the control variable which in turn produces a more aggressive controller (higher insulin infusion at meal times). Parameter k_e was adjusted for each patient in order to ensure the robust stability condition $\beta < 1$. Notice that by norm properties $\beta \leq \eta$, nevertheless forcing $\eta < 1$ might result in a very conservative controller design. For this reason, the parameter k_e for each patient was selected (by trial and error) according to the gain β. From Table 4.2 it is clear that those subjects with higher uncertainty bound γ_{ws} require lower values of k_e, which implies a lower performance, i.e., a worse glucose regulation, given the conservativeness imposed over the controller due to the high uncertainty.

Closed-loop simulations were performed considering the following conditions: (i) the UVA/Padova distribution simulator; (ii) a meal of 70 g of CHO is ingested at hour 7; (iii) the aggressive controller is triggered exactly at meal time and commands the insulin infusion; (iv) one hour after meal time, the conservative controller automatically takes over the insulin delivery; and (v) a CGM and an insulin pump with a delivery resolution of 0.1 U. It is worth clarifying that meal
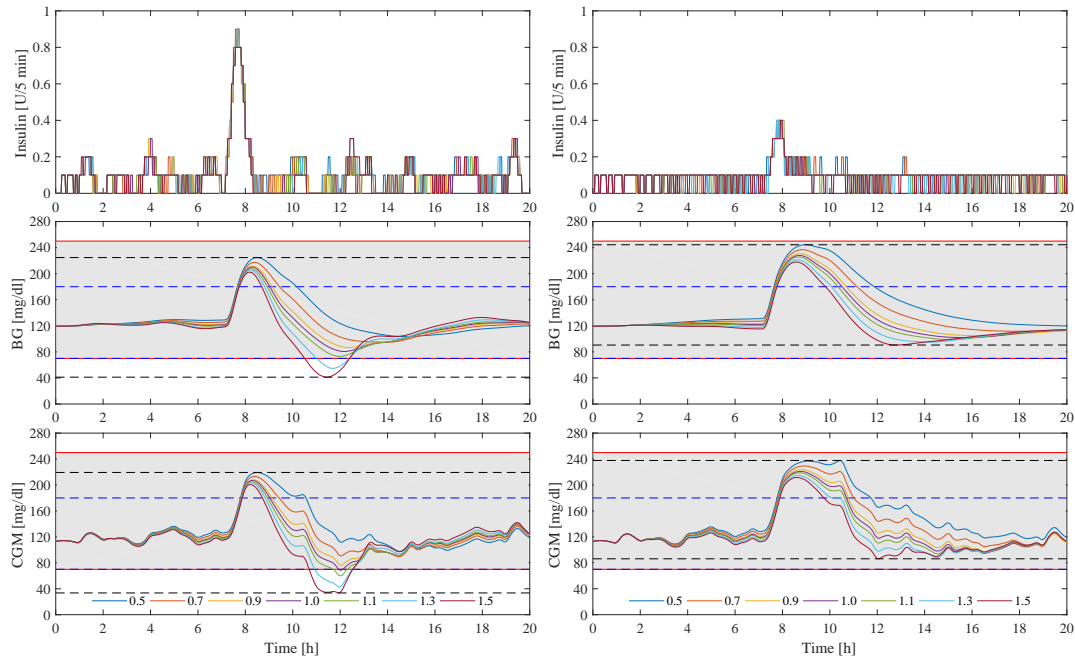
Figure 4.4: Closed-loop responses for one *in-silico* adult to a meal of 70 g of CHO at the hour 7, using the nominal controller (left) and the robust controller (right). Seven variations of S_I are considered and the same CGM noise is applied in all cases for comparison purposes. The continuous red lines represent the limits of the 70-250 mg/dl range, the dashed blue lines indicate the limits of the 70-180 mg/dl range, and the dashed black lines indicate the minimum and maximum glucose values.

announcement is made only for triggering the aggressive controller, but no information regarding the carbohydrate amount is required by the controller, and therefore, no pre-meal insulin boluses are infused.

Figure 4.4 presents simulations of the closed-loop system for one *in-silico* adult, where each line corresponds to a particular subject's S_I indicated in Section 4.1. Plots on the right correspond to the closed-loop system with the robust controller designed as mentioned in this section. Plots on the left show the closed-loop responses with a nominal controller, i.e., a controller designed considering only the performance objective (4.6) and not the model set (3.8) (model uncertainty is excluded) with the same $k_{u,j}$ and $k_e = 1$. Comparing both responses, it can be observed that the nominal controller is more aggressive than the robust one, applying higher insulin doses. This result is suitable for S_I values close to $S_{I,nom}$, but not when the S_I is far from the nominal value. This is clear in the case of a more sensitive value as $S_I = 1.5 S_{I,nom}$ in which a significant postprandial glucose drop can be observed (minimum blood glucose around 40 mg/dl). On the other hand, the robust controller is more conservative, using lower insulin values, but produces a more uniform response for all S_I cases (minimum blood glucose around 90 mg/dl). These results are reasonable from the point of view of robust control theory: a controller that aims for a particular (nominal) model representation of the patient will show its worst performance when the model does not match the actual patient. Instead, a robust controller that should manage a set of models (a more realistic representation of the patient) already considers possible uncertainties in
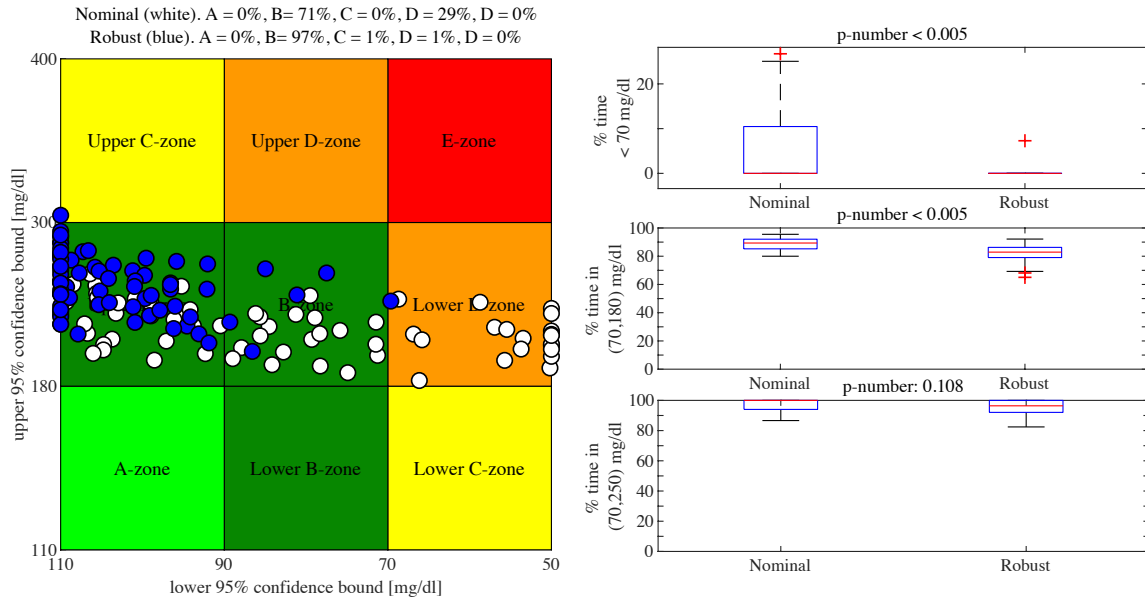
Figure 4.5: Left: Control Variability Grid Analysis (CVGA) plots of the closed-loop responses of all *in-silico* adults and their S_I variations for the nominal (white) and the robust controllers (blue). Right: Time-in-range plots.

both model's structure and parameters, and therefore will perform at its best in general, although in a more conservative fashion.

Figure 4.5 provides the closed-loop results for all *in-silico* adults in a CVGA (left) and time-in-range (right) plots. Time-in-range results are computed from the meal time to the end of the simulation. A comparison is made between the nominal and robust controller designs over all subjects, including their S_I variations. From the CVGA plot, the nominal controller presents a higher number of subjects in the lower D-zone (nominal: 29%, robust: 1%), indicating risk of hypoglycemia. Instead, the robust controller is located in the B- and upper B-zones, achieving a significant reduction in hypoglycemic events, compared to the nominal one. This situation is also shown in the time-in-range plot, where a significant reduction of time in hypoglycemia ($<$ 70 mg/dl) is achieved (nominal: 2.67% vs. robust: 0.05%, $p < 0.05$), without significantly reducing the percentage of time in range [70, 250] mg/dl (nominal: 96.85% vs. robust: 95.48%, $p = 0.108$). Although there is a significant reduction in percentage of time in range [70, 180] mg/dl when the robust controller is used (nominal: 88.75% vs. robust: 82.19%, $p < 0.05$), time in range achieved with the robust controller is still acceptable. Hyperglycemic behavior arises as a consequence of the conservative tendency of the robust controller, coming from a large uncertainty bound, and therefore, it can be reduced by further refining of the uncertainty bounds by means of more (and better) information of each patient.

4.3   Concluding remarks

In this Chapter, an LPV invalidation technique has been applied to a control-oriented LPV model in order to expand the insulin-glucose description to a set of LPV models. Here is worth highlighting:

- The invalidation procedure can be employed with clinical data. In this way, personalization can be achieved, and parametric uncertainties different from those related to the subject's S_I could be accounted for.

- This model-set set is instrumental for robust controller design, which in this work has been carried out by a switched LPV procedure. The controller design based on this model set has proved useful when structural and parametric uncertainties appear in the problem.

- An illustrative example presents a robust controller that successfully copes with uncertainties in the nonlinear dynamics (changes in the glucose values) and variations in S_I, as compared to a nominal design.

- The resulting performance of the controller can be enhanced by using more complex nominal models which would allow making the model more consistent with the experiments.

Chapter 5

Control-Oriented Model with Intra-patient Variations

In Chapter 4, a model-set that includes S_I variations through dynamic uncertainty bounds for each patient was obtained. This approach "covers" intra-patient variations with bounded uncertainty that can be taken into account in the controller design procedure.

In this Chapter, an alternative is proposed, embedding S_I variations into the model. This represents a better way of considering these variations in the synthesis stage since the dynamic effects of intra-patient variations are included in the controller dynamics. In this way, more specific and less conservative controllers can be designed.

The proposed model is an extension of [57] that includes S_I variations while maintaining its low-order model structure. Intra-patient variability is included using a second time-varying parameter to the LPV structure. The model now includes intra- and inter-patient variations because it still preserves the possibility of personalizing it to a particular patient. Moreover, this personalization is also based on the 1800-rule, through a procedure that can be carried out in real patients in a non-invasive way.

The Chapter is organized as follows: In Section 5.1 the procedure to obtain the LPV model with intra-patient variations is presented. Then, Section 5.2 presents the open- and closed- loop evaluation of the model efficiency. Finally, some concluding remarks are drawn in Section 5.3.

5.1 LPV$_g$ with intra-patient variations

Following a similar procedure than [57], an extension of model (3.4) that includes intra-patient variability is developed, defined as LPV$_i$ model. Linearizations of the UVA/Padova model are obtained for each *in-silico* adult of the distribution version, from the subcutaneous insulin delivery (pmol/min) to the subcutaneous glucose concentration deviation (mg/dl) at different steady-state glucose concentrations g and Insulin Sensitivity Variation Factor ($S_{I,VF}$) values. To this end, for each subject and each g and $S_{I,VF}$, the insulin infusion rate needed to maintain the glucose level constant was computed. To fully cover all scenarios discussed in [49, 106], parameters V_{mx} and k_{p3} of the simulator are modulated by an $S_{I,VF}$ within the range [0.4, 1.7]. Here, $S_{I,VF} = S_I/S_{I,nom}$,

where $S_{I,nom}$ represents the nominal values of V_{mx} and k_{p3} in the simulator.

Figure 5.1 and Figure 5.2 show the average variation of the BW and DCG, respectively, for LPV_g and all *in-silico* adults linearized at different g and $S_{I,VF}$ values. Note that both bandwidths and continuous gains coincide exactly at $S_{I,VF} = 1$.
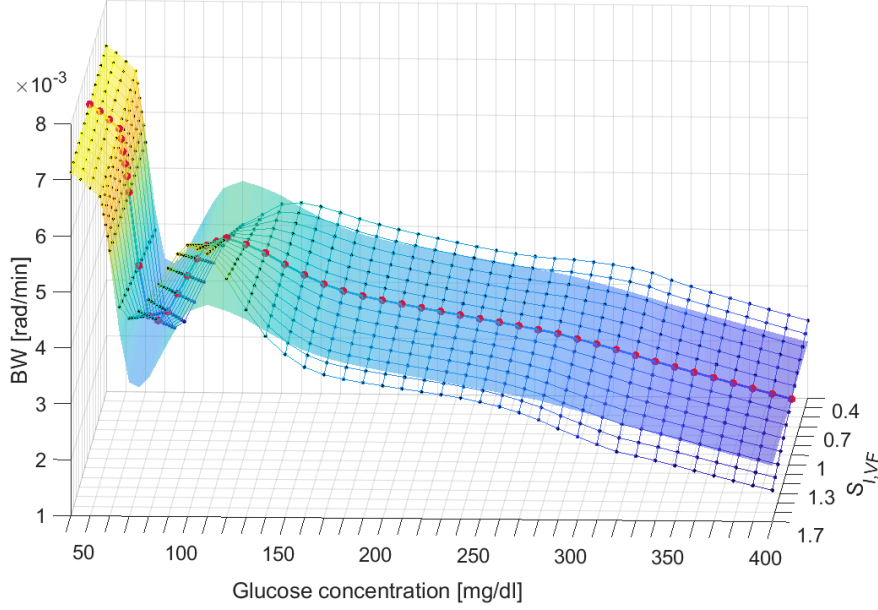
Figure 5.1: BW of LPV_g (smooth surface) and average BW for all *in-silico* adults from the UVA/Padova simulator linearized at different g and $S_{I,VF}$ values (gridded surface). The red dotted line indicates the BW at $S_{I,VF} = 1$.
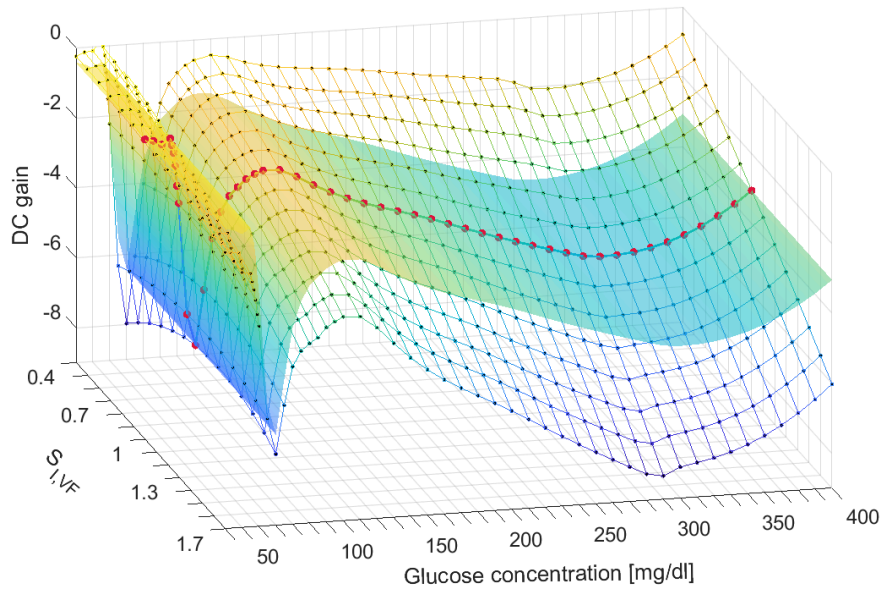
Figure 5.2: DCG of LPV_g (smooth surface) and average DCG for all *in-silico* adults from the UVA/Padova simulator linearized at different g and $S_{I,VF}$ values (gridded surface). The red dotted line indicates the DCG at $S_{I,VF} = 1$.

Bearing in mind that the DCG of model (3.1) is $\frac{kz}{p_1 p_2 p_3}$ and that the BW is independent on k, an extension to model LPV$_g$ is proposed by making parameter k dependent on g and S$_{I,VF}$ as depicted in Figure 5.3. Following this approach, the observed variations of the model's gain due to S$_I$ changes (see Figure 5.2) can be reproduced, without affecting the previous BW fitting.
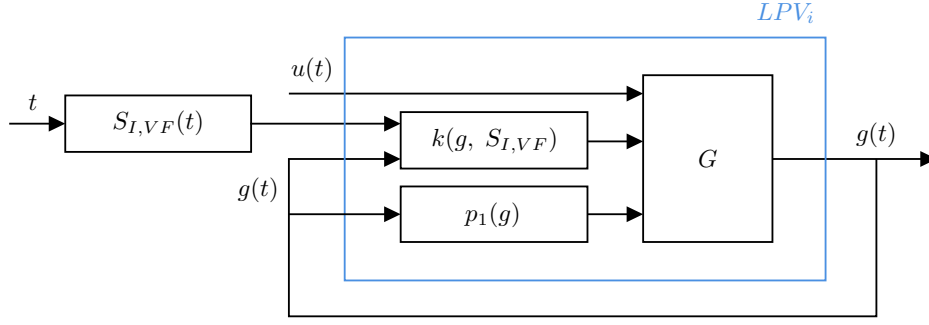
Figure 5.3: Average LPV$_i$ model structure.

In this way, k is used to compensate both inter-patient variations through the 1800-rule and intra-patient variations by making k change according to a suitable S$_I$ profile. The latter could be a general profile (such as those in [47, 104, 106]) or a profile obtained from clinical data. This grants flexibility to the selected model structure, so it can be used together with the S$_I$ profile that best suits subject-specific circadian variations in S$_I$, or even considering other factors that influence S$_I$ such as physical exercise or stress [62, 91, 100, 147], which have yet to be included in control-oriented models [64, 148].

In order to characterize the dependence of parameter k on g and S$_{I,VF}$, the average DCG for all *in-silico* adults linearized at different $(g, S_{I,VF})$ pairs, i.e., DCG$_{NL}(g, S_{I,VF})$ is used for determining k_{avg} as:

$$k_{avg}(g, S_{I,VF}) = \frac{p_2 p_3}{z} p_1(g) \text{DCG}_{NL}(g, S_{I,VF}) \tag{5.1}$$

where $p_1(g)$ corresponds to the polinomial function given in (3.2). The result was fitted using the following piecewise polynomial function:

$$
\begin{aligned}
k_{avg}(g,\ S_{I,VF}) = & \lambda_{1,n} + \lambda_{2,n}\, g \\
& + \lambda_{3,n}\, S_{I,VF} + \lambda_{4,n}\, g\, S_{I,VF} \\
& + \lambda_{5,n}\, g^2 + \lambda_{6,n}\, S_{I,VF}{}^2 \\
& + \lambda_{7,n}\, g^2\, S_{I,VF} + \lambda_{8,n}\, g\, S_{I,VF}{}^2 \quad \text{with} \quad n = \begin{cases} 1 & \text{if } g \geq 300 \\ 2 & \text{if } 120 \geq g < 300 \\ 3 & \text{if } 50 \geq g < 120 \\ 4 & \text{if } g \leq 50 \end{cases} \\
& + \lambda_{9,n}\, g^2\, S_{I,VF}{}^2 + \lambda_{10,n}\, g^3 \\
& + \lambda_{11,n}\, S_{I,VF}{}^3 + \lambda_{12,n}\, g^3\, S_{I,VF} \\
& + \lambda_{13,n}\, g\, S_{I,VF}{}^3 + \lambda_{14,n}\, g^4
\end{aligned}
\tag{5.2}
$$

Table 5.1: Parameter values for $k_{avg}(g, S_{I,VF})$ from (5.2).

n	1	2	3	4
$\lambda_{1,n}$	-7.641×10^{-03}	5.514×10^{-05}	8.356×10^{-05}	-2.011×10^{-05}
$\lambda_{2,n}$	9.024×10^{-05}	-1.186×10^{-06}	-2.645×10^{-06}	2.942×10^{-06}
$\lambda_{3,n}$	4.785×10^{-04}	3.262×10^{-05}	-5.145×10^{-05}	-1.352×10^{-04}
$\lambda_{4,n}$	-4.296×10^{-06}	-6.907×10^{-07}	8.635×10^{-07}	7.641×10^{-06}
$\lambda_{5,n}$	-3.971×10^{-07}	9.342×10^{-09}	2.470×10^{-08}	-1.323×10^{-07}
$\lambda_{6,n}$	-4.243×10^{-05}	3.838×10^{-06}	5.062×10^{-06}	8.139×10^{-05}
$\lambda_{7,n}$	1.225×10^{-08}	3.270×10^{-09}	-4.359×10^{-09}	-1.399×10^{-07}
$\lambda_{8,n}$	1.885×10^{-07}	-3.542×10^{-08}	-5.847×10^{-08}	-3.266×10^{-06}
$\lambda_{9,n}$	-1.966×10^{-10}	6.014×10^{-11}	0	2.696×10^{-08}
$\lambda_{10,n}$	7.718×10^{-10}	-3.175×10^{-11}	-7.066×10^{-11}	2.400×10^{-09}
$\lambda_{11,n}$	5.622×10^{-06}	-2.428×10^{-06}	0	-1.458×10^{-05}
$\lambda_{12,n}$	-1.153×10^{-11}	-5.211×10^{-12}	0	8.254×10^{-10}
$\lambda_{13,n}$	-1.546×10^{-08}	8.127×10^{-09}	0	3.713×10^{-07}
$\lambda_{14,n}$	-5.588×10^{-13}	3.937×10^{-14}	0	-1.575×10^{-11}
FIT	97.11	97.22	15.03	92.75

Parameter values and goodness of fit for each interval are presented in Table 5.1. The goodness of fit was expressed as a fitting percentage obtained by:

$$\text{FIT} = 100 \left(1 - \frac{\|k_p - k\|_2}{\|k - \overline{k}\|_2} \right) \tag{5.3}$$

where k_p is the predicted value, k the real value and $\overline{k}$ its mean. Figure 5.4 presents the results for k_{avg} and its smooth polynomial fitting. Note that as shown in Figure 5.1, there is an abrupt change at 60 mg/dl. The reason for this discontinuity is that the insulin-dependent glucose utilization in the UVA/Padova simulator is associated with a risk function that increases when glucose decreases below the subject's basal glucose concentration and saturates when glucose reaches 60 mg/dl. To avoid translating this artifact discontinuity to the glucose output, a smooth surface was fitted instead, as evidenced in the low fitting coefficient interval $n = 3$.

In this way, the state-space representation of the average LPV_i model is the same as (3.3), but now with:

$$A(p_1) = \begin{bmatrix} 0 & 1 & 0 \\ 0 & 0 & 1 \\ 0 & -p_2 p_3 & -(p_2 + p_3) \end{bmatrix} + p_1 \begin{bmatrix} 0 & 0 & 0 \\ 0 & 0 & 0 \\ -p_2 p_3 & -(p_2 + p_3) & -1 \end{bmatrix},$$
$$B = \begin{bmatrix} 0 & 0 & 1 \end{bmatrix}^T,$$
$$C = k_{avg}(g, S_{I,VF}) \begin{bmatrix} z & 1 & 0 \end{bmatrix}. \tag{5.4}$$
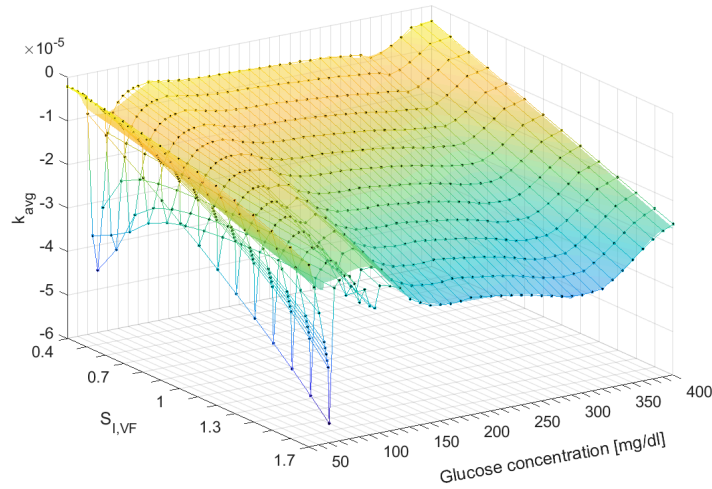
Figure 5.4: Parameter k_{avg} for different values of g and S$_{I,VF}$ (gridded surface) and piecewise polinomial function $k_{avg}(g, \text{S}_{I,VF})$ (smooth surface).

5.1.1 Model personalization

In Section 5.1, it was shown how k could be used to tackle intra-patient variability. In this Section, k is tuned to reduce inter-patient uncertainty. This model personalization is carried out similarly as in [57], i.e., by adjusting the model's k through the 1800-rule.

For this, a suitable gain $k^\star$ is found, making the model achieve the same glucose drop as the one predicted by the 1800-rule when excited with a 1 U insulin bolus at $g =235$ mg/dl and S$_{I,VF} = 1$. Then, k_{avg} is scaled by means of a constant k_j, in order to satisfy $k^\star = k_j k^\star_{avg}$, where $k^\star_{avg} = -1.822 \times 10^{-5}$ corresponds to $k_{avg}(235, 1)$. Results are presented in Table 5.2. Model personalization is thus achieved by replacing $k_{avg}(g, \text{S}_{I,VF})$ in (5.4) with parameter $k_s(g, \text{S}_{I,VF}) = k_j k_{avg}(g, \text{S}_{I,VF})$.

Table 5.2: Scaling factor k_j for each *in-silico* adult.

Adult	TDI [U/day]	$k^\star \times 10^{-5}$	k_j
#001	42	-1.7888	0.9818
#002	43	-1.7451	0.9578
#003	52	-1.4343	0.7872
#004	35	-2.1396	1.1743
#005	40	-1.8650	1.0236
#006	72	-1.0343	0.5677
#008	52	-1.4379	0.7892
#009	34	-2.2024	1.2088
#010	47	-1.5919	0.8737
#011	39.9	-1.8864	1.0354

Variations of k_s for the average *in-silico* subject, and the most and least sensitive subjects are presented in Figure 5.5. Note that the most sensitive subject (Adult #009), whose TDI is

the lowest, is associated with the highest scaling factor k_j, and therefore, higher values of k_s. Moreover, the same subjects, a comparison of the fit accomplished by the personalized LPV_i model to the DCG of the linearized models are presented in Figures 5.6 to 5.8. Note that in each case, the fit of the personalized LPV_i is better than if just k_{avg} is used (average LPV_i), even for the case when k_{avg} fitting was softened. Additionally, for the average subject, both the personalized LPV_i and the average LPV_i coincide, since his/her parameters are considered to be the average of the *in silico* population.
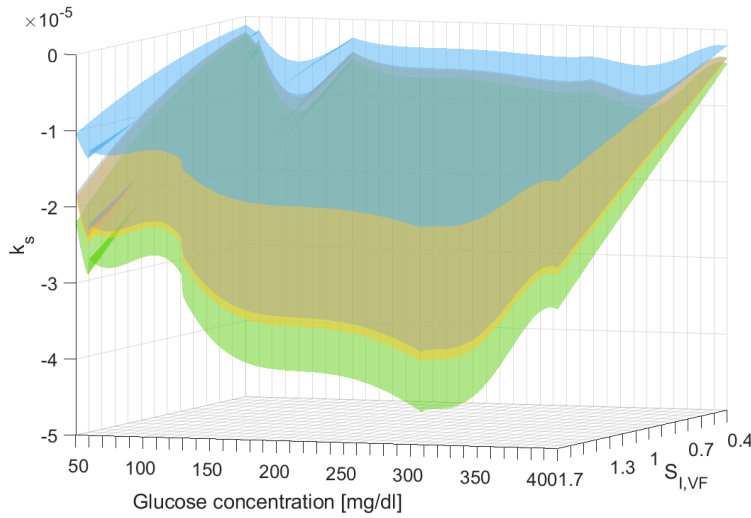
Figure 5.5: k_{avg} (gray surface) and personalized k_s for the average subject (yellow surface), Adult #006 (blue surface) and Adult #009 (green surface)
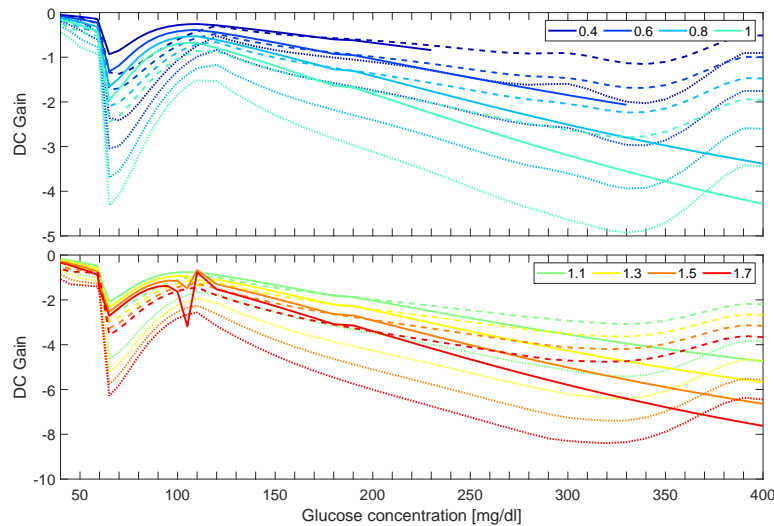
Figure 5.6: DCG of average LPV_i (dotted lines), personalized LPV_i (dashed lines) and linearized UVA/Padova model (solid lines) for Adult #006, for sensibilities lower (upper panel) and higher (lower pannel) than nominal.
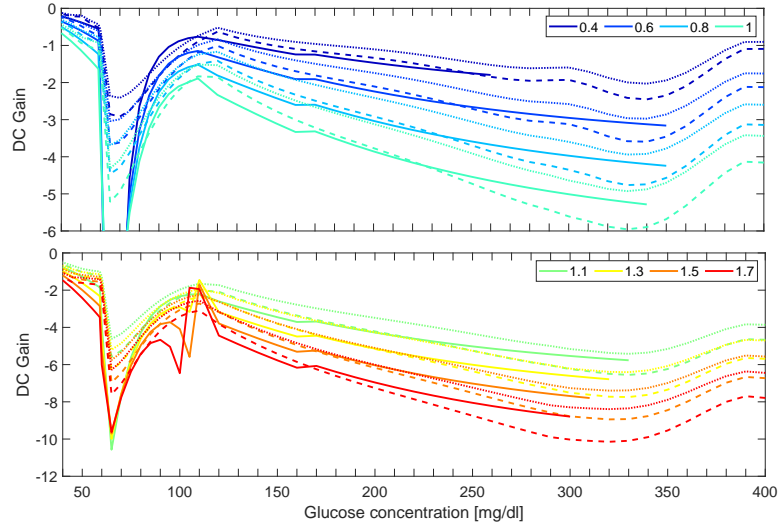
Figure 5.7: DCG of average LPV$_i$ (dotted lines), personalized LPV$_i$ (dashed lines) and linearized UVA/Padova model (solid lines) for Adult #009, for sensibilities lower (upper panel) and higher (lower pannel) than nominal.
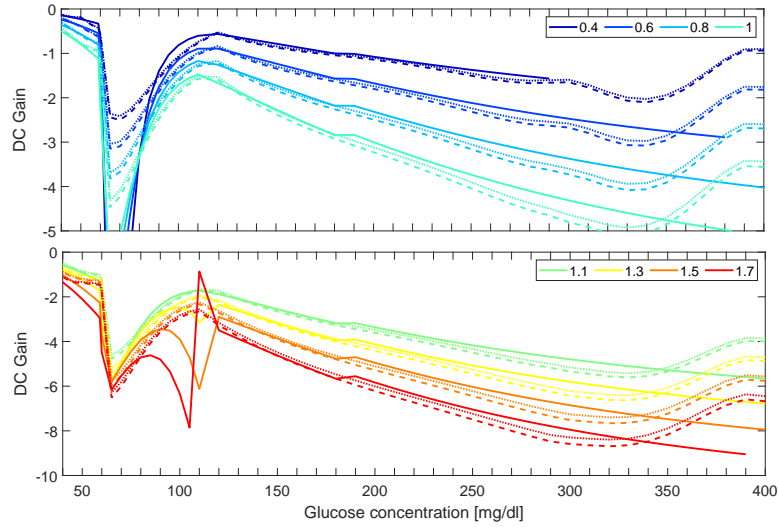
Figure 5.8: DCG of average LPV$_i$ (dotted lines), personalized LPV$_i$ (dashed lines) and linearized UVA/Padova model (solid lines) for Adult #011, for sensibilities lower (upper panel) and higher (lower pannel) than nominal.

5.2 Results and Discussion

A good simulation model, i.e., one that fits properly the experimental data, is not necessarily a good candidate to design controllers [86]. Therefore, in this Section, a comparison of both LPV$_g$ and LPV$_i$ with respect to the UVA/Padova model is carried out not only for simulation (open-loop) purposes, but also for controller synthesis (closed-loop). No other models are considered here, since in [57], it was found that LPV$_g$ has lower closed- and open-loop errors than previous control-oriented models [21, 50, 65].

5.2.1 Open-loop comparison

For each of the 10 *in-silico* subjects of the distribution version of the UVA/Padova simulator, an insulin bolus of 1 U was applied at different operating points to test the personalized LPV_i and LPV_g models in comparison with the UVA/Padova nonlinear simulator. Figure 5.10 presents the time-responses to a 1 U insulin bolus for multiple $S_{I,VF}$ values at basal glucose concentrations of 120, 180, and 240 mg/dl, for Adult #009 (most sensitive subject), Adult #006 (least sensitive subject) and Adult #011 (average subject). Variation in parameters p_1 and k_s for the LPV_g and LPV_i models are also depicted.
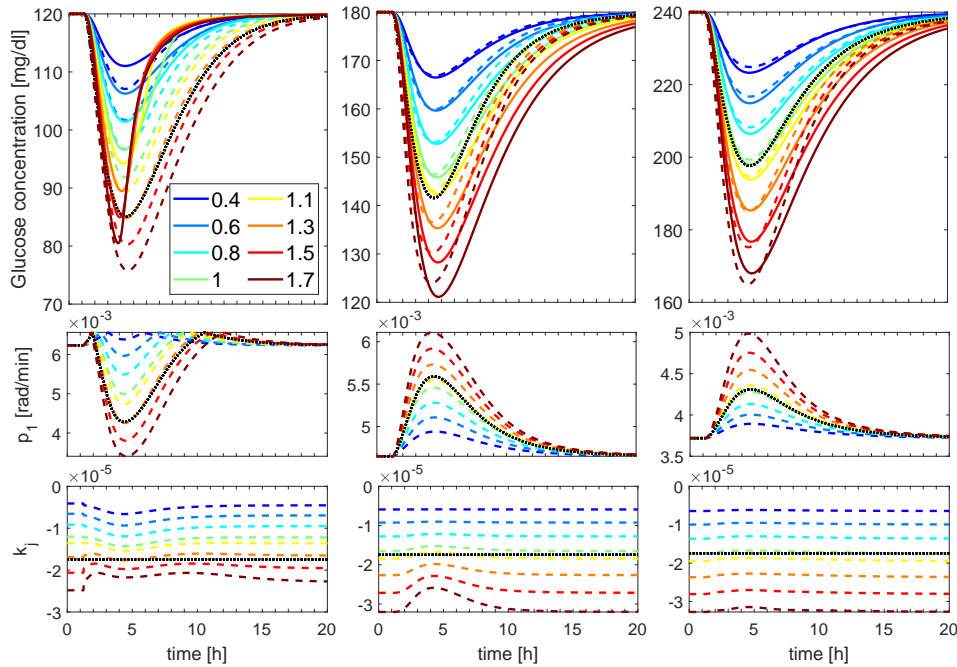
Figure 5.9: Responses to a 1 U insulin bolus starting from 120 mg/dl, 180 mg/dl and 240 mg/dl for Adult #011 at different $S_{I,VF}$ values for models LPV_g (dotted black line), LPV_i (dashed lines) and the UVA/Padova nonlinear model (solid lines). Top: Glucose drop. Middle: Evolution of parameter p_1. Bottom: Evolution of parameter k_s.

Note that a better fit is achieved with LPV_i than with LPV_g for most $S_{I,VF}$ values. The reason is that only LPV_i adjusts its gain to reflect changes in S_I. In addition, it is worth clarifying that despite the LPV_i model is an extension of the LPV_g model, its behavior for $S_{I,nom}$ is the same only at 235 mg/dl as an operating point, i.e., the glucose concentration at which they were both identified. For other glucose concentrations, the gain adjustment through variation of parameter $k_s(g, S_{I,VF})$ generates the differences between both models. Moreover, the average subject presents a similar behavior since it exhibits the average variations captured by parameters p_1 and k_{avg}. However, the model is able to adjust to each patient due to its personalization (see Figures 5.6 and 5.7), and obtain similar responses to those of the non-linear model for each subject.
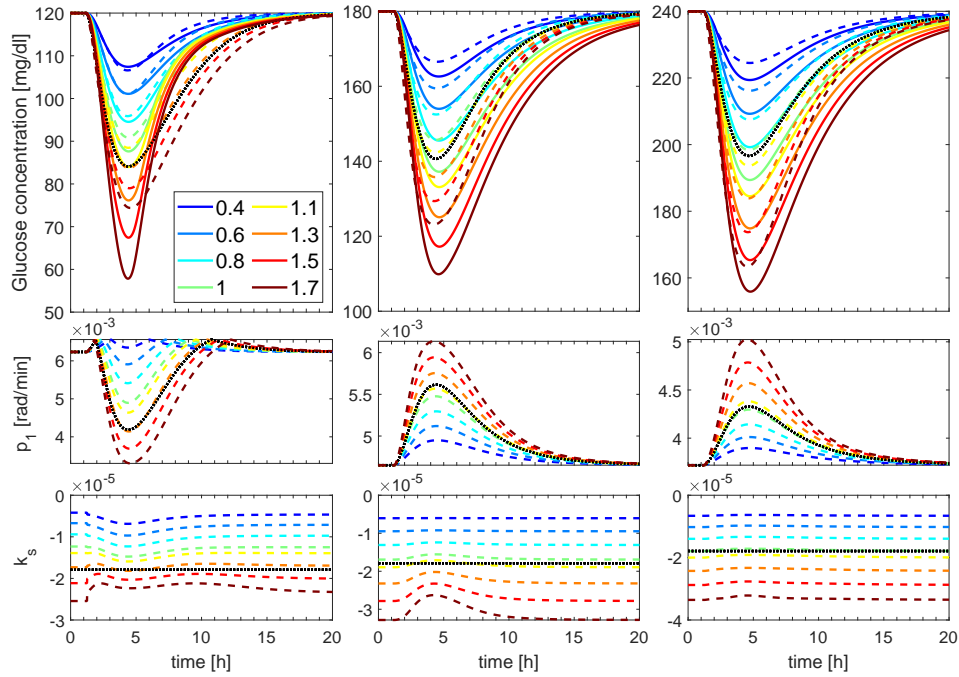
Figure 5.10: Responses to a 1 U insulin bolus starting from 120 mg/dl, 180 mg/dl and 240 mg/dl for Adult #009 at different $S_{I,VF}$ values for models LPV_g (dotted black line), LPV_i (dashed lines) and the UVA/Padova nonlinear model (solid lines). Top: Glucose drop. Middle: Evolution of parameter p_1. Bottom: Evolution of parameter k_s.
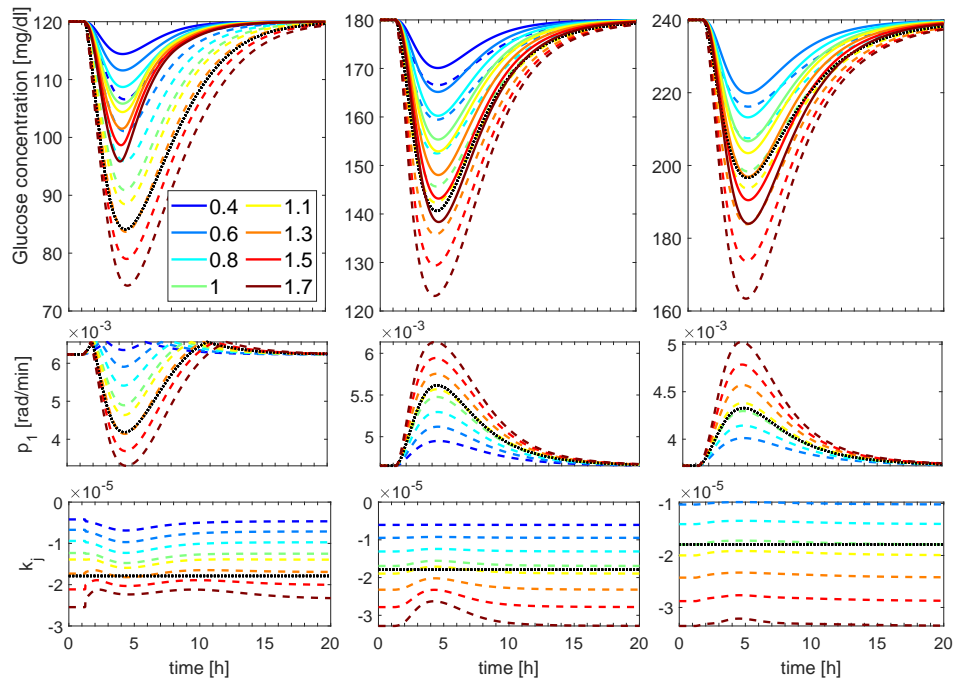
Figure 5.11: Responses to a 1 U insulin bolus starting from 120 mg/dl, 180 mg/dl and 240 mg/dl for Adult #006 at different $S_{I,VF}$ values for models LPV_g (dotted black line), LPV_i (dashed lines) and the UVA/Padova nonlinear model (solid lines). Top: Glucose drop. Middle: Evolution of parameter p_1. Bottom: Evolution of parameter k_s.

For the three LPV models, i.e. the average LPV$_i$, the personalized LPV$_i$ and the LPV$_g$, the RMSE between their time-responses ($\boldsymbol{y_p}$) and the UVA/Padova model ($\boldsymbol{y}$), for each subject at each operating point on the (g,S$_{\mathrm{I,VF}}$) grid, was computed according to the following equation:

$$\text{RMSE} = \frac{\|\boldsymbol{y_p} - \boldsymbol{y}\|_2 \Delta t}{n_t} \tag{5.5}$$

where n_t is the number of samples in the signals ($\boldsymbol{y_p}$ or $\boldsymbol{y}$) and Δt the sample time. In order to capture the complete glucose variation at each point, a number of $n_t = 1200$ points and $\Delta t = 1$ min were selected. In Figure 5.12, average values of the RMSE for all 10 *in-silico* adults at different g and S$_{\mathrm{I,VF}}$ values are shown. Note that a lower RMSE can be obtained with LPV$_i$ than with LPV$_g$ for most glucose concentrations. Considering S$_\mathrm{I}$ variations, for the least sensitive case (S$_{\mathrm{I,VF}} = 0.4$), LPV$_i$ outperforms LPV$_g$ for the whole glucose range. For S$_{\mathrm{I,nom}}$ (S$_{\mathrm{I,VF}} = 1$), both LPV models have approximately the same RMSE, except for glucose concentrations around 90-180 mg/dl, where the increased sensitivity of the UVA/Padova model is further adjusted by the variation of the k_s parameter in LPV$_i$. For a glucose concentration of 235 mg/dl, similar errors are observed since, as discussed before, at this point both models are equivalent. For the most sensitive case (S$_{\mathrm{I,VF}} = 1.7$), LPV$_i$ has a similar RMSE as LPV$_g$ for $g < 140$ mg/dl, but at higher g values the difference in the DCG between both models becomes larger and LPV$_i$ provides a better fit. Moreover, the benefits of model personalization are evidenced, since the personalized LPV$_i$ model achieves smaller errors than the average LPV$_i$ in all cases.
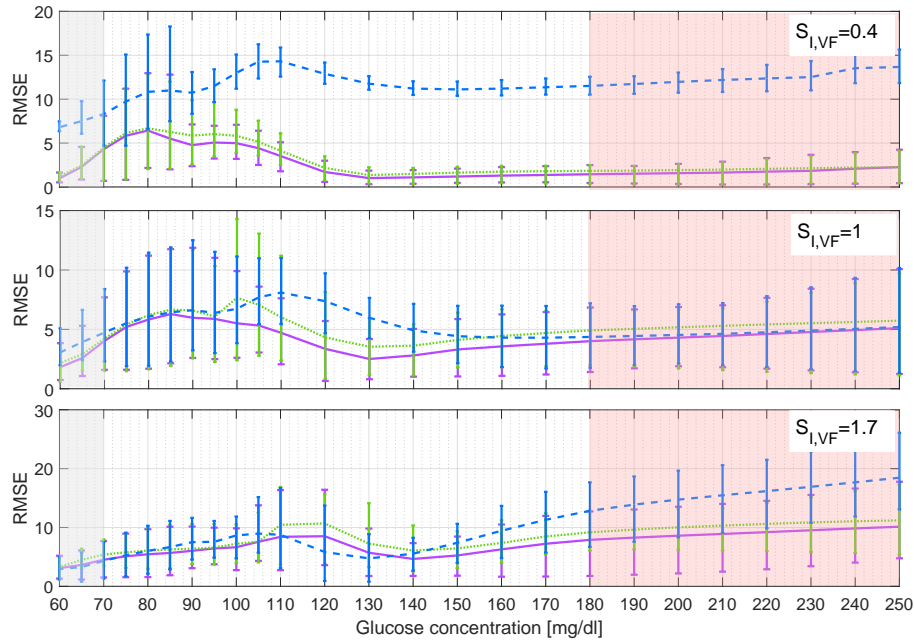
Figure 5.12: Average RMSE between the time-responses of the personalized LPV$_g$ (blue dashed lines), average LPV$_i$ (green dotted lines) and personalized LPV$_i$ (violet solid lines), as compared with the UVA/Padova nonlinear model to an insulin bolus of 1 U for different S$_{\mathrm{I,VF}}$ values. Top: most resistant case (S$_{\mathrm{I,VF}}$=0.4), middle: nominal case (S$_{\mathrm{I,VF}}$=1), bottom: most sensitive case (S$_{\mathrm{I,VF}}$=1.7). Vertical bars are limited by maximum and minimum values.

5.2.2 Closed-loop comparison

In this case, the ν-gap distance [139, 140] between each personalized LPV model and the UVA/Padova model linearized at different points of the $(g, S_{I,VF})$ grid is computed. This metric allows the closed-loop performance of two models to be compared without specifically designing the controller, which is required for a comparison through the RMSE. As mentioned in Section 3.3, a smaller δ_ν means that the differences between two models of the same system are not important from a feedback perspective [139]. Figure 5.13 presents the average ν-gap for all 10 adults for three different $S_{I,VF}$ values, obtaining similar results as for the RMSE analysis discussed in Section 5.2.1.
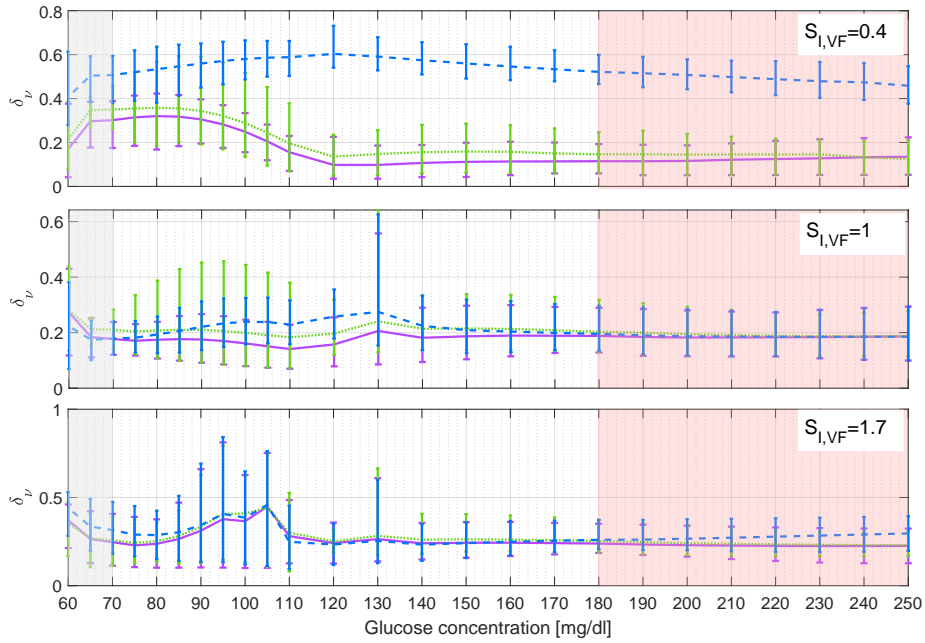
Figure 5.13: Average ν-gap (δ_ν) between the linearizations of the UVA/Padova nonlinear model and models LPV$_g$ (blue dashed lines), average LPV$_i$ (green dotted lines) and personalized LPV$_i$ (violet solid lines) for different $S_{I,VF}$ values. Top: most resistant case ($S_{I,VF}$=0.4), middle: nominal case ($S_{I,VF}$=1), bottom: most sensitive case ($S_{I,VF}$=1.7). Vertical bars are limited by maximum and minimum values.

5.2.3 Overall comparison

The difference between the RMSE and ν-gap obtained with the three LPV models was computed for all $(g, S_{I,VF})$ values considered, and all 10 *in-silico* adults, according to:

$$\delta_{\nu,d} = \delta_{\nu,\text{LPV}_i} - \delta_{\nu,\text{LPV}_g}; \qquad \text{RMSE}_d = \text{RMSE}_i - \text{RMSE}_g \qquad (5.6)$$

In this way, negative values of $\delta_{\nu,d}$ or RMSE$_d$ indicate points where the personalized LPV$_i$ outperforms LPV$_g$. For all subjects, RMSE and ν-gap differences are shown in Figures 5.14 to 5.18. Although a definitive improvement over all $(g, S_{I,VF})$ values with the LPV$_i$ model is not obtained, the reduction is greater in terms of its magnitude than cases where the LPV$_g$ outperforms the

personalized LPV$_i$, where the ν-gap difference between both models does not exceed 0.1. This is clearer in the case of the closed-loop performance (for example, in Adults #001, 002, 008 and 010), which evidences the benefits of including the S$_I$ variation in the controller design stage.
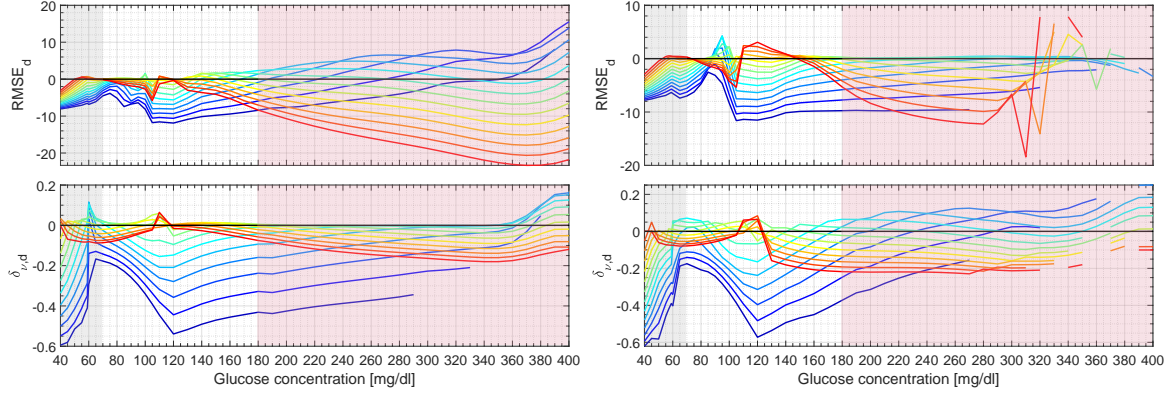
Figure 5.14: RMSE$_d$ (top) and $\delta_{\nu,d}$ (bottom) for Adult #001 (left) and Adult #002 (right).
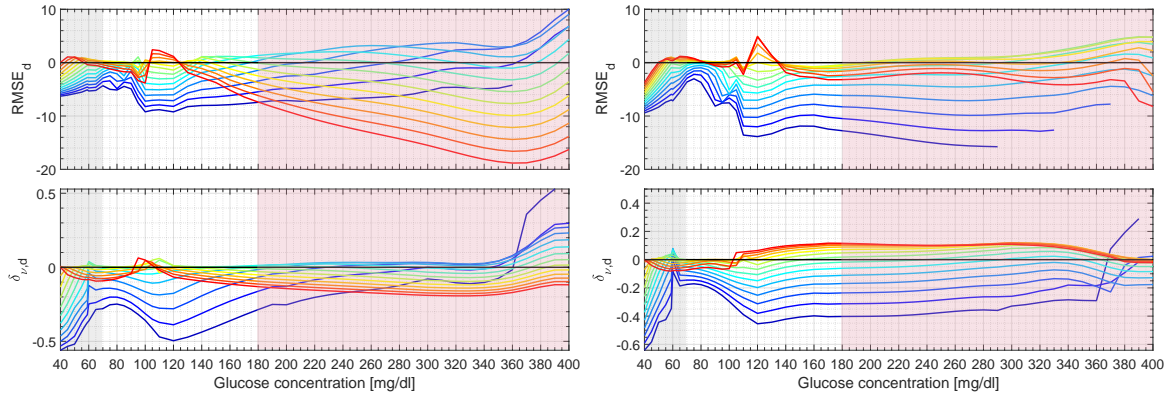
Figure 5.15: RMSE$_d$ (top) and $\delta_{\nu,d}$ (bottom) for Adult #003 (left) and Adult #004 (right).
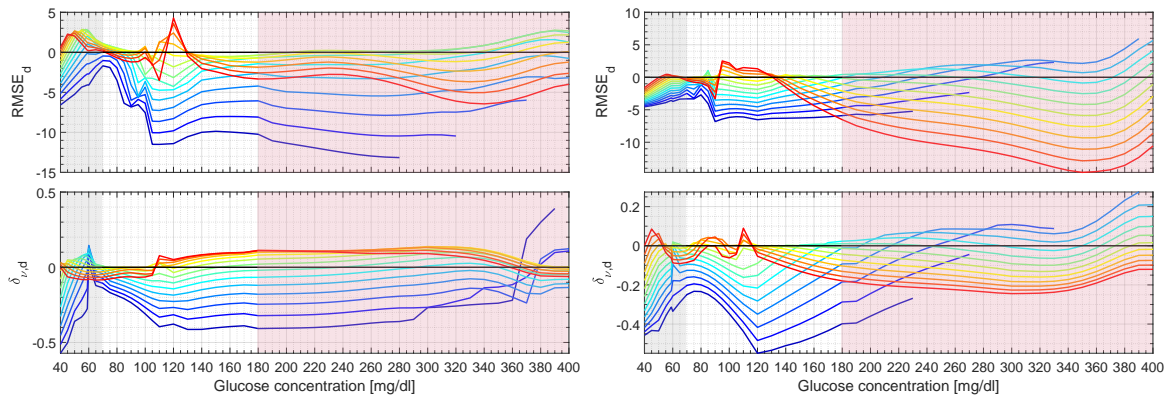
Figure 5.16: RMSE$_d$ (top) and $\delta_{\nu,d}$ (bottom) for Adult #005 (left) and Adult #006 (right).
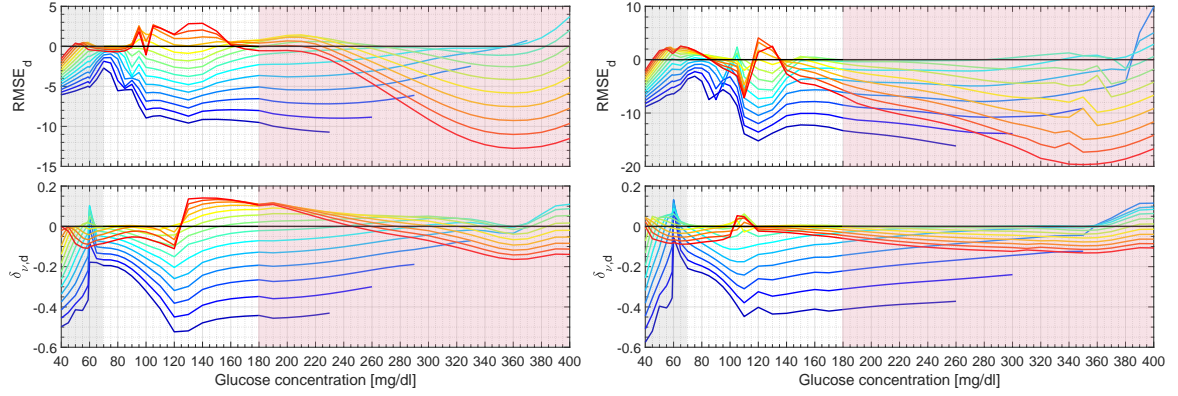
Figure 5.17: RMSE$_d$ (top) and $\delta_{\nu,d}$ (bottom) for Adult #008 (left) and Adult #009 (right).
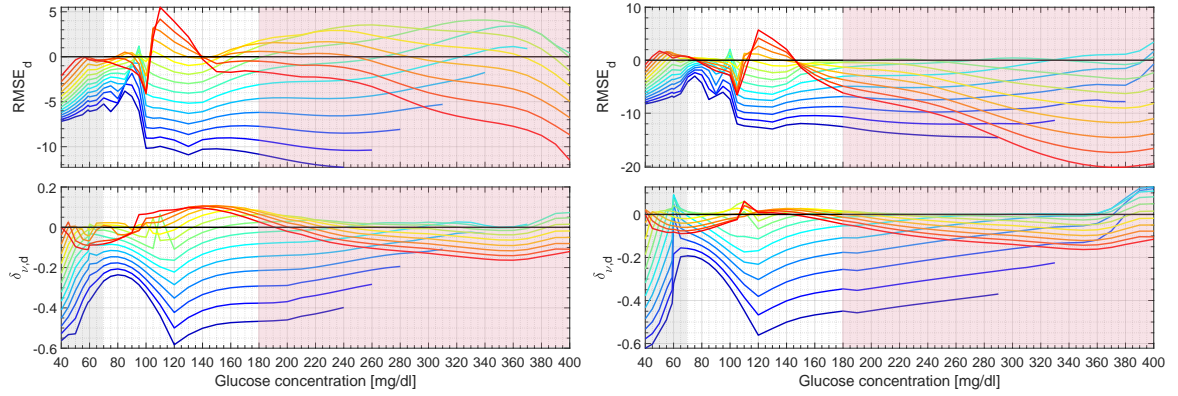
Figure 5.18: RMSE$_d$ (top) and $\delta_{\nu,d}$ (bottom) for Adult #010 (left) and Adult #011 (right).

Differences between the average LPV$_i$ and personalized LPV$_i$ relative to the LPV$_g$ are presented in Figure 5.19. Note that for some subjects both models have approximately the same errors both in open- and closed-loop, but mostly, the personalized LPV$_i$ has the same or better performance than the average LPV$_i$. Considering these similarities, a two-sample t-test was carried out for each *in-silico* adult, to determine if the LPV$_i$ achieved a significant improvement for both RMSE and ν-gap. Differences were computed according to (5.6), with the average LPV$_i$ in place of the LPV$_g$. Test results are presented in Table 5.3, with the percentaje of cases in which the personalized LPV$_i$ outperforms the average LPV$_i$. Note that subjects for whom low (or none) improvement with the personalized LPV$_i$ was achieved, a significant difference was not observed according to the t-test, and therefore, no detriment on the model's performance was obtained through personalization. For the subjects were this difference was significant, the personalized LPV$_i$ was better in over 79% of cases. For the whole *in-silico* population, despite no difference in the RMSE of both LPV$_i$ models was found, the personalized LPV$_i$ presents a better closed-loop performance. This highlights the relevance of model personalization considering the different dynamics that can be exhibit by different subjects.
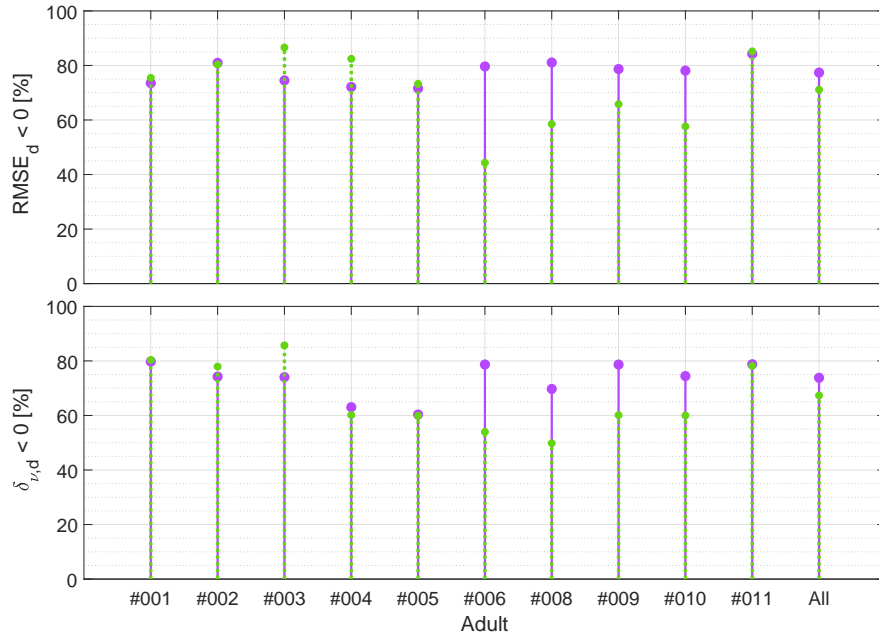
Figure 5.19: Percentage of cases of model improvement in terms of the RMSE ($RMSE_d < 0$) (top) and ν-gap ($\delta_{\nu,d} < 0$) (bottom) obtained with the average LPV$_i$ (green dotted lines) and personalized LPV$_i$ (violet solid lines) compared to the personalized LPV$_g$ for each *in silico* adult of the UVA/Padova simulator.

Table 5.3: Percentage of cases of model improvement in terms of the RMSE and ν-gap obtained with the personalized LPV$_i$ compared to the average LPV$_i$. h$_{RMSE}$ or h$_{\nu\text{-gap}}$ equal to one indicate a significant reduction on the average RMSE or ν-gap with the personalized LPV$_i$, considering a 5% significance.

Adult	$RMSE_d < 0$	h$_{RMSE}$	$\delta_{\nu,d} < 0$	h$_{\nu\text{-gap}}$
#001	20.83	0	46.28	0
#002	53.60	0	23.20	0
#003	27.42	0	33.53	0
#004	44.39	0	33.94	0
#005	24.92	0	36.47	0
#006	85.23	1	63.61	1
#008	79.65	1	81.70	1
#009	87.27	0	78.83	1
#010	95.24	1	82.86	1
#011	22.58	0	45.00	0
All	53.60	0	52.81	1

To determine if the average RMSE obtained with LPV$_i$ is lower than the one obtained with LPV$_g$ at all (g,S$_{I,VF}$) values, a two-sampled t-test was carried out for each *in-silico* adult. The same analysis was performed for the ν-gap to determine if including the S$_I$ variation in the controller design stage could lead to a better closed-loop performance. Test results for each adult and the whole population (row 'All') are presented in Table 5.4, along with the percentage of

$(g, S_{I,VF})$ values in which an improvement over LPV_g is obtained, both in open- and closed-loop.

Table 5.4: Percentage of cases of model improvement in terms of the RMSE and ν-gap obtained with the personalized LPV_i compared to the personalized LPV_g. $h_{RMSE,i}$ or $h_{\nu\text{-gap},i}$ equal to one indicate a significant reduction on the average RMSE or ν-gap with the personalized LPV_i, considering a 5% significance.

Adult	$RMSE_d < 0$	h_{RMSE}	$\delta_{\nu,d} < 0$	$h_{\nu\text{-gap}}$
#001	73.51	1	79.76	1
#002	80.96	0	74.24	1
#003	74.52	1	74.07	1
#004	72.12	1	63.03	1
#005	71.58	1	60.33	1
#006	79.63	1	78.69	1
#008	81.07	1	69.72	1
#009	78.68	1	78.68	1
#010	78.10	1	74.44	1
#011	84.24	1	78.79	1
All	77.39	1	73.82	1

According to Table 5.4, the open-loop and closed-loop metrics show an overall improvement using LPV_i above 73.8%. Take into account that the comparison measures were computed based on a simulated population and has an average significance. A better and more personalized result could be obtained by having clinical data from the S_I variations for a particular patient.

5.3 Concluding remarks

In this Chapter, a low-order model to design control laws for an AP including intra-patient variations is obtained from the UVA/Padova metabolic simulator, with a structure amenable for LPV controller design. Here, it is worth highlighting:

- The model is able to capture: *(i)* the nonlinear behavior of the glucose-insulin system, *(ii)* intra-patient variations related to daily insulin sensitivity (S_I) changes, and *(iii)* the large inter-subject variability, by personalizing the model based on *a priori* patient information.

- This model depends on two parameters, $p_1(g)$ and $k_s(g, S_{I,VF})$, which in turn are functions of the glucose concentration and insulin sensitivity factors, that can be computed in real-time.

- Model personalization is achieved by only adjusting the values of k_j, and not the average model structure, by using the subject's TDI, information that is available in real life for each patient, through a non-invasive procedure.

- A general average structure that is not dependent on a particular model that describes changes in S_I is obtained, so that it can be used in combination with any real-time S_I estimator.

- The proposed LPV_i was compared to the LPV_g model without the intra-patient variations in terms of its open- and closed-loop characteristics, through the RMSE and ν-gap, respectively. The proposed LPV_i showed better performance with smaller errors, highlighting the advantages of including S_I variations in the model's structure.

Chapter 6

Control-Oriented Model including hyperinsulinemia induced insulin resistance.

The delay in subcutaneous insulin absorption may lead to insulin "stacking" when the controller continues to infuse insulin in response to increasing glucose concentrations. This phenomena, together with prolonged glucose appearance after meal ingestion, might lead to situations of Hyperglycemic-Hyperinsulinemic (HGHI), which is associated to impaired insulin action in T1DM subjects. In Chapters 4 and 5 two different approaches to account for S_I variations were considered, without including the insulin-induced Insulin Resistance (IR) (reduced S_I).

Considering the relevance of this phenomenon in closed-loop control, in this chapter the LPV_g model is extended to include the HI effect on S_I, so it can also describe the HGHI region, by adding the patient's IOB as a model input. First, the effects of HGHI over S_I are described in Section 6.1. The identification procedure is described in Section 6.2, and the identified model with illustrative simulations that compare the proposed model with the UVA/Padova simulator are presented in Section 6.3. Finally, some conclusions are addressed in Section 6.4.

6.1 Hyperglycemia/Hyperinsulinemia in T1DM

IR is defined as a decreased biological response to a certain concentration in insulin [149]. This impairment in insulin action comprises both reduced insulin sensitivity and insulin responsiveness [150]. Several mechanisms can induce IR by interfering with the insulin signaling cascade, like hyperglucemia, elevated blood lipids and amino acids, and inherited variations in the signaling molecules. Additionally, evidences of HI-induced IR had been found in *in-vivo* studies in T1DM patients [42].

Glucose concentration plays a role in S_I. In severe hypoglycemia, a lower S_I is found induced by increased secretion of counter-regulatory hormones to protect against further decreases in plasma glucose concentration [42, 151]. Hyperglycemia also contributes to IR [42, 149] which might be a reflection of hypoinsulinemia, as increased peripheral insulin has been associated with down-regulation of peripheral insulin receptors [42–46].

Hyperglucemic/Hyperinsulinemic clamps evidenced decreased insulin response results in lower glycogen synthesis and increased gluconeogenesis, and thus enhanced EGP [150]. This last fact was also demonstrated in euglycemic/Hyperinsulinemic clamps, which indicate decreased hepatic S_I in subjects with T1DM. Moreover, hyperinsulinemia appears to increase whole-body and hepatic insulin resistance via abnormal mitochondrial function and prolonged oxidative stress [150]. This increased IR is considered a risk factor for development of micro and macrovascular complications [42, 149].

Designing a control law without considering the expected HI reduced S_I might prevent post-prandial hypoglycemic events, but would increase the risk for postprandial Hyperglycemia (HG). Therefore, considering this HI-induced reduced S_I would allow for a more reliable controller to be designed. Considering that these effects have not been considered in previous control-oriented models, next section focuses on developing a low-order model including the effect of HI in S_I.

6.2   Model Identification Procedure

In order to characterize the HGHI effects on S_I, the identification procedure is repeated to include the active IOB in the LPV_g model's structure, obtaining a new model, defined as LPV_{ins}.

The proposed structure is identified by starting from the linearization of the UVA/Padova metabolic model around a basal working point representing the steady state of the patient during fasting periods. Steady-state glucose concentrations ($g \in [40, 400]$ mg/dl) were achieved by only accommodating the insulin infusion rate. For each particular initial glucose concentration, the corresponding initial states of the UVA/Padova model were calculated, and the Insulin Infusion Rate (IIR) to maintain that glucose level was determined. Once each glucose concentration is achieved, HI was induced by increasing the IIR in a way that each patient's IOB reaches levels in the set $\{1, 2, 3, 4, 5, 6, 7, 8\}$ U. In order to maintain the steady-state glucose concentration for HI conditions, a plasmatic dextrosae infusion was computed for each HI level, as in hyperinsulinemic clamp methods [112]. Subsequently, for each *in-silico* adult, a linearized model from the subcutaneous-insulin delivery (pmol/min) to the subcutaneous-glucose concentration deviation (mg/dl) is calculated for each point of the (g, IOB) grid.

Since an average structure is pursued, instead of insulin infusion values, the IOB will be computed, because of its physiological significance (active insulin not yet used by the body). The IOB can be obtained from the past amounts of insulin following a simple model, specific to each subject, like the insulin compartment model in [152] (used in this work), or other IOB models [153].

Figure 6.1 and Figure 6.2 present the average variation of the BW and DCG, respectively, for LPV_g and all *in-silico* adults linearized at different g and IOB values.

Note that, for the basal case, both models coincide. For each glucose concentration a sensitivity decrease in HI conditions can be noted, due to the decrease in the constant gain of the
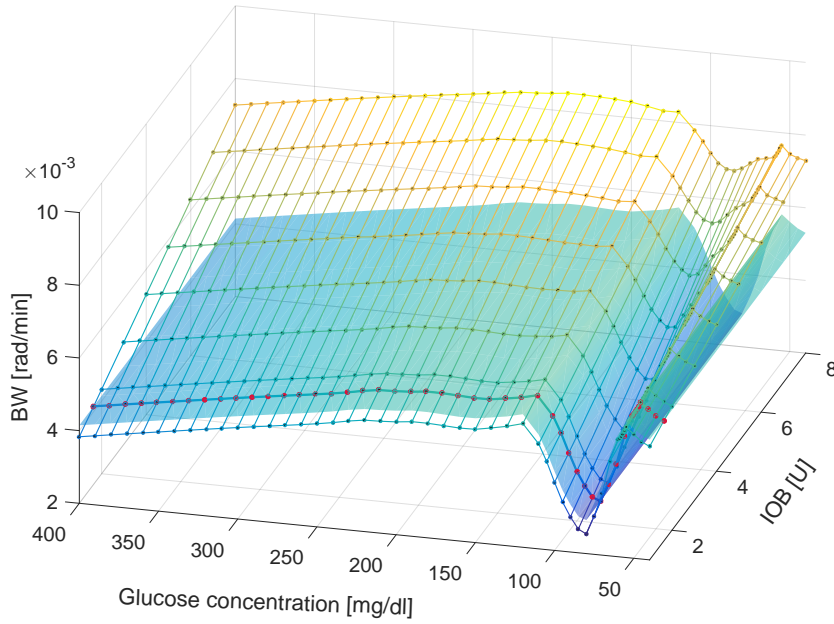
Figure 6.1: BW of LPV$_g$ (smooth surface) and average BW for all *in-silico* adults from the UVA/Padova simulator linearized at different g and IOB values (gridded surface). The red dotted line indicates the BW at basal IOB.
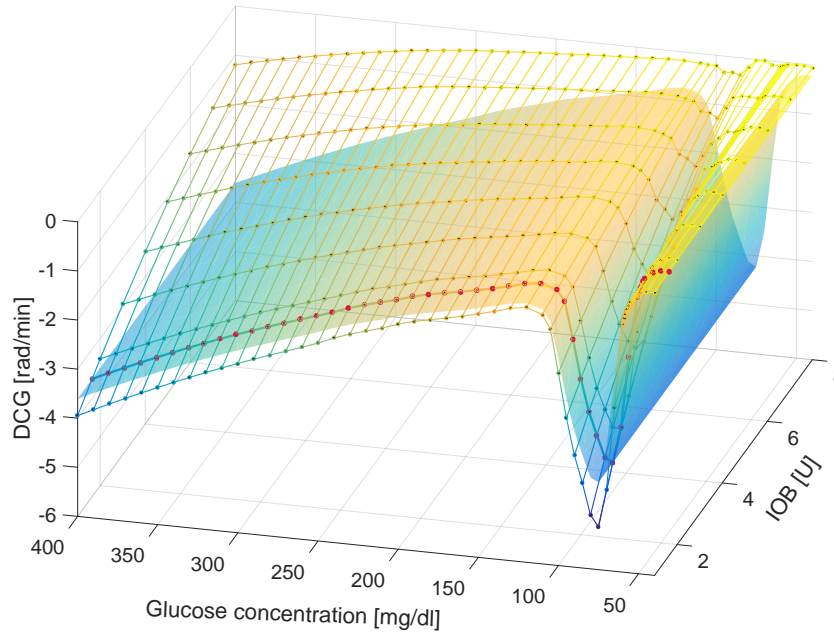
Figure 6.2: DCG of LPV$_g$ (smooth surface) and average DCG for all *in-silico* adults from the UVA/Padova simulator linearized at different g and IOB values (gridded surface). The red dotted line indicates the DCG at basal IOB.

model at high insulin infusions. These differences are more evident at high glucose concentrations (HG). The decrease in the model's gain module produces an increase in its BW, which will be reflected in the LPV model as a variation in pole p_1 as a function of both, g and IOB. Therefore, the LPV$_{ins}$ model has the average structure depicted in Figure 6.3
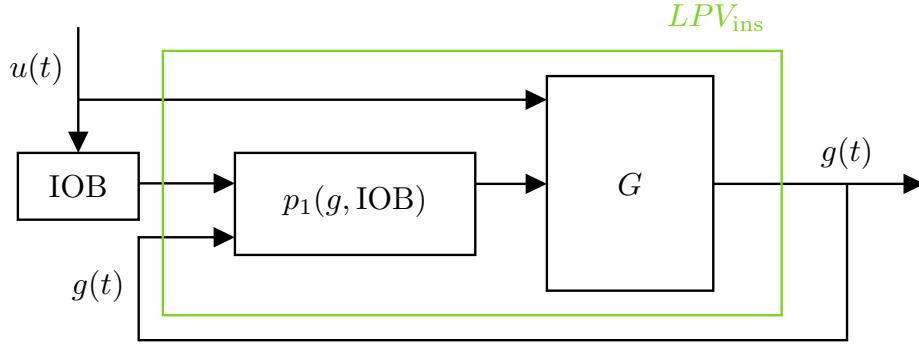
Figure 6.3: Average LPV$_{\text{ins}}$ model structure.

The BW definition is used to represent the S$_{\text{I}}$ variation detected in Figure 6.1, by making the BW of the proposed LPV$_{\text{ins}}$ model vary with the subcutaneous-glucose concentration g and IOB appropriately. As in [57], with variations of parameter p_1 the measured BW values can be reproduced. A decrease in the model's BW is associated with a decrease in the value of p_1, and as a consequence, an increase in the absolute value of the model's static gain. Therefore, the S$_{\text{I}}$ variations evidenced in Figure 6.2 would also be described by the p_1 variations.

Parameter p_1 is computed in order to make the BW of model (3.1) coincide with the BW of each linearized model in the (g, IOB) grid, through the following equation, considering all other parameters fixed at the values indicated in Section 3.3:

$$\frac{\left|\frac{j\omega^*}{z} + 1\right|}{\left|\frac{j\omega^*}{p_1} + 1\right|\left|\frac{j\omega^*}{p_2} + 1\right|\left|\frac{j\omega^*}{p_3} + 1\right|} = 10^{-3/20} \tag{6.1}$$

The result was then fitted by a piecewise polynomial function:

$$
\begin{aligned}
p_1(g, \text{ IOB}) = &\alpha_{1,n} + \alpha_{2,n}\, g \\
&+ \alpha_{3,n}\, \text{IOB} + \alpha_{4,n}\, g\, \text{IOB} \\
&+ \alpha_{5,n}\, g^2 + \alpha_{6,n}\, \text{IOB}^2 \\
&+ \alpha_{7,n}\, g^2\, \text{IOB} + \alpha_{8,n}\, g\, \text{IOB}^2 \quad \text{with} \quad n = \begin{cases} 1 & \text{if } g \geq 300 \\ 2 & \text{if } 130 \geq g < 300 \\ 3 & \text{if } 65 \geq g < 130 \\ 4 & \text{if } 59 \geq g < 65 \\ 5 & \text{if } g \leq 59 \end{cases} \\
&+ \alpha_{9,n}\, g^2\, \text{IOB}^2 + \alpha_{10,n}\, g^3 \\
&+ \alpha_{11,n}\, \text{IOB}^3 + \alpha_{12,n}\, g^3\, \text{IOB} \\
&+ \alpha_{13,n}\, g\, \text{IOB}^3 + \alpha_{14,n}\, g^4
\end{aligned}
\tag{6.2}
$$

Parameter values and goodness of fit for each interval are presented in Table 6.1. The goodness of fit was expressed as a fitting percentage obtained by:

$$\text{FIT} = 100\left(1 - \frac{\|p_{1,p} - p_1\|_2}{\|p_1 - \overline{p_1}\|_2}\right) \tag{6.3}$$

where $p_{1,p}$ is the predicted value, p_1 the real value and $\overline{p_1}$ its mean. Figure 6.4 presents the results

Table 6.1: Parameter values for $p_1(g, \text{IOB})$ from (6.2).

n	1	2	3	4	5
$\alpha_{1,n}$	7.278×10^{-03}	-4.573×10^{-03}	1.187×10^{-01}	5.850×10^{-01}	-6.614×10^{-01}
$\alpha_{2,n}$	-6.137×10^{-06}	1.971×10^{-04}	-3.814×10^{-03}	-3.057×10^{-02}	5.587×10^{-02}
$\alpha_{3,n}$	1.600×10^{-03}	-2.188×10^{-03}	7.762×10^{-03}	4.289×10^{-02}	7.431×10^{-02}
$\alpha_{4,n}$	-6.407×10^{-06}	4.283×10^{-05}	-1.218×10^{-04}	-1.348×10^{-03}	-4.541×10^{-03}
$\alpha_{5,n}$	5.998×10^{-10}	-1.184×10^{-06}	4.005×10^{-05}	5.376×10^{-04}	-1.753×10^{-03}
$\alpha_{6,n}$	2.337×10^{-04}	-3.653×10^{-04}	-5.392×10^{-04}	-2.768×10^{-04}	-4.430×10^{-04}
$\alpha_{7,n}$	1.585×10^{-08}	-8.068×10^{-08}	5.528×10^{-07}	1.071×10^{-05}	9.266×10^{-05}
$\alpha_{8,n}$	-1.132×10^{-06}	-1.509×10^{-06}	3.598×10^{-06}	3.933×10^{-06}	1.799×10^{-05}
$\alpha_{9,n}$	0	0	0	0	-1.977×10^{-07}
$\alpha_{10,n}$	-3.184×10^{-11}	2.049×10^{-09}	-1.340×10^{-07}	-3.145×10^{-06}	2.444×10^{-05}
$\alpha_{11,n}$	2.594×10^{-05}	8.247×10^{-05}	2.849×10^{-05}	1.221×10^{-05}	-4.097×10^{-06}
$\alpha_{12,n}$	0	0	0	0	-6.245×10^{-07}
$\alpha_{13,n}$	0	0	0	0	3.199×10^{-07}
$\alpha_{14,n}$	0	0	0	0	-1.275×10^{-07}
FIT	99.96	99.35	98.99	99.98	95.03

for $p_1(g, \text{IOB})$ and its smooth polynomial fitting. Note that a decrease in the model's BW is associated with a decrease in the value of p_1, and as a consequence, an increase in the absolute value of the model's static gain. Also, the higher pole values for HI conditions at each glucose concentration reflect the expected behavior of reduced S_I (since a lower DC gain is achieved).
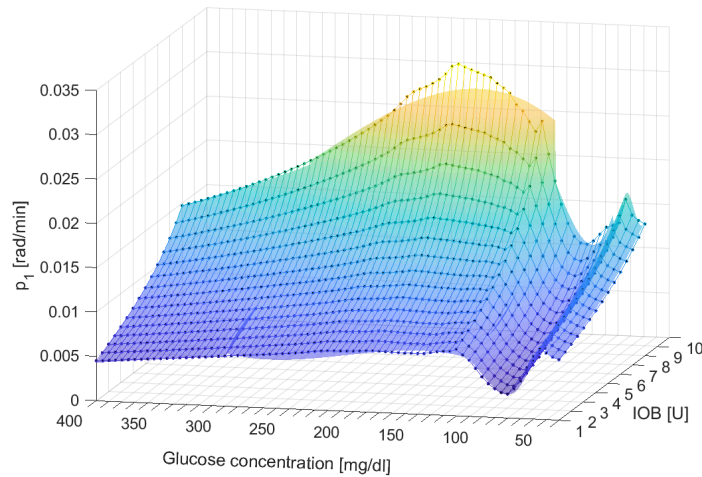
Figure 6.4: Parameter p_1 for different values of g and IOB (gridded surface) and piecewise polinomial function $p_1(g, \text{IOB})$ (smooth surface).

Finally, the average LPV_ins model with the state-space representation (3.4) can be obtained by including the glucose-varying parameter $p_1(g, \text{IOB})$ into the model structure (3.4).

6.2.1   Model tuning

As mentioned before, the inter-patient variability is considering by tuning the model to each patient according to the 1800-rule. Since each patient has a different TDI (TDI_j) a 1U insulin bolus produces a different glucose drop for each Adult #j. Hence, to tune the LPV_{ins} model, it is excited with a 1 U insulin bolus, starting from a glucose concentration g of 235 mg/dl and its correspondent IIR, and a suitable gain k_j is calculated to achieve the corresponding glucose drop given by $1800/TDI_j$. The personalized values of gain k for all *in-silico* adults are presented in Table 6.2.

Table 6.2: Personalized gain k_j for each *in-silico* adult.

Adult	TDI [U/day]	$k_j \times 10^{-5}$
#001	42	-2.3874
#002	43	-2.2290
#003	52	-1.9426
#004	35	-2.7706
#005	40	-2.3444
#006	72	-1.4160
#008	52	-1.7911
#009	34	-2.7764
#010	47	-2.0022
#011	39.9	-2.4198

6.3   Results and Discussion

In this Section, a comparison of both LPV_g and LPV_{ins} with respect to the UVA/Padova model is carried out both for simulation (open-loop) and controller synthesis (closed-loop) purposes. As in Chapter 5, the comparison is only made with the LPV_g considering it has a better fit to the UVA/Padova model than other previous control-oriented models [21, 50, 65].

6.3.1   Open-loop comparison

For each of the 10 *in-silico* subjects of the distribution version of the UVA/Padova simulator, an insulin bolus of 1 U was applied at different operating points on the (g, IOB) grid to test the three LPV models: *(i)* the average LPV_{ins} , *(ii)* the personalized LPV_{ins} and *(iii)* the LPV_g model in comparison with the UVA/Padova nonlinear models. Figures 6.5 to 6.7 presents the time-responses to a 1 U insulin bolus for multiple IOB values at basal glucose concentrations of 120, 180, and 240 mg/dl, for Adults #009 (most sensitive subject), #006 (least sensitive subject) and #011 (average subject).

Note that the reduced S_I is evidenced in the UVA/Padova model at higher IOB levels, and
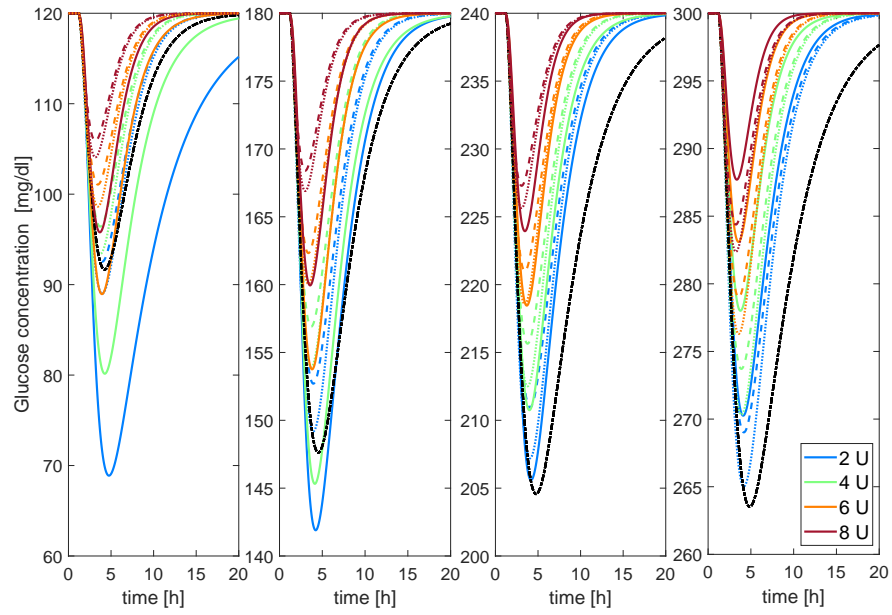
Figure 6.5: Responses to a 1 U insulin bolus starting from 120 mg/dl, 180 mg/dl, 240 mg/dl and 300 mg/dl at different IOB levels for models LPV$_g$ (black dash-dotted line), average LPV$_{ins}$ (dotted lines), personalized LPV$_{ins}$ (dashed lines) and the UVA/Padova nonlinear model (solid lines) for Adult #011.
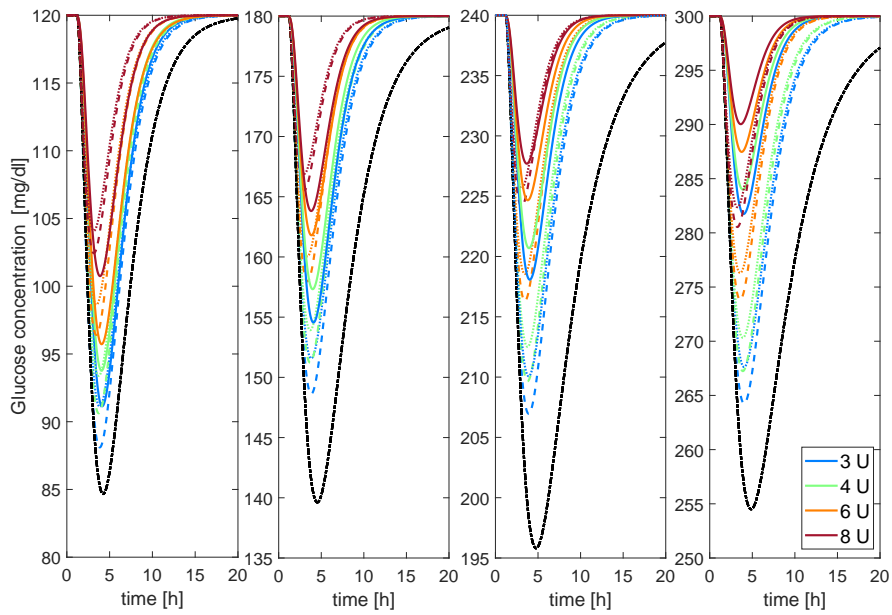
Figure 6.6: Responses to a 1 U insulin bolus starting from 120 mg/dl, 180 mg/dl, 240 mg/dl and 300 mg/dl at different IOB levels for models LPV$_g$ (black dash-dotted line), average LPV$_{ins}$ (dotted lines), personalized LPV$_{ins}$ (dashed lines) and the UVA/Padova nonlinear model (solid lines) for Adult #006.

that this behavior is captured by both the average and personalized LPV$_{ins}$ models, and not by the LPV$_g$ model, and this adjustment improves at hyperglucemic concentrations. In this case, despite differences between the responses of the average and personalized LPV$_{ins}$ models, personalization
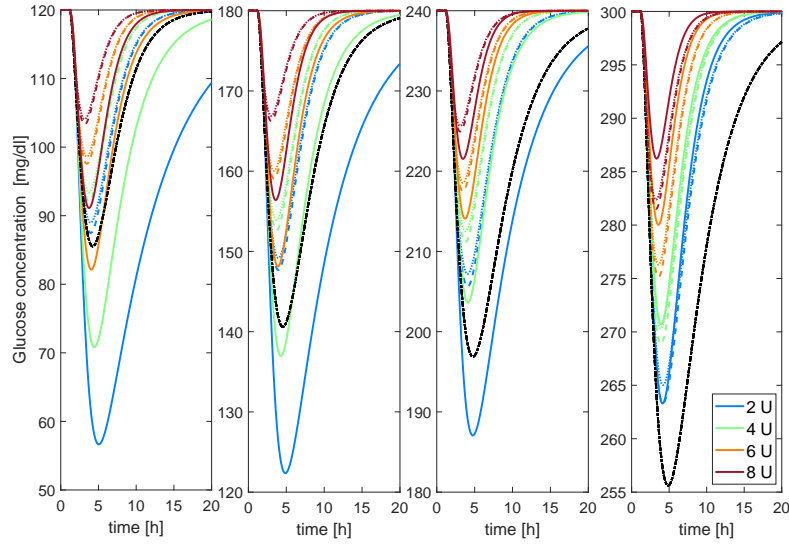
Figure 6.7: Responses to a 1 U insulin bolus starting from 120 mg/dl, 180 mg/dl, 240 mg/dl and 300 mg/dl at different IOB levels for models LPV_g (black dash-dotted line), average LPV_{ins} (dotted lines), personalized LPV_{ins} (dashed lines) and the UVA/Padova nonlinear model (solid lines) for Adult #009.

only improves the response of the LPV_{ins} for Adult #006.

For the three LPV models, the RMSE between their time-responses ($\boldsymbol{y_p}$) and the UVA/Padova model ($\boldsymbol{y}$), for each subject at each operating point on the (g,IOB) grid, was computed according to (5.5):

$$\text{RMSE} = \frac{\|\boldsymbol{y_p} - \boldsymbol{y}\|_2 \Delta t}{n_t} \tag{5.5}$$

In order to capture the complete glucose variation at each point, a number of $n_t = 1200$ points and $\Delta t = 1$ min were selected. In Figure 6.8, average values of the RMSE for all 10 *in-silico* adults at different g and IOB values are shown. Note that a lower RMSE can be obtained with LPV_{ins} (average and personalized) than with LPV_g for most glucose concentrations, and that this improvement becomes larger as HI increases (higher IOB). In this case, however, it appears that personalization through parameter k does not provide a large improvement, obtaining very similar RMSE with the average LPV_{ins} than with the personalized LPV_{ins}. It is also important to highlight that close to the basal IOB, the three models present similar errors, since in these cases parameters $p_1(g)$ and $p_1(g, \text{IOB})$ are very similar (given their relation through the UVA/Padova model's BW).

6.3.2   Closed-loop comparison

In this case, the ν-gap distance [139, 140] between each personalized LPV model and the UVA/Padova model linearized at all points of the (g, IOB) grid is computed. Figure 6.9 presents the average ν-gap for all 10 adults for three different levels of IOB, obtaining similar results as in the open loop comparison.
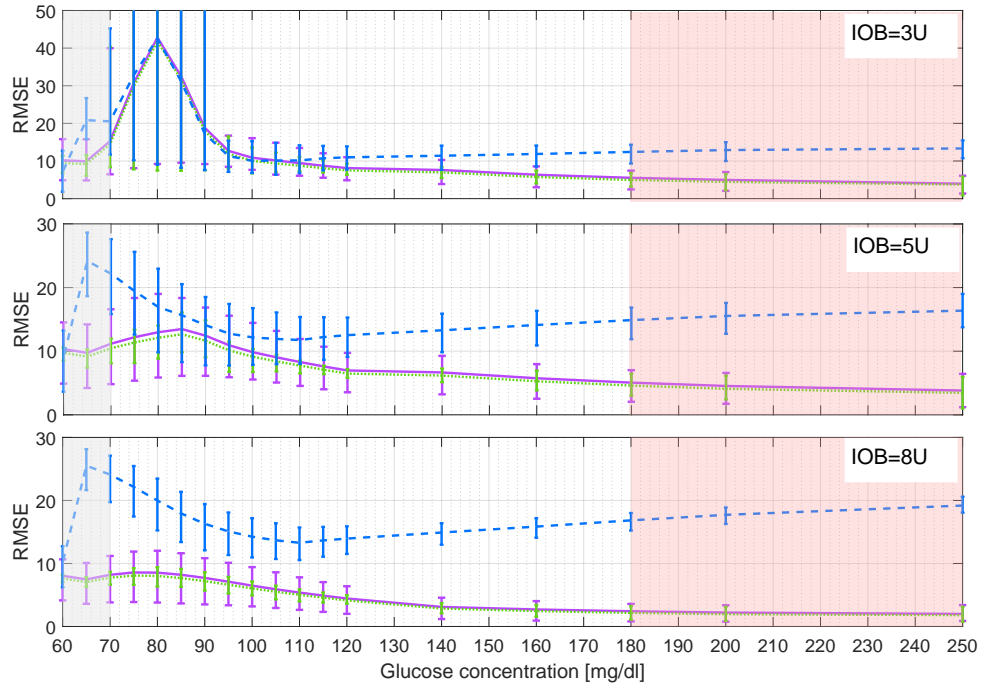
Figure 6.8: Average RMSE between the time-responses of the personalized LPV$_g$ (blue dashed lines), average LPV$_{ins}$ (green dotted lines) and personalized LPV$_{ins}$ (violet solid lines), as compared with the UVA/Padova nonlinear model to an insulin bolus of 1 U for IOB at 3U (top), 5U (middle) and 8U (bottom).
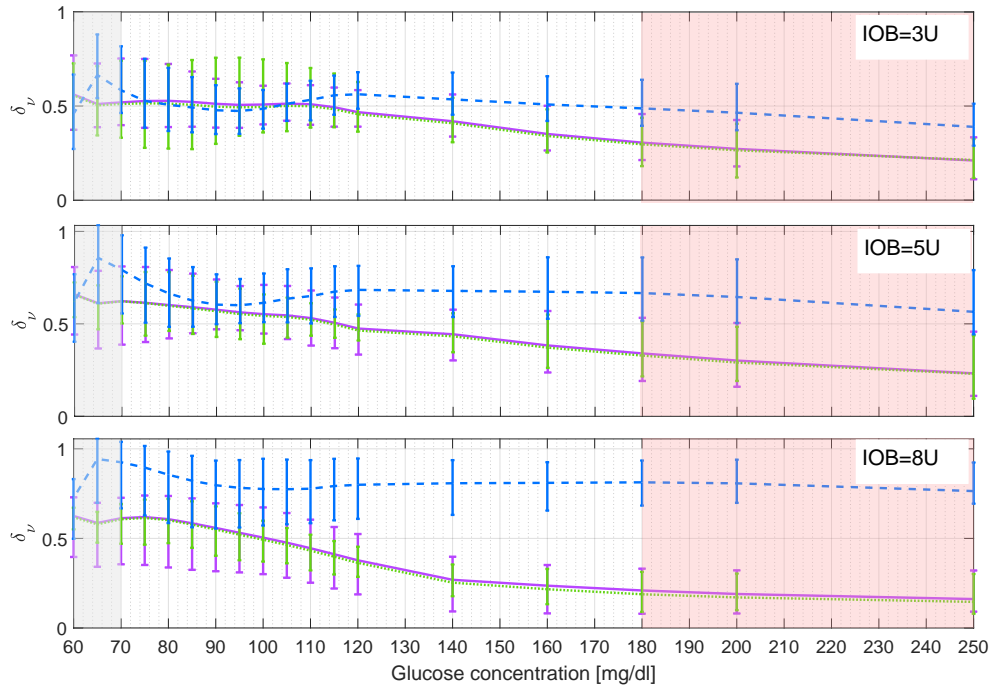
Figure 6.9: Average ν-gap (δ_ν) between the linearizations of the UVA/Padova nonlinear model and models LPV$_g$ (blue dashed lines), average LPV$_{ins}$ (green dotted lines) and personalized LPV$_{ins}$ (violet solid lines), as compared with the UVA/Padova nonlinear model to an insulin bolus of 1 U for IOB at 3U (top), 5U (middle) and 8U (bottom).

6.3.3   Overall comparison

The difference between the RMSE and ν-gap obtained with the three LPV models was computed for all (g,IOB) values considered, and all 10 *in-silico* adults, according to:

$$\delta_{\nu,d} = \delta_{\nu,\mathrm{LPV}_i} - \delta_{\nu,\mathrm{LPV}_g}; \qquad \mathrm{RMSE}_d = \mathrm{RMSE}_i - \mathrm{RMSE}_g \qquad (5.6)$$

Therefore, negative values of $\delta_{\nu,d}$ or RMSE_d indicate points where the personalized $\mathrm{LPV}_{\mathrm{ins}}$ outperforms the average $\mathrm{LPV}_{\mathrm{ins}}$ or the LPV_g .

Differences between the average $\mathrm{LPV}_{\mathrm{ins}}$ and personalized $\mathrm{LPV}_{\mathrm{ins}}$ relative to the LPV_g are presented in Figure 6.10. In this case, as suspected from the average RMSE and ν-gap, personalization does not imply a model improvement for all subjects, obtaining cases in which the average $\mathrm{LPV}_{\mathrm{ins}}$ outperforms the personalized $\mathrm{LPV}_{\mathrm{ins}}$.
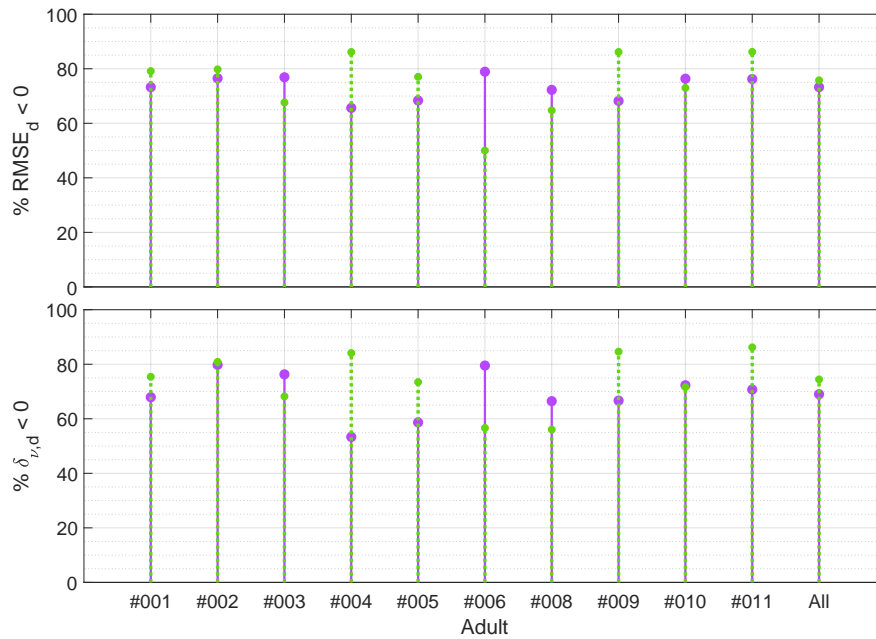
Figure 6.10: Percentage of cases of model improvement in terms of the RMSE (top) and ν-gap (bottom) obtained with the average $\mathrm{LPV}_{\mathrm{ins}}$ (green dotted lines) and personalized $\mathrm{LPV}_{\mathrm{ins}}$ (violet solid lines) compared to the personalized LPV_g for each *in silico* adult of the UVA/Padova simulator.

In order to determine if the differences found between the two models are significant, a two-sampled t-test was carried out for each *in-silico* adult, to determine whether the personalized $\mathrm{LPV}_{\mathrm{ins}}$ represents an improvement or not over the average $\mathrm{LPV}_{\mathrm{ins}}$. Results presented in Table 6.3 indicate that a significant improvement is achieved with the personalized $\mathrm{LPV}_{\mathrm{ins}}$ for the same number of cases than those to whom the average $\mathrm{LPV}_{\mathrm{ins}}$ is better. In most cases, no significant differences are found between these models, both in open- and closed-loop.

To determine if the average RMSE obtained with $\mathrm{LPV}_{\mathrm{ins}}$ is lower than the one obtained with

Table 6.3: Improvement analysis over the RMSE and ν-gap for all *in-silico* subjects, with a 5% significance. The $\surd$ marks indicate a significant improvement with the personalized LPV$_{ins}$, $\mathcal{X}$ where the average LPV$_{ins}$ is better, and $\varnothing$ where there are no significant differences between the two models.

Adult	RMSE$_d$	$\delta_{\nu,d}$
#001	$\varnothing$	$\varnothing$
#002	$\varnothing$	$\varnothing$
#003	$\surd$	$\surd$
#004	$\mathcal{X}$	$\mathcal{X}$
#005	$\varnothing$	$\mathcal{X}$
#006	$\surd$	$\surd$
#008	$\surd$	$\surd$
#009	$\mathcal{X}$	$\mathcal{X}$
#010	$\varnothing$	$\mathcal{X}$
#011	$\mathcal{X}$	$\mathcal{X}$
All	$\varnothing$	$\varnothing$

LPV$_g$ at all (g,IOB) values, a two-sampled t-test was carried out for each *in-silico* adult. The same analysis was performed for the ν-gap to determine if including the HI effects in the controller design stage could lead to a better closed-loop performance. Test results for each adult and the whole population (row 'All') are presented in Table 6.4, along with the percentage of (g,IOB) values in which an improvement over LPV$_g$ is obtained, both in open- and closed-loop.

According to Table 5.4, a significant improvement in RMSE and ν-gap is obtained in above 69% of cases with the LPV$_{ins}$ model, except for the RMSE of two subjects. However, further adjustment of the model, by fitting the gain variations could lead to better results than the sole representation of the influence of HI trough the pole's variation, as suggested from the results presented in Table 6.3. Figure 6.11 presents a comparison of the fitting of the linearized UVA/Padova models DCG and BW achieved with the personalized LPV$_{ins}$ model for the average subject. Note that the desired fitting of the BW variations is obtained, but further adjustment of the DCG would be necessary to improve the model's capabilities.

It must be noted that the validity of the UVA/Padova simulator is not always guaranteed in this region. However, these results evidence the importance of considering the HI effects over the glucose regulation dynamics on the controller design stage. Moreover, evidence on HI effects on glucose turnover during excercise have also been found [150, 154] and overall, HI effects continue to be studied since they are not fully understood.

Bearing in mind that *(i)* the effect of HI influences S$_I$, *(ii)* IOB effects are evidenced both in BW and DCG of the linearized UVA/Padova model, and *(iii)* S$_I$ effects are observed mostly in the DCG of the linearized UVA/Padova model, and *(iv)* further fitting of the DCG is needed, Figure 6.12 presents a possible model structure that could be explored to fully include the HI effects

Table 6.4: Percentage of cases of model improvement in terms of the RMSE and ν-gap obtained with the personalized LPV$_{ins}$ compared to the personalized LPV$_g$. $h_{RMSE,i}$ or $h_{\nu\text{-gap},i}$ equal to one indicate a significant reduction on the average RMSE or ν-gap with the personalized LPV$_{ins}$, considering a 5% significance.

Adult	RMSE$_d < 0$	h$_{RMSE}$	$\delta_{\nu,d} < 0$	h$_{\nu\text{-gap}}$
#001	73.3	0	67.9	1
#002	76.5	1	79.8	1
#003	76.9	1	76.3	1
#004	65.6	1	53.3	1
#005	68.4	0	58.7	1
#006	78.9	1	79.5	1
#008	72.2	1	66.5	1
#009	68.2	1	66.7	1
#010	76.4	1	72.3	1
#011	76.2	1	70.7	1
All	73.2	0	69.0	1
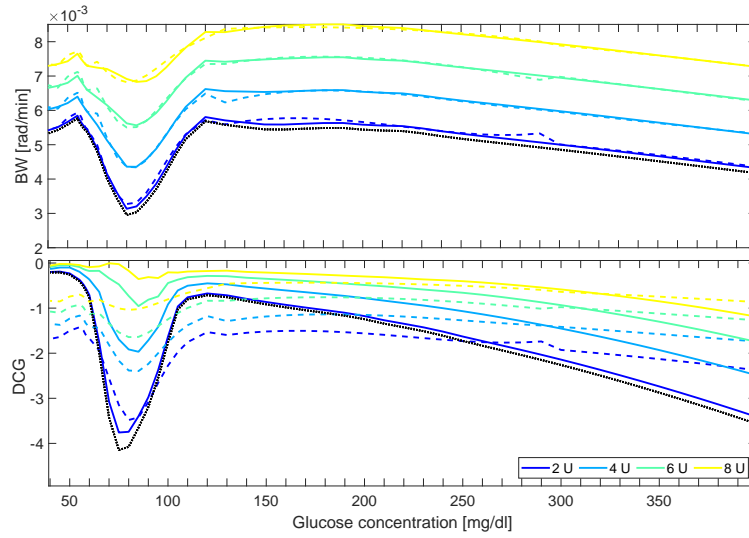
Figure 6.11: DCG (top) and BW (bottom) of average LPV$_{ins}$ (dotted lines), personalized LPV$_{ins}$ (dashed lines) and linearized UVA/Padova model (solid lines) for Adult #011, for different IOB above basal levels.

over glucose regulation. Here, parameters $p_1(g, \text{IOB})$ in (6.2) and $k_{avg}(g, S_{I,VF})$ in (5.2) could be used together with an S_I estimator that, among others, also considers IOB as a parameter. Moreover, the average structure with $p_1(g, \text{IOB})$ could be used in IOB-based safety mechanisms in order to inform this layer of the effects of insulin stacking.
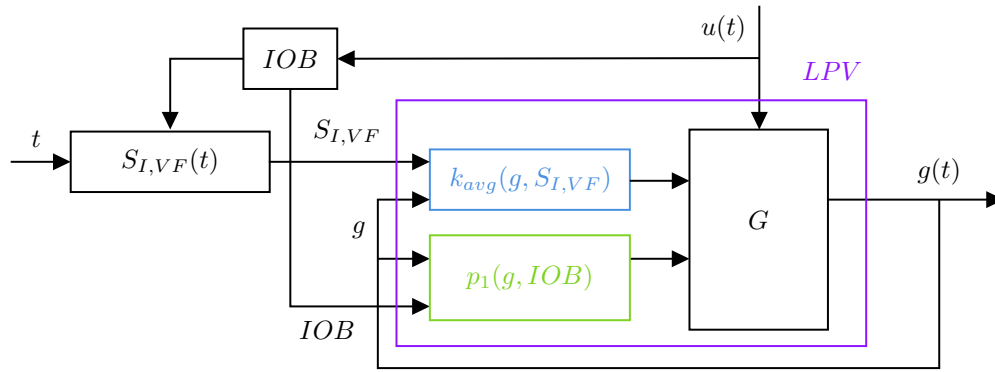
Figure 6.12: Proposed control-oriented LPV model structure

6.4 Concluding remarks

Here a control-oriented model of the HGHI region has been presented, which extends previous results to variations with glucose and insulin. The latter is represented here by the IOB which has an important significance for control performance, particularly to avoid hypoglycemic and sustained hyperglycemic events. Here, it is worth highlighting:

- An average (affine) LPV model is obtained, which allows to include the effect of active insulin on the patient's S_I. The effectiveness of the model compared to the LPV_g evidenced the importance of including the effects of insulin stacking during the controller-design stage.

- This model would be helpfull during post-prandial periods by informing the continuous controller of possible increased insulin resistance so it is able to adjust insulin infusion accordingly, while actively considering past insulin infusions. Moreover, it could be useful in safety IOB-based mechanisms, giving the controller a more informed effect of the active insulin in the organism.

- Further research needs to be done in order to obtain more definite results on the inclusion of the effects of active insulin concentration on glucose regulation and obtaining a more effective model that considers them.

Chapter 7

Conclusions and Future Work

This work presented a review of the current challenges in the design of control algorithms for AP, highlighting the relevance of control-oriented model personalization for improving the performance of the controller and the inclusion of dynamic and parametric uncertainties, specially related to variations in S_I.

Previous models of intra-patient variability have been developed considering average S_I profiles. In terms of the large inter-patient variability, it is not possible to obtain a single diurnal S_I pattern for the T1DM population as a whole, and therefore, the specific S_I variation for each subject should be considered when designing control algorithms.

The main strategy for model personalization is to adapt the model according to physiological parameters like CR, TDI or by personalized identification based on historical clinical data. Previous models do not consider intra-day variations of S_I and parametric uncertainty has not been directly addressed, specially for robust control techniques that would be more suitable for the time-varying nature of the problem.

Starting from a previously developed LPV (LPV_g) model for the glucose-insulin dynamics, in this thesis two approaches for including S_I variations in control-oriented models are explored:

1. Use of dynamic uncertainty bounds for covering S_I variations, obtaining an LPV model set. This was carried out by means of an invalidation procedure, that allowed to obtain an LPV model-set that accounts for both dynamic and parametric uncertainties. This model-set is an essential elemental for robust control design, and was used for obtaining a switched LPV controller. The controller design based on this model set proved to be advantageous when dynamic and parametric uncertainties appear in the problem. An illustrative example presents a robust controller that successfully copes with uncertainties in the nonlinear dynamics (changes in the glucose values) and variations in S_I, as compared to a nominal design, where these uncertainties are not considered. In this way, robustness to uncertain model dynamics or modelling errors, which is an essential feature for AP control, is achieved.

2. Include S_I variations into the model structure. In this regard, a low-order model was obtained from the UVA/Padova metabolic simulator, with a structure amenable for LPV controller

design. This model depends on two parameters, $p_1(g)$ and $k_s(g, S_{I,VF})$, which in turn are functions of the glucose concentration and insulin sensitivity factors, that can be computed in real-time. In this way, the model structure is able to capture the nonlinear behavior of the glucose-insulin system, intra-patient variations related to S_I changes, and inter-subject variability, by personalizing the model based on *a priori* patient information. This is achieved with an average structure that is not dependent on a particular model that describes changes in S_I and therefore, can be used together with any available S_I temporal profile, or even one including other factors that influence S_I suitable for the specific subject. The proposed LPV$_i$ showed better performance with smaller errors, both for simulation and controller design purposes, highlighting the advantages of including S_I variations in the model's structure.

Additionally, an LPV model including the HGHI induced IR (reduced S_I) effects was developed as an extension of the LPV$_g$. An improvement on the closed-loop performance of the new model was obtained, evidencing the importance of considering this phenomenon in the controller design stage. However, future work is needed to improve the simulation capabilities of this model.

After completing this work, the following aspects could be explored towards complementing the outcome of this thesis:

1. Development of a S_I model that is able to reflect its variations due to several factors, like physical exercise, stress, sleep cycles and active insulin concentrations, that allows the real-time estimation of the subject's S_I. In this way, not only circadian variations could be considered, but also slow but consistent changes in insulin needs beyond the scope of a single day.

2. Development of a complete LPV model that accounts for both S_I variations and HI effects, that allow to condense the results obtained with the LPV$_i$ and LPV$_{ins}$ models and in turn, improve controller performance by anticipating these effects inside its structure.

3. The invalidation procedure carried out in Chapter 4 considered the worst case uncertainty bound for each patient. An LPV uncertainty weight could be developed exploiting the S_I variations. Moreover, this time-varying uncertainty weight can be used together with the LPV$_i$ model as the nominal model in the invalidation procedure. This would allow to obtain tighter uncertainty bounds for the LPV model family, and possibly better performance of the controllers designed with this model, in terms of reduction of hyperglycemic events.

4. Extension of the LPV$_i$ model and S_I models for adolescents and children. These are the age groups at higher risk of hypoglycemia given their increased activity levels and changing hormonal systems influenced by puberty (increased growth hormone and sex hormone secretion). Moreover, the consequences of hypoglycemic events are distinctly different between adults and children. These factors would need to be addressed for a better and safer control design for this population.

Bibliography

[1] Centers for Disease Control and Prevention, "National diabetes statistics report: Estimates of diabetes and its burden in the United States, 2014," *Atlanta, GA: US Department of Health and Human Services*, 2014.

[2] Diabetes Control and Complications Trial Research Group, "The effect of intensive treatment of diabetes on the development and progression of long-term complications in insulin-dependent diabetes mellitus," *New England Journal of Medicine*, vol. 329, no. 14, pp. 977–986, 1993.

[3] A. Chait and K. E. Bornfeldt, "Diabetes and atherosclerosis: Is there a role for hyperglycemia?," *J. Lipid Res.*, vol. 50, pp. S335–S339, Apr. 2009.

[4] J. Mastrototaro, "The minimed continuous glucose monitoring system (cgms)," *J Pediatr Endocrinol Metab*, vol. 12, no. 13, pp. 751–758, 1999.

[5] D. C. Klonoff, "Continuous glucose monitoring: roadmap for 21st century diabetes therapy," *Diabetes care*, vol. 28, no. 5, pp. 1231–1239, 2005.

[6] J. Pickup, H. Keen, J. Parsons, and K. Alberti, "Continuous subcutaneous insulin infusion: an approach to achieving normoglycaemia.," *Br Med J*, vol. 1, no. 6107, pp. 204–207, 1978.

[7] A. Haidar, "The artificial pancreas: How closed-loop control is revolutionizing diabetes," *IEEE Control Systems*, vol. 36, no. 5, pp. 28–47, 2016.

[8] T. Ly, A. Roy, B. Grosman, J. Shin, A. Campbell, S. Monirabbasi, B. Liang, R. von Eyben, S. Shanmugham, P. Clinton, and B. A. Buckingham, "Day and night closed-loop control using the integrated Medtronic hybrid closed-loop system in type 1 diabetes at diabetes camp," *Diabetes Care*, vol. 38, pp. 1205–1211, Jul 2015.

[9] L. Bally, H. Thabit, H. Kojzar, J. K. Mader, J. Qerimi-Hyseni, S. Hartnell, M. Tauschmann, J. M. Allen, M. E. Wilinska, T. R. Pieber, M. L. Evans, and R. Hovorka, "Day-and-night glycaemic control with closed-loop insulin delivery versus conventional insulin pump therapy in free-living adults with well controlled type 1 diabetes: An open-label, randomised, crossover study," *Lancet Diabetes Endocrinol.*, vol. 5, pp. 261–270, Apr 2017.

[10] B. P. Kovatchev, P. Cheng, S. M. Anderson, J. E. Pinsker, F. Boscari, B. A. Buckingham, F. J. Doyle III, K. K. Hood, S. A. Brown, M. D. Breton, D. Chernavvsky, W. C. Bevier, P. K. Bradley, D. Bruttomesso, S. Del Favero, R. Calore, C. Cobelli, A. Avogaro, T. T. Ly, S. Shanmugham, E. Dassau, C. Kollman, J. W. Lum, and R. W. Beck, "Feasibility of long-term closed-loop control: A multicenter 6-month trial of 24/7 automated insulin delivery," *Diabetes Technol. Ther.*, vol. 19, no. 1, pp. 18–24, 2017.

[11] G. P. Forlenza, S. Deshpande, T. T. Ly, D. P. Howsmon, F. Cameron, N. Baysal, E. Mauritzen, T. Marcal, L. Towers, B. W. Bequette, L. M. Huyett, J. E. Pinsker, R. Gondhalekar, F. J. Doyle III, D. M. Maahs, B. A. Buckingham, and E. Dassau, "Application of zone model predictive control artificial pancreas during extended use of infusion set and sensor: A randomized crossover-controlled home-use trial," *Diabetes Care*, vol. 40, no. 8, pp. 1096–1102, 2017.

[12] M. Messori, J. Kropff, S. Del Favero, J. Place, R. Visentin, R. Calore, C. Toffanin, F. Di Palma, G. Lanzola, A. Farret, F. Boscari, S. Galasso, A. Avogaro, P. Keith-Hynes, B. P. Kovatchev, D. Bruttomesso, L. Magni, J. H. DeVries, E. Renard, C. Cobelli, and for the AP@home consortium, "Individually adaptive artificial pancreas in subjects with type 1 diabetes: A one-month proof-of-concept trial in free-living conditions," *Diabetes Technol. Ther.*, vol. 19, no. 10, pp. 560–571, 2017.

[13] G. Marchetti, M. Barolo, L. Jovanovič, H. Zisser, and D. E. Seborg, "An improved PID switching control strategy for type 1 diabetes," *IEEE Transactions on Biomedical Engineering*, vol. 55, no. 3, pp. 857–865, 2008.

[14] J. L. Sherr, E. Cengiz, C. C. Palerm, B. Clark, N. Kurtz, A. Roy, L. Carria, M. Cantwell, W. V. Tamborlane, and S. A. Weinzimer, "Reduced hypoglycemia and increased time in target using closed-loop insulin delivery during nights with or without antecedent afternoon exercise in type 1 diabetes," *Diabetes Care*, vol. 36, no. 10, pp. 2909–2914, 2013.

[15] R. Hovorka, D. Elleri, H. Thabit, J. Allen, L. Leelarathna, R. El-Khairi, K. Kumareswaran, K. Caldwell, P. Calhoun, C. Kollman, H. Murphy, C. Acerini, M. Wilinska, M. Nodale, and D. Dunger, "Overnight closed-loop insulin delivery in young people with type 1 diabetes: A free-living, randomized clinical trial," *Diabetes Care*, vol. 37, no. 5, pp. 1204–1211, 2014.

[16] F. Cameron, G. Niemeyer, D. M. Wilson, B. W. Bequette, K. S. Benassi, P. Clinton, and B. A. Buckingham, "Inpatient trial of an artificial pancreas based on multiple model probabilistic predictive control with repeated large unannounced meals," *Diabetes Technology & Therapeutics*, vol. 16, no. 11, pp. 728–734, 2014.

[17] P. Colmegna, F. Garelli, H. D. Battista, and R. Sánchez-Peña, "Automatic regulatory control in type 1 diabetes without carbohydrate counting," *Control Eng. Pract.*, vol. 74, pp. 22–32, 2018.

[18] M. Messori, G. P. Incremona, C. Cobelli, and L. Magni, "Individualized model predictive control for the artificial pancreas: In silico evaluation of closed-loop glucose control," *IEEE Contr. Syst. Mag.*, vol. 38, no. 1, pp. 86–104, 2018.

[19] P. Soru, G. De Nicolao, C. Toffanin, C. Dalla Man, C. Cobelli, L. Magni, and on behalf of the AP@home consortium, "MPC based Artificial Pancreas : Strategies for individualization and meal compensation," *Annu. Rev. Control*, vol. 36, pp. 118–128, 2012.

[20] R. Gondhalekar, E. Dassau, and F. J. Doyle III, "Periodic zone-MPC with asymmetric costs for outpatient-ready safety of an artificial pancreas to treat type 1 diabetes," *Automatica*, vol. 71, pp. 237–246, Sept. 2016.

[21] P. Colmegna, R. S. Sánchez-Peña, R. Gondhalekar, E. Dassau, and F. J. Doyle III, "Switched LPV glucose control in type 1 diabetes," *IEEE Trans. Biomed. Eng.*, vol. 63, pp. 1192–1200, June 2016.

[22] P. Colmegna, R. S. Sánchez-Peña, R. Gondhalekar, E. Dassau, and F. J. Doyle III, "Reducing glucose variability due to meals and postprandial exercise in T1DM using switched LPV control: In silico studies," *J. Diabetes Sci. Technol.*, vol. 10, pp. 744–753, May 2016.

[23] R. S. Sánchez-Peña and A. Ghersin, "LPV control of glucose for diabetes type I," in *32nd Annual International Conference* (IEEE EMBS, ed.), (Buenos Aires, Argentina), pp. 680–683, 2010.

[24] P. Colmegna and R. Sánchez-Peña, "Linear parameter-varying control to minimize risks in type 1 diabetes," *IFAC Proceedings Volumes*, vol. 47, no. 3, pp. 9253 – 9257, 2014. 19th IFAC World Congress.

[25] L. Kovács, B. Kulcsár, J. Bokor, and Z. Benyó, "Model-based nonlinear optimal blood glucose control of type I diabetes patients," in *30th Annual International IEEE EMBS Conference*, (Vancouver, BC, Canada), pp. 1607–1610, 2008.

[26] L. Kovács, B. Benyó, J. Bokor, and Z. Benyó, "Induced $\mathcal{L}_2$-norm minimization of glucose-insulin system for type I diabetic patients," *Comput. Meth. Progr. Bio.*, vol. 102, pp. 105–118, May 2011.

[27] P. Colmegna, R. S. Sánchez-Peña, R. Gondhalekar, E. Dassau, and F. J. Doyle III, "Reducing risks in type 1 diabetes using $\mathcal{H}_\infty$ control," *IEEE Trans. Biomed. Eng.*, vol. 61, pp. 2939–2947, Dec. 2014.

[28] E. Ruiz-Velázquez, R. Femat, and D. Campos-Delgado, "Blood glucose control for type I diabetes mellitus: A robust tracking $\mathcal{H}_\infty$ problem," *Control Engineering Practice*, vol. 12, no. 9, pp. 1179–1195, 2004.

[29] R. S. Parker, F. J. Doyle III, J. H. Ward, and N. A. Peppas, "Robust $\mathcal{H}_\infty$ glucose control in diabetes using a physiological model," *AIChE Journal*, vol. 46, no. 12, pp. 2537–2549, 2000.

[30] C. C. Palerm, H. Zisser, L. Jovanovič, and F. J. Doyle III, "A run-to-run control strategy to adjust basal insulin infusion rates in type 1 diabetes," *Journal of Process Control*, vol. 18, pp. 258–265, 2008.

[31] K. Turksoy, L. Quinn, E. Littlejohn, and A. Cinar, "Multivariable adaptive identification and control for artificial pancreas systems," *IEEE Trans. Biomed. Eng.*, vol. 61, no. 3, pp. 883–891, 2014.

[32] D. Shi, E. Dassau, and F.J. Doyle III, "Adaptive zone model predictive control of artificial pancreas based on glucose- and velocity-dependent control penalties," *IEEE Transactions on Biomedical Engineering*, 2018.

[33] R. S. Sánchez-Peña and D. Cherñavvsky, eds., *The Artificial Pancreas: Current Situation and Future Directions*. Academic Press (Elsevier), 2019.

[34] D. S. Carrasco, Y. Fu, and G. C. Goodwin, "Performance limitations arising in closed loop control of blood glucose in type 1 diabetes," *19th IFAC World Congress*, vol. 1, no. 3, pp. 2082–2087, 2014.

[35] L. M. Huyett, E. Dassau, H. C. Zisser, and F. J. Doyle III, "Glucose sensor dynamics and the artificial pancreas: The impact of lag on sensor measurement and controller performance," *IEEE Control Systems*, vol. 38, no. 1, pp. 30–46, 2018.

[36] H. Wolpert, M. Kavanagh, A. Atakov-Castillo, and G. Steil, "The artificial pancreas: evaluating risk of hypoglycaemia following errors that can be expected with prolonged at-home use," *Diabetic Medicine*, vol. 33, no. 2, pp. 235–242, 2016.

[37] E. R. Damiano, F. H. El-Khatib, H. Zheng, D. M. Nathan, and S. J. Russell, "A comparative effectiveness analysis of three continuous glucose monitors," *Diabetes Care*, vol. 36, no. 2, pp. 251–259, 2013.

[38] C. Cobelli, E. Renard, and B. P. Kovatchev, "Artificial pancreas: Past, present, future," *Diabetes*, vol. 60, pp. 2672–2682, Nov. 2011.

[39] G. M. Steil, A. E. Panteleon, and K. Rebrin, "Closed-loop insulin delivery-the path to physiological glucose control," *Adv. Drug Deliv. Rev.*, vol. 56, pp. 125–144, Feb 2004.

[40] J. Walsh, R. Roberts, and L. Heinemann, "Confusion regarding duration of insulin action: A potential source for major insulin dose errors by bolus calculators," *J. Diabetes Sci. Technol.*, vol. 8, pp. 170–178, Jan 2014.

[41] B. W. Bequette, "Challenges and recent progress in the development of a closed-loop artificial pancreas," *Annu. Rev. Control*, vol. 36, pp. 255–266, Dec 2012.

[42] C. L. Chan, L. Pyle, R. Morehead, A. Baumgartner, M. Cree-Green, and K. J. Nadeau, "The role of glycemia in insulin resistance in youth with type 1 and type 2 diabetes," *Pediatric diabetes*, vol. 18, no. 6, pp. 470–477, 2017.

[43] J. R. Gavin, J. Roth, D. M. Neville, P. De Meyts, and D. N. Buell, "Insulin-dependent regulation of insulin receptor concentrations: a direct demonstration in cell culture," *Proceedings of the National Academy of Sciences*, vol. 71, no. 1, pp. 84–88, 1974.

[44] M. H. Shanik, Y. Xu, J. Škrha, R. Dankner, Y. Zick, and J. Roth, "Insulin resistance and hyperinsulinemia," *Diabetes Care*, vol. 31, no. Supplement 2, pp. S262–S268, 2008.

[45] H.-Y. Liu, S. Y. Cao, T. Hong, J. Han, Z. Liu, and W. Cao, "Insulin is a stronger inducer of insulin resistance than hyperglycemia in mice with type 1 diabetes mellitus (t1dm)," *Journal of Biological Chemistry*, pp. jbc–M109, 2009.

[46] Y. Lee, J. D. Fluckey, S. Chakraborty, and M. Muthuchamy, "Hyperglycemia-and hyperinsulinemia-induced insulin resistance causes alterations in cellular bioenergetics and activation of inflammatory signaling in lymphatic muscle," *The FASEB Journal*, vol. 31, no. 7, pp. 2744–2759, 2017.

[47] F. León-Vargas, F. Garelli, H. De Battista, and J. Vehí, "Postprandial response improvement via safety layer in closed-loop blood glucose controllers," *Biomedical Signal Processing and Control*, vol. 16, pp. 80–87, 2015.

[48] G. M. Steil, C. C. Palerm, N. Kurtz, G. Voskanyan, A. Roy, S. Paz, and F. R. Kandeel, "The effect of insulin feedback on closed loop glucose control," *The Journal of Clinical Endocrinology & Metabolism*, vol. 96, no. 5, pp. 1402–1408, 2011.

[49] L. Hinshaw, C. Dalla Man, D. K. Nandy, A. Saad, A. E. Bharucha, J. A. Levine, R. A. Rizza, R. Basu, R. E. Carter, C. Cobelli, *et al.*, "Diurnal pattern of insulin action in type 1 diabetes: implications for a closed loop system," *Diabetes*, p. DB_121759, 2013.

[50] K. van Heusden, E. Dassau, H. C. Zisser, D. E. Seborg, and F. J. Doyle III, "Control-relevant models for glucose control using *a priori* patient characteristics," *IEEE Trans. Biomed. Eng.*, vol. 59, pp. 1839–1849, July 2012.

[51] C. Toffanin, S. Del Favero, E. Aiello, M. Messori, C. Cobelli, and L. Magni, "Glucose-insulin model identified in free-living conditions for hypoglycaemia prevention," *Journal of Process Control*, vol. 64, pp. 27–36, 2018.

[52] C. Toffanin, H. Zisser, F. J. Doyle III, and E. Dassau, "Dynamic insulin on board: Incorporation of circadian insulin sensitivity variation.," *Journal of Diabetes Science and Technology*, vol. 7, no. 4, pp. 928–940, 2013.

[53] M. Messori, M. Ellis, C. Cobelli, P. D. Christofides, and L. Magni, "Improved postprandial glucose control with a customized model predictive controller," in *2015 American Control Conference (ACC)*, pp. 5108–5115, July 2015.

[54] M. Messori, C. Toffanin, S. D. Favero, G. De Nicolao, C. Cobelli, and L. Magni, "Model individualization for artificial pancreas," *Comput. Meth. Prog. Bio.*, vol. (2016). DOI: 10.1016/j.cmpb.2016.06.006, 2016.

[55] I. Hajizadeh, M. Rashid, K. Turksoy, S. Samadi, J. Feng, M. Sevil, N. Frantz, C. Lazaro, Z. Maloney, E. Littlejohn, *et al.*, "Multivariable recursive subspace identification with application to artificial pancreas systems," *IFAC-PapersOnLine*, vol. 50, no. 1, pp. 886–891, 2017.

[56] I. Contreras, S. Oviedo, M. Vettoretti, R. Visentin, and J. Vehí, "Personalized blood glucose prediction: A hybrid approach using grammatical evolution and physiological models," *PloS one*, vol. 12, no. 11, p. e0187754, 2017.

[57] P. Colmegna, R. Sánchez-Peña, and R. Gondhalekar, "Linear parameter-varying model to design control laws for an artificial pancreas," *Biomed. Signal Process. Control*, vol. 40, pp. 204–213, Feb 2018.

[58] L. Magni, D. M. Raimondo, C. Dalla Man, M. Breton, S. Patek, G. De Nicolao, C. Cobelli, and B. P. Kovatchev, "Evaluating the efficacy of closed-loop glucose regulation via control-variability grid analysis," *J. Diabetes Sci. Technol.*, vol. 2, pp. 630–635, July 2008.

[59] D. de Pereda, S. Romero-Vivo, B. Ricarte, and J. Bondia, "On the prediction of glucose concentration under intra-patient variability in type 1 diabetes: A monotone systems approach," *Comput. Meth. Prog. Bio.*, vol. 108, no. 3, pp. 993–1001, 2012.

[60] E. Van Cauter, K. S. Polonsky, and A. J. Scheen, "Roles of circadian rhythmicity and sleep in human glucose regulation," *Endocrine Reviews*, vol. 18, no. 5, pp. 716–738, 1997.

[61] S. E. La Fleur, "Daily rhythms in glucose metabolism: Suprachiasmatic nucleus output to peripheral tissue," *Journal of Neuroendocrinology*, vol. 15, no. 3, pp. 315–322, 2003.

[62] E. Haus, "Chronobiology in the endocrine system," *Advanced Drug Delivery Reviews*, vol. 59, no. 9, pp. 985–1014, 2007.

[63] C. Cobelli, C. Dalla Man, M. Schiavon, A. Basu, and Y. C. Kudva, "Estimation of insulin sensitivity from CGM and subcutaneous insulin delivery in type 1 diabetes," 2013. US Patent App. 13/661,755.

[64] S. Oviedo, J. Vehí, R. Calm, and J. Armengol, "A review of personalized blood glucose prediction strategies for t1dm patients," *International Journal for Numerical Methods in Biomedical Engineering*, vol. 33, no. 6, pp. e2833–n/a, 2017.

[65] J. Lee, E. Dassau, D. Seborg, and F. J. Doyle III, "Model-based personalization scheme of an artificial pancreas for type 1 diabetes applications," in *American Control Conference (ACC)*, (Washington, DC, USA), pp. 2911–2916, 2013.

[66] J. Bondia, S. Romero-Vivo, B. Ricarte, and J. L. Diez, "Insulin estimation and prediction: A review of the estimation and prediction of subcutaneous insulin pharmacokinetics in closed-loop glucose control," *IEEE Contr. Syst. Mag.*, vol. 38, no. 1, pp. 47–66, 2018.

[67] S. Miller, R. Nimri, E. Atlas, E. A. Grunberg, and M. Phillip, "Automatic learning algorithm for the md-logic artificial pancreas system," *Diabetes technology & therapeutics*, vol. 13, no. 10, pp. 983–990, 2011.

[68] J. E. Youssef, J. R. Castle, D. L. Branigan, R. G. Massoud, M. E. Breen, P. G. Jacobs, B. W. Bequette, and W. K. Ward, "A controlled study of the effectiveness of an adaptive closed-loop algorithm to minimize corticosteroid-induced stress hyperglycemia in type 1 diabetes," *Journal of diabetes science and technology*, pp. 1312–1326, 2011.

[69] F. H. El-Khatib, S. J. Russell, D. M. Nathan, R. G. Sutherlin, and E. R. Damiano, "A bi-hormonal closed-loop artificial pancreas for type 1 diabetes," *Science translational medicine*, vol. 2, no. 27, pp. 27ra27–27ra27, 2010.

[70] S. A. Weinzimer, G. M. Steil, K. L. Swan, J. Dziura, N. Kurtz, and W. V. Tamborlane, "Fully automated closed-loop insulin delivery versus semiautomated hybrid control in pediatric patients with type 1 diabetes using an artificial pancreas," *Diabetes Care*, vol. 31, pp. 934–939, May 2008.

[71] A. S. Brazeau, H. Mircescu, K. Desjardins, C. Leroux, I. Strychar, J. M. Ekoé, and R. Rabasa-Lhoret, "Carbohydrate counting accuracy and blood glucose variability in adults with type 1 diabetes," *Diabetes Res. Clin. Pract.*, vol. 99, pp. 19–23, Jan 2013.

[72] A. Haidar, D. Farid, A. St-Yves, V. Messier, V. Chen, D. Xing, A.-S. Brazeau, C. Duval, B. Boulet, L. Legault, *et al.*, "Post-breakfast closed-loop glucose control is improved when accompanied with carbohydrate-matching bolus compared to weight-dependent bolus," *Diabetes & metabolism*, vol. 40, no. 3, pp. 211–214, 2014.

[73] F. H. El-Khatib, C. Balliro, M. A. Hillard, K. L. Magyar, L. Ekhlaspour, M. Sinha, D. Mondesir, A. Esmaeili, C. Hartigan, M. J. Thompson, S. Malkani, J. P. Lock, D. M. Harlan, P. Clinton, E. Frank, D. M. Wilson, D. DeSalvo, L. Norlander, T. Ly, B. A. Buckingham, J. Diner, M. Dezube, L. A. Young, A. Goley, M. S. Kirkman, J. B. Buse, H. Zheng, R. R. Selagamsetty, E. R. Damiano, and S. J. Russell, "Home use of a bihormonal bionic pancreas versus insulin pump therapy in adults with type 1 diabetes: A multicentre randomised crossover trial," *Lancet*, vol. 389, pp. 369–380, Jan 2017.

[74] V. Gingras, R. Rabasa-Lhoret, V. Messier, M. Ladouceur, L. Legault, and A. Haidar, "Efficacy of dual-hormone artificial pancreas to alleviate the carbohydrate-counting burden of type 1 diabetes: A randomized crossover trial," *Diabetes Metab.*, vol. 42, pp. 47–54, Feb 2016.

[75] V. Gingras, A. Haidar, V. Messier, L. Legault, M. Ladouceur, and R. Rabasa-Lhoret, "A simplified semiquantitative meal bolus strategy combined with single- and dual-hormone closed-loop delivery in patients with type 1 diabetes: A pilot study," *Diabetes Technol. Ther.*, vol. 18, pp. 464–471, Aug 2016.

[76] L. Kovács, B. Kulcsár, J. Bokor, and Z. Benyó, "LPV fault detection of glucose-insulin system," in *14th Mediterranean Conference on Control and Automation*, (Ancona, Italy), pp. 1–5, 2006.

[77] F. Bianchi, **M. Moscoso-Vásquez**, P. Colmegna, and R. Sánchez-Peña, "Invalidation and low-order model set for artificial pancreas robust control design," *Journal of Process Control*, 2019. https://doi.org/10.1016/j.jprocont.2019.02.004.

[78] R. N. Bergman, Y. Ider, C. Bowden, and C. Cobelli, "Quantitative estimation of insulin sensitivity," *Am. J. Physiol.*, vol. 236, pp. E667–677, June 1979.

[79] R. Hovorka, L. Chassin, S. D. Luzio, R. Playle, and D. R. Owens, "Pancreatic β-cell responsiveness during meal tolerance test: model assessment in normal subjects and subjects with newly diagnosed noninsulin-dependent diabetes mellitus," *The Journal of Clinical Endocrinology & Metabolism*, vol. 83, no. 3, pp. 744–750, 1998.

[80] P. G. Fabietti, V. Canonico, M. O. Federici, M. M. Benedetti, and E. Sarti, "Control oriented model of insulin and glucose dynamics in type 1 diabetics," *Medical and Biological Engineering and Computing*, vol. 44, no. 1-2, pp. 69–78, 2006.

[81] C. Dalla Man, F. Micheletto, D. Lv, M. Breton, B. P. Kovatchev, and C. Cobelli, "The UVA/PADOVA type 1 diabetes simulator: New features," *J. Diabetes Sci. Technol.*, vol. 8, pp. 26–34, Jan. 2014.

[82] B. P. Kovatchev, M. Breton, C. Dalla Man, and C. Cobelli, "*In silico* preclinical trials: A proof of concept in closed-loop control of type 1 diabetes," *J. Diabetes Sci. Technol.*, vol. 3, pp. 44–55, Jan. 2009.

[83] R. Visentin, E. Campos-Náñez, M. Schiavon, D. Lv, M. Vettoretti, M. Breton, B. P. Kovatchev, C. D. Man, and C. Cobelli, "The uva/padova type 1 diabetes simulator goes from single meal to single day," *Journal of Diabetes Science and Technology*, vol. 12, no. 2, pp. 273–281, 2018.

[84] J. T. Sorensen, *A physiologic model of glucose metabolism in man and its use to design and assess improved insulin therapies for diabetes*. PhD thesis, Massachusetts Institute of Technology, 1985.

[85] M. E. Wilinska, L. J. Chassin, C. L. Acerini, J. M. Allen, D. B. Dunger, and R. Hovorka, "Simulation environment to evaluate closed-loop insulin delivery systems in type 1 diabetes.," *Journal of Diabetes Science and Technology*, vol. 4, no. 1, pp. 132–144, 2010.

[86] R. S. Sánchez-Peña and F. Bianchi, "Model selection: from LTI to switched-LPV," in *American Control Conference (ACC)*, (Montreal, Canada), pp. 1561–1566, 2012.

[87] L. Kovács and B. Kulcsár, "LPV modeling of type I diabetes mellitus," in *8th International Symposium of Hungarian Researchers*, (Budapest, Hungary), pp. 163–173, 2007.

[88] R. S. Sánchez-Peña, A. Ghersin, and F. Bianchi, "Time varying procedures for diabetes type 1 control," *Journal of Electrical and Computer Engineering*, 2011. Special Issue Electrical and Computer Technology for Effective Diabetes Management and Treatment.

[89] R. Sánchez-Peña, P. Colmegna, F. Garelli, H. De Battista, D. García-Violini, **M. Moscoso-Vásquez**, N. Rosales, E. Fushimi, E. Campos-Náñez, M. Breton, *et al.*, "Artificial pancreas: Clinical study in latin america without premeal insulin boluses," *Journal of diabetes science and technology*, vol. 12, no. 5, pp. 914–925, 2018.

[90] P. Colmegna, F. Garelli, E. Fushimi, **M. Moscoso-Vásquez**, N. Rosales, D. García-Violini, H. D. Battista, and R. Sánchez-Peña, "Artificial pancreas: The argentine experience," *Science Reviews*, vol. 1, no. 1, 2019.

[91] **M. Moscoso-Vásquez**, P. Colmegna, and R. Sánchez-Peña, "Intra-patient dynamic variations in type 1 diabetes: A review," in *2016 IEEE Conference on Control Applications (CCA)*, pp. 416–421, Sept 2016.

[92] **M. Moscoso-Vásquez**, P. Colmegna, and R. Sánchez-Peña, "Control-oriented model with intra-patient variations for glucose regulation in type 1 diabetes." Submitted to Biomedical Signal Processing and Control, February 4th 2019.

[93] **M. Moscoso-Vásquez**, P. Colmegna, and R. Sánchez-Peña, "Model of Hyperglycemia-Hyperinsulinemia effects for the Artificial Pancreas control," Oct 2019. *submitted to 2019 IEEE Colombian Conference Automatic Control (CCAC)*.

[94] W. G. Blackard, C. Barlascini, J. N. Clore, and J. E. Nestler, "Morning insulin requirements: Critique of dawn and meal phenomena," *Diabetes*, vol. 38, no. 3, pp. 273–277, 1989.

[95] M. García-Jaramillo, R. Calm, J. Bondia, and J. Vehí, "Prediction of postprandial blood glucose under uncertainty and intra-patient variability in type 1 diabetes: A comparative study of three interval models," *Comput. Meth. Prog. Bio.*, vol. 108, no. 1, pp. 224–233, 2012.

[96] T. Gibson, L. Stimmler, R. J. Jarrett, P. Rutland, and M. Shiu, "Diurnal variation in the effects of insulin on blood glucose, plasma non-esterified fatty acids and growth hormone," *Diabetologia*, vol. 11, no. 1, pp. 83–88, 1975.

[97] F. Porcellati, P. Lucidi, G. B. Bolli, and C. G. Fanelli, "Thirty years of research on the dawn phenomenon: Lessons to optimize blood glucose control in diabetes," *Diabetes Care*, vol. 36, no. 12, pp. 3860–3862, 2013.

[98] G. Perrielo, P. De Feo, E. Torlone, C. G. Fanelli, F. Santeusanio, P. Brunetti, and G. B. Bolli, "The dawn phenomenon in type 1 (insulin-dependent) diabetes mellitus: Magnitude, frequency, variability and dependence on glucose counterregulation and insulin sensitivity," *Diabetologia*, vol. 34, pp. 21–28, 1991.

[99] G. Scheiner and B. A. Boyer, "Characteristics of basal insulin requirements by age and gender in type-1 diabetes patients using insulin pump therapy," *Diabetes Research and Clinical Practice*, vol. 69, no. 1, pp. 14–21, 2005.

[100] M. Schiavon, L. Hinshaw, A. Mallad, C. Dalla Man, G. Sparacino, M. Johnson, R. Carter, R. Basu, Y. Kudva, C. Cobelli, and A. Basu, "Postprandial glucose fluxes and insulin sensitivity during exercise: A study in healthy individuals," *American Journal of Physiology. Endocrinology and Metabolism*, vol. 305, no. 4, pp. E557–566, 2013.

[101] R. N. Bergman, L. S. Phillips, and C. Cobelli, "Physiologic evaluation of factors controlling glucose tolerance in man: Measurement of insulin sensitivity and beta-cell glucose sensitivity from the response to intravenous glucose.," *Journal of Clinical Investigation*, vol. 68, no. 6, pp. 1456–1467, 1981.

[102] N. Moøller and J. O. L. Jørgensen, "Effects of growth hormone on glucose, lipid, and protein metabolism in human subjects," *Endocrine Reviews*, vol. 30, no. 2, pp. 152–177, 2009.

[103] M. Schiavon, C. Dalla Man, Y. C. Kudva, A. Basu, and C. Cobelli, "Quantitative estimation of insulin sensitivity in type 1 diabetic subjects wearing a sensor augmented insulin pump," *Diabetes care*, vol. 37, no. 5, pp. 39–49, 2013.

[104] P. Herrero, P. Pesl, J. Bondia, M. Reddy, N. Oliver, P. Georgiou, and C. Toumazou, "Method for automatic adjustment of an insulin bolus calculator: In silico robustness evaluation under intra-day variability," *Computer Methods and Programs in Biomedicine*, vol. 119, no. 1, pp. 1–8, 2015.

[105] R. Hovorka, V. Canonico, L. J. Chassin, U. Haueter, M. Massi-Benedetti, M. O. Federici, T. R. Pieber, H. C. Schaller, L. Schaupp, T. Vering, *et al.*, "Nonlinear model predictive control of glucose concentration in subjects with type 1 diabetes," *Physiological Measurement*, vol. 25, no. 4, pp. 905–920, 2004.

[106] R. Visentin, C. Dalla Man, Y. C. Kudva, A. Basu, and C. Cobelli, "Circadian variability of insulin sensitivity: Physiological input for in silico artificial pancreas," *Diabetes Technology & Therapeutics*, vol. 17, no. 1, pp. 1–7, 2015.

[107] C. Dalla Man, D. M. Raimondo, R. Rizza, and C. Cobelli, "GIM, simulation software of meal glucose-insulin model," *J. Diabetes Sci. Technol.*, vol. 1, pp. 323–330, May 2007.

[108] C. Cobelli, C. Dalla Man, G. Sparacino, L. Magni, G. De Nicolao, and B. P. Kovatchev, "Diabetes: Models, signals, and control," *IEEE Reviews in Biomedical Engineering*, vol. 2, pp. 54–96, 2009.

[109] B. P. Kovatchev, M. Breton, C. Dalla Man, and C. Cobelli, "In silico preclinical trials: A proof of concept in closed-loop control of type 1 diabetes," *J. Diabetes Sci. Technol.*, vol. 3, pp. 44–55, Jan. 2009.

[110] P. Herrero, P. Pesl, M. Reddy, N. Oliver, P. Georgiou, and C. Toumazou, "Advanced insulin bolus advisor based on run-to-run control and case-based reasoning," *IEEE journal of biomedical and health informatics*, vol. 19, no. 3, pp. 1087–1096, 2015.

[111] J. Tuo, H. Sun, D. Shen, H. Wang, and Y. Wang, "Optimization of insulin pump therapy based on high order run-to-run control scheme," *Computer Methods and Programs in Biomedicine*, vol. 120, no. 3, pp. 123–134, 2015.

[112] R. A. DeFronzo, J. D. Tobin, and R. Andres, "Glucose clamp technique: a method for quantifying insulin secretion and resistance.," *American Journal of Physiology-Endocrinology And Metabolism*, vol. 237, no. 3, p. E214, 1979.

[113] C. Dalla Man, A. Caumo, R. Basu, R. Rizza, G. Toffolo, and C. Cobelli, "Minimal model estimation of glucose absorption and insulin sensitivity during an oral test: validation of a nontracer against a tracer method," *American Journal of Physiology-Endocrinology and Metabolism*, 2004.

[114] A. Caumo, R. N. Bergman, and C. Cobelli, "Insulin sensitivity from meal tolerance tests in normal subjects: A minimal model index," *Journal of Clinical Endocrinology and Metabolism*, vol. 85, no. 11, pp. 4396–4402, 2000.

[115] M. Schiavon, R. Visentin, C. Dalla Man, and C. Cobelli, "Modeling inter-day variability of insulin sensitivity in type 1 diabetic subjects from 1 month outpatient artificial pancreas data," in *Diabetes Technology & Therapeutics*, vol. 20, pp. A17–A17, 2018.

[116] A. J. Laguna, P. Rossetti, F. J. Ampudia-Blasco, J. Vehí, and J. Bondia, "Identification of intra-patient variability in the postprandial response of patients with type 1 diabetes," *Biomed. Signal Proces.*, vol. 12, no. 1, pp. 39–46, 2014.

[117] S. S. Kanderian, S. Weinzimer, G. Voskanyan, and G. M. Steil, "Identification of intraday metabolic profiles during closed-loop glucose control in individuals with type 1 diabetes," *Journal of Diabetes Science and Technology*, vol. 3, no. 5, pp. 1047–1057, 2009.

[118] P. Vicini, A. Caumo, and C. Cobelli, "The hot ivgtt two-compartment minimal model: indexes of glucose effectiveness and insulin sensitivity," *American Journal of Physiology-Endocrinology And Metabolism*, vol. 273, no. 5, pp. E1024–E1032, 1997.

[119] E. D. Lehmann and T. Deutsch, "A physiological model of glucose-insulin interaction in type 1 diabetes mellitus," *J. Biomed. Eng.*, vol. 14, pp. 235–242, May 1992.

[120] P. Colmegna and R. Sánchez-Peña, "Analysis of three T1DM simulation models for evaluating robust closed-loop controllers," *Comput. Meth. Prog. Bio.*, vol. 113, no. 1, pp. 371–382, 2014.

[121] P. G. Fabietti, V. Canonico, M. O. Federici, M. M. Benedetti, and E. Sarti, "Control oriented model of insulin and glucose dynamics in type 1 diabetics," *Med. Biol. Eng. Comput.*, vol. 44, pp. 69–78, Mar. 2006.

[122] E. Dassau, H. Zisser, R. Harvey, M. Percival, B. Grosman, W. Bevier, E. Atlas, S. Miller, R. Nimri, L. Jovanovič, and F. J. Doyle III, "Clinical evaluation of a personalized artificial pancreas," *Diabetes Care*, vol. 36, pp. 801–809, Apr. 2013.

[123] S. Schaller, S. Willmann, J. Lippert, L. Schaupp, T. R. Pieber, A. Schuppert, and T. Eissing, "A generic integrated physiologically based whole-body model of the glucose-insulin-glucagon regulatory system," *CPT: Pharmacometrics & Syst. Pharmacol.*, vol. 2, pp. 1–10, Aug. 2013.

[124] S. S. Kanderian, S. A. Weinzimer, and G. M. Steil, "The identifiable virtual patient model: Comparison of simulation and clinical closed-loop study results," *J. Diabetes Sci. Technol.*, vol. 6, pp. 371–379, Mar. 2012.

[125] Q. Wang, P. Molenaar, S. Harsh, K. Freeman, J. Xie, C. Gold, M. Rovine, and J. Ulbrecht, "Personalized state-space modeling of glucose dynamics for type 1 diabetes using continuously monitored glucose, insulin dose, and meal intake: An extended Kalman filter approach," *J. Diabetes Sci. Technol.*, vol. 8, pp. 331–345, Mar. 2014.

[126] J. Walsh and R. Roberts, *Pumping Insulin*. Torrey Pines Press, San Diego, CA, 4 ed., 2006.

[127] F. M. Cameron, G. Niemeyer, and B. W. Bequette, "Extended multiple model prediction with application to blood glucose regulation," *J. Process Contr.*, vol. 22, pp. 1422–1432, Sep 2012.

[128] N. Magdelaine, L. Chaillous, I. Guilhem, J. Poirier, M. Krempf, C. H. Moog, and E. Le Carpentier, "A long-term model of the glucose–insulin dynamics of type 1 diabetes," *IEEE Transactions on Biomedical Engineering*, vol. 62, pp. 1546–1552, June 2015.

[129] L. F. Colorado, J. L. Godoy, and P. S. Rivadeneira, "Parametric identification of a new model for type 1 diabetic patients," in *2017 IEEE 3rd Colombian Conference on Automatic Control (CCAC)*, pp. 1–6, Oct 2017.

[130] Y. Ruan, M. E. Wilinska, H. Thabit, and R. Hovorka, "Modeling day-to-day variability of glucose–insulin regulation over 12-week home use of closed-loop insulin delivery," *IEEE Transactions on Biomedical Engineering*, vol. 64, pp. 1412–1419, June 2017.

[131] L. Griva, M. Breton, and M. Basualdo, "Análisis del método wiener para modelado del sistema endocrino de pacientes con diabetes mellitus tipo 1," in *V Simposio Argentino de Informática Industrial (SII 2016)-JAIIO 45 (Tres de Febrero, 2016)*, 2016.

[132] E. I. Georga, V. C. Protopappas, D. Ardigò, M. Marina, I. Zavaroni, D. Polyzos, and D. I. Fotiadis, "Multivariate prediction of subcutaneous glucose concentration in type 1 diabetes patients based on support vector regression," *IEEE Journal of Biomedical and Health Informatics*, vol. 17, pp. 71–81, Jan 2013.

[133] D. K. Rollins, N. Bhandari, J. Kleinedler, K. Kotz, A. Strohbehn, L. Boland, M. Murphy, D. Andre, N. Vyas, G. Welk, and W. E. Franke, "Free-living inferential modeling of blood glucose level using only noninvasive inputs," *Journal of Process Control*, vol. 20, no. 1, pp. 95 – 107, 2010.

[134] C. Toffanin, A. Sandri, M. Messori, C. Cobelli, and L. Magni, "Automatic adaptation of basal therapy for type 1 diabetic patients: a run-to-run approach," *IFAC Proceedings Volumes*, vol. 47, no. 3, pp. 2070–2075, 2014.

[135] J. Garcia-Tirado, C. Zuluaga-Bedoya, and M. D. Breton, "Identifiability analysis of three control-oriented models for use in artificial pancreas systems," *Journal of diabetes science and technology*, p. 1932296818788873, 2018.

[136] P. Szalay, G. Eigner, and L. A. Kovács, "Linear matrix inequality-based robust controller design for type-1 diabetes model," in *19th IFAC World Congress*, (Cape Town, South Africa), pp. 9247–9252, 2014.

[137] J. T. Sorensen, *A physiologic Model of Glucose Metabolism in Man and its Use to Design and Asses Improved Insulin Therapies for Diabetes*. PhD thesis, Massachusetts Institute of Technology, Cambridge, MA, USA, 1985.

[138] R. Hovorka, F. Shojaee-Moradie, P. Carroll, L. Chassin, I. Gowrie, N. Jackson, R. Tudor, A. Umpleby, and R. Jones, "Partitioning glucose distribution/transport, disposal, and endogenous production during IVGTT," *Am. J. Physiol. Endocrinol. Metab.*, vol. 282, pp. E992–1007, May 2002.

[139] G. Vinnicombe, *Uncertainty and Feedback: $\mathcal{H}_\infty$ Loop-shaping and the ν-gap metric*. London: Imperial College Press, 2001.

[140] G. Vinnicombe, "Frequency domain uncertainty and the graph topology," *IEEE Trans. Autom. Control*, vol. 38, pp. 1371–1383, Sept. 1993.

[141] R. Smith, G. Dullerud, S. Rangan, and K. Poolla, "Model validation for dynamically uncertain systems," *Math. Comp. Model. Dyn*, vol. 3, no. 1, pp. 43–58, 1997.

[142] R. S. Smith, *Model validation for uncertain systems*. PhD thesis, California Institute of Technology, 1990.

[143] M. Sznaier and M. C. Mazzaro, "An LMI approach to control-oriented identification and model (in)validation of LPV systems," *IEEE Trans Automat Contr*, vol. 48, no. 9, pp. 1619–1624, 2003.

[144] K. R. Popper, *Conjectures and Refutations: The Growth of Scientific Knowledge*. London: Routledge, 1963.

[145] F. D. Bianchi and R. S. Sánchez-Peña, "Robust identification/invalidation in an lpv framework," *International Journal of Robust and Nonlinear Control*, vol. 20, no. 3, pp. 301–312, 2010.

[146] C. Dalla Man, F. Micheletto, D. Lv, M. Breton, B. P. Kovatchev, and C. Cobelli, "The UVA/PADOVA type 1 diabetes simulator: New features," *J. Diabetes Sci. Technol.*, vol. 8, pp. 26–34, Jan. 2014.

[147] R. Basu, M. L. Johnson, Y. C. Kudva, and A. Basu, "Exercise, hypoglycemia, and type 1 diabetes," *Diabetes Technology & Therapeutics*, vol. 16, no. 6, p. 331, 2014.

[148] K. Turksoy, L. Quinn, E. Littlejohn, and A. Cinar, "Multivariable adaptive identification and control for artificial pancreas systems," *IEEE Transactions on Biomedical Engineering*, vol. 61, no. 3, pp. 883–891, 2014.

[149] E. Donga, O. M. Dekkers, E. P. Corssmit, and J. A. Romijn, "Insulin resistance in patients with type 1 diabetes assessed by glucose clamp studies: systematic review and meta-analysis," *European journal of endocrinology*, vol. 173, no. 1, pp. 101–109, 2015.

[150] K. Kaul, M. Apostolopoulou, and M. Roden, "Insulin resistance in type 1 diabetes mellitus," *Metabolism*, vol. 64, no. 12, pp. 1629–1639, 2015.

[151] B. P. Kovatchev, L. S. Farhy, D. J. Cox, M. Straume, V. I. Yankov, L. A. Gonder-Frederick, and W. L. Clarke, "Modeling insulin-glucose dynamics during insulin induced hypoglycemia. evaluation of glucose counterregulation," *Computational and Mathematical Methods in Medicine*, vol. 1, no. 4, pp. 313–323, 1999.

[152] C. Dalla Man, R. Rizza, and C. Cobelli, "Meal simulation model of the glucose-insulin system," *IEEE Trans. Biomed. Eng.*, vol. 54, pp. 1740–1749, Oct. 2007.

[153] M. E. Wilinska, L. J. Chassin, H. C. Schaller, L. Schaupp, T. R. Pieber, and R. Hovorka, "Insulin kinetics in type-1 diabetes: continuous and bolus delivery of rapid acting insulin," *IEEE Transactions on Biomedical Engineering*, vol. 52, no. 1, pp. 3–12, 2005.

[154] D. Romeres, A. Basu, M. Schiavon, C. Cobelli, C. Dalla Man, and R. Basu, "Effects of hyperglycemia and hyperinsulinemia on glucose turnover during exercise in type 1 diabetes," *Diabetes*, vol. 67, no. Supplement 1, 2018.